Investigations of wood treated by mild pyrolysis in a semi-industrial reactor for sustainable material production: thermal behavior, property changes and kinetic modeling

Bo-Jhih Lin

THÈSE DE DOCTORAT

DE

L'UNIVERSITÉ DE LORRAINE

ÉCOLE DOCTORALE SCIENCES ET INGÉNIERIE DES MOLÉCULES, DES PRODUITS, DES PROCÉDÉS ET DE L'ÉNERGIE (SIMPPÉ)

Présentée et soutenue publiquement par

LIN Bo-Jhih

Pour obtenir le grade de

DOCTEUR

Spécialité: Sciences du bois et des fibres

Option: Energétique, génie des procédés

Etudes de bois traités par pyrolyse douce dans un réacteur semi-industriel pour une production de matériaux durable: comportement thermique, changements de propriétés et modélisation cinétique

Investigations of wood treated by mild pyrolysis in a semi-industrial reactor for sustainable material production: thermal behavior, property changes and kinetic modeling

Soutenue publiquement le 3 Avril 2019 à l'IUT Épinal - Hubert Curien

COMPOSITION DU JURY

Mme. DUPONT Capucine	Ingénieur de Recherche, IHE Delft Institute for Water Education	Rapporteur
M. GOURDON Christophe	Professeur, Institut National Polytechnique de Toulouse	Rapporteur
Mme. ARLABOSSE Patricia	Professeur, IMT Mines Albi-Carmaux	Examinateur
M. PETRISSANS Mathieu	Professeur, Université de Lorraine	Directeur de thèse
M. CHEN Wei-Hsin	Professeur, National Cheng Kung University	Co-directeur de thèse
Mme. PETRISSANS Anélie	Maître de Conférences, Université de Lorraine	Examinateur
M. COLIN Baptiste	Maître de Conférences, Université de Lorraine	Invité

Laboratoire d'Etudes et de Recherches sur le Matériau Bois, LERMaB
IUT Epinal - Hubert Curien, 7 rue des fusillés de la résistance, 88000 Epinal, France

Résumé long -français

Mots clés: Cinétique de pyrolyse, Comportement thermique, Dévolatilisation, Pyrolyse légère, Traitement thermique du bois, Torréfaction

La pyrolyse douce est un procédé prometteur qui permet de modifier thermiquement de la biomasse comme le bois, soit pour produire un matériau durable: le bois traité thermiquement, soit pour produire un combustible solide : le bois torréfié. Après traitement, les propriétés de la biomasse ou du bois sont améliorées par l'obtention d'une meilleure stabilité dimensionnelle, une faible reprise en humidité et une résistance vis-à-vis des attaques fongiques. Un point faible de ce traitement pour le bois utilisé comme matériaux est l'affaiblissement des propriétés mécaniques. Ce point faible devient un avantage dans la production de combustible biomasse dont la broyabilité se trouve considérablement améliorée. Il devient alors plus facile et économique de produire un combustible dispersé. Classiquement, la pyrolyse douce est menée à une température située entre 180 et 300 °C. Afin d'atteindre la température de traitement, plusieurs vitesses de montée en température peuvent être adoptées, suivant l'usage visé pour le matériau, les vitesses de montée en température usuelles sont comprises entre 0,1 et 2 °C min^{-1} pour le traitement thermique et dans une gamme de 20 à 40 °C min^{-1} pour la torréfaction.

Le traitement thermique est un procédé qui favorise la production écologique de matériaux utiles pour l'ameublement ou la construction, pour un usage intérieur et/ou extérieur ; ou pour la production de combustible. Basé sur des produits biosourcés il favorise le stockage du carbone dans notre société en valorisant du carbone végétal et en utilisant très peu de carbone fossile. En ne faisant pas appel aux produits chimiques adjuvantés, en fin de vie (pour la partie matériaux) la planche de bois est très facilement

recyclable dans la filière énergie sans avoir à la décontaminer. Durant son usage en société le matériau ne contamine pas l'environnement, comme par exemple par lessivage à l'eau de pluie des produits de préservation. La principale faiblesse de ce procédé réside dans le manque de connaissance sur le comportement thermique de la biomasse, sur le détail des mécanismes de dégradation et sur la modélisation du processus et cela malgré des décennies de recherche sur le sujet. Cet écueil vient très probablement de l'hétérogénéité chimique du matériau et de son caractère anisotrope, qui en font un produit très variable suivant son essence, son mode de culture et l'action du climat. Il devient alors très difficile d'envisager un comportement unique de la biomasse et ainsi de pouvoir facilement prédire et piloter les unités de traitement de la biomasse.

Néanmoins la littérature issue des précédents travaux du LERMaB (Laboratoire d'Etudes et de Recherches sur le Matériau Bois) a mis en évidence les corrélations qui peuvent exister entre la perte de masse du matériau au cours du traitement (mass loss ML), l'intensité du traitement (température, durée et vitesse de montée en température) et la durabilité conférée. Par ailleurs, ces travaux ont montré que la dégradation thermique du bois est un ensemble complexe de réactions dont la majorité s'établissent dans les parois cellulaires du bois qui sont principalement composées d'hémicelluloses, de cellulose et de lignine. De ces résultats sont également ressorties d'importantes corrélations entre les propriétés du matériau obtenu et les réactions de dégradation du bois.

La bibliographie a révélé que de nombreux travaux se sont attachés à l'étude des phénomènes physiques, chimiques et biologiques impliqués par le traitement thermique des essences bois. Cependant, il existe peu d'informations concernant la dégradation thermique du bois traité dans les réacteurs à l'échelle pilote, nécessaires au changement d'échelle. Pour ce faire, il est important d'évaluer les relations entre les paramètres du procédé, les mécanismes de dégradation et les propriétés du bois produit dans l'industrie. D'après la

littérature, il apparait que la modélisation de la modification thermique du bois pourrait fournir un outil adapté aux applications industrielles en permettant la prédiction du comportement thermique de la biomasse du bois traités dans les fours industriels.

En tenant compte de cet état de la littérature nous avons souhaité développer une étude portant sur le comportement thermique de la biomasse et en particulier du bois soumis à une pyrolyse douce, dans des conditions semi-industrielle (masse supérieure au kilo, temps de traitement long et vitesse de montée en température très faibles). Nous espérons ainsi produire des jeux de données proches des données industrielles, permettant ainsi de valider des modèles existants et ainsi de pouvoir prédire le comportement industriel des unités de production.

Nous avons ainsi mené une étude sur deux essences de bois, un feuillu et un résineu, très utilisées dans l'industrie européenes et dont les comportements sont attendus comme étant éloignés :le peuplier (***Populus Nigra***) et le sapin (***Abies Pectinata***).

Les recherches présentées dans ce manuscrit sont divisées en trois parties. La première partie examine le comportement thermique du bois dans un réacteur à l'échelle semi-industrielle dans lequel un environnement sous vide est utilisé pour maintenir le taux d'oxygène bas et permettre ainsi une dégradation par pyrolyse. Deux espèces de bois différentes, peuplier et sapin,ainsi que quatre températures de traitement (200, 210, 220 et 230 °C) ont été utilisées, cela permet de balayer largement les différents comportements thermiques du bois et l'échelle des températures industrielles de le pyrolyse douce. A partir des courbes de perte de masse (ML) il apparait que la dégradation thermique du matériau bois peut être divisée en quatre principales étapes. Il est également observé que la sensibilité thermique du feuillu (peuplier) est plus importante que celle du résineux (sapin), ce qui mène à une plus grande perte de masse. Une analyse thermogravimétrique des bois avant et après traitement semi-industriel, suivie d'une analyse des signaux ATG, DTG et

DTG seconde permet de clairement identifier la dégradation des hémicelluloses, de la cellulose et de la lignine. Les analyses immédiates et élémentaires indiquent que les réactions de déhydrogénation et de déoxygénation sont plus importantes chez le sapin que chez le peuplier. Par ailleurs, les ratios atomiques H/C et O/C ainsi que l'indice de dévolatilisation sont corrélés linéairement à la perte de masse. La forte relation entre l'indice de dévolatilisation et la perte de masse fait de cet indice un outil simple et efficace pour évaluer la perte de masse de différents bois subissant un traitement thermique sous conditions variables de température, de durée et d'atmosphère (azote, air et vide).

La deuxième partie de l'étude s'attache à l'examen des changements de propriétés comme la structure chimique, la cristallinité, la couleur, l'hygroscopicité et la mouillabilité des bois traités thermiquement. Pour ce faire, des analyses comme l'infrarouge à transformée de Fourier (FTIR), la diffraction des rayons X (XRD) ainsi que des mesures de colorimétrie, d'humidité d'équilibre (EMC) et d'angle de contact ont été réalisées. Les phénomènes observés sont alors discutés en détail et des corrélations entre les modifications élémentaires et le changement de couleur ainsi que les variations hygroscopiques sont établies. Les résultats indiquent que les changements de structure chimique lors du traitement peuvent être évalués par l'analyse des spectres infrarouges. Ceux-ci permettent de mettre en évidence les mécanismes de déacétylation des hémicelluloses, de dépolymérisation et de déshydratation des hémicelluloses et de la cellulose ainsi que les mécanismes de condensation et de scission de la lignine durant le traitement. La diffraction des rayons X apporte des informations sur la dégradation de la cellulose amorphe au cours du traitement ce qui mène à une augmentation du taux de cristallinité. Les changements colorimétriques mesurés suivant le référentiel CIELAB indiquent que la clarté (L^*) est le facteur déterminant de la modification colorimétrique totale (ΔE^*). Les valeurs de ΔE^* sont dans la gamme 41,49 - 51,66 pour les deux bois et

augmentent avec la perte de masse et la sévérité du traitement. Une mesure du taux de réduction de l'hygroscopie est introduite pour quantifier les modifications de cette propriété au sein du matériau. Globalement, le taux de réduction de l'hygroscopie pour le peuplier et le sapin traités est dans la gamme 34,50 - 57,39 %, ce qui suggère d'importantes modifications du matériau. Par ailleurs, les angles de contact d'une goutte d'eau posée sur les échantillons augmentent rapidement avec l'intensité du traitement. Les angles de contact sont supérieurs à 90 ° (dans la gamme 94-113 °) pour tous les bois traités ce qui met également en évidence le caractère hydrophobe de la surface des matériaux produits par traitement thermique. De plus, il apparait que les angles de contact obtenus sur du sapin traité sont plus importants que ceux obtenus sur du peuplier traité, ce qui peut être attribué à une plus grande production de goudrons, en raison du taux d'extractibles très élevés (résines) qui condensent lors du traitement thermique du sapin. Enfin, les taux de décarbonisation (DC), de déhydrogénation (DH) et de déoxygénation (DO) lors du traitement thermique ont été évalués et une forte corrélation linéaire ($R^2 > 0,87$) a été observée entre ces trois indices et la variation colorimétrique ΔE^* ainsi que le taux de réduction de l'hygroscopie.

Dans la dernière partie de l'étude, les cinétiques du traitement thermique du bois sont évaluées à l'aide d'un modèle cinétique à deux étapes. Ce modèle, adapté à partir des essais sur le réacteur à l'échelle semi-industrielle, est utilisé pour prédire les dynamiques de perte de masse (ou de rendement massique). Un modèle de prédiction de la composition élémentaire, basé sur le modèle cinétique, a également été établi pour prédire l'évolution de la composition en C, H et O du bois au cours du traitement. La prédiction du rendement massique montre un bon accord avec les résultats expérimentaux pour des valeurs de R^2 dans la gamme 0,9656 - 0,9997. Les évolutions des trois types de solides présents dans le modèle (bois brut A, intermédiaire B et résidu C) suggèrent que l'intermédiaire B est le

principal composant du matériau final avec des teneurs allant de 74,2 à 82,8 %. Les résultats obtenus sont similaires à des bois ayant subi une torréfaction légère. Par ailleurs, les taux de libération des matières volatiles lors du traitement du peuplier et du sapin à 230 °C sont de 17,05 et 12,44 % respectivement. Les prédictions permises par les modèles mettent en évidence que les ratios atomiques H/C et O/C commencent à diminuer significativement après l'étape d'homogénéisation thermique (> 170 °C) lorsque la dévolatilisation débute. Le pouvoir calorifique supérieur (PCS) des bois peut être déduit des prédictions de composition élémentaire par l'intermédiaire d'une formule empirique. Ceci a permis de déterminer que le PCS des bois traités est dans la gamme 19,62 - 20,55 MJ kg^{-1} ce qui correspond à un facteur d'augmentation situé entre 1,01 et 1,07 par rapport au bois brut.

Pour conclure, les résultats obtenus et les cinétiques établies dans ces travaux contribuent à l'identification des mécanismes de dégradation thermique du bois et pourront être utiles à la conduite des procédés et à l'élaboration des réacteurs dans l'industrie.

Acknowledgements

First of all, I would like to express my grateful thanks to my supervisor, Prof. Mathieu Pétrissans, and Dr. Patrick Rousset for giving me such a good opportunity and recommendation for the PhD study in France. Thanks for the financial support from Laboratory of Excellence ARBRE (ANR-11-LABX-0002-01) and Lorraine Region Council in France. During my PhD study in Épinal, I am very glad to work with LERMaB research team in IUT-Épinal. I would like to express my thanks for Prof. Anelie Pétrissans, Dr. Baptiste Colin, and Dr. François Leconte. Thanks for not only the assistance of research work, but also the aid for the daily life. Thanks very much to the technicians and the administrative staffs in IUT-Épinal for the help during these three years. Thanks to my classmate and also my friend, Edgar. Because of the help from him in the beginning of my PhD study in Épinal, I can concentrate on my study quickly without warring about the dormitory and living. Thanks to my Chinese friends in Épinal. They gave furniture and provided information to me to have a convenient living.

I would like to give special thanks to Prof. Wei-Hsin Chen for his teaching and guiding, and it makes me be on the right way during my research journey. Thanks to GENFUEL team in NCKU for the assistance of measurements and analysis on my study. My sincere thanks also goes to Prof. Christophe Gourdon, Prof. Capucine Dupont, and Prof. Patricia Arlabosse. I appreciate very much for their participation for my PhD thesis jury, and they share the experience and inspire me to have ideas for the future research work.

Last but not the least, I would like to thank my family. They devote every effort to making me have good education and living, as well as they also always encourage me in all of my pursuits and inspire me to follow my dreams.

Thank you all once again. Merci beaucoup.

Bo-Jhih LIN

Épinal, France

April 5, 2019

Content

List of Tables

List of Figures

Nomenclature

$\boldsymbol{A_i}$	Pre-exponential factor (s^{-1})
DC	decarbonization (%)
DH	dehydrogenation (%)
DO	deoxygenation (%)
DI	devolatilization index
$\boldsymbol{DML}$	differential mass loss (% min^{-1})
DTG	derivative thermogravimetric (% min^{-1})
$\boldsymbol{Diff}$	The root mean square of the difference
$\boldsymbol{Ea}$	Activation energy (J mol^{-1})
EMC	Equilibrium moisture content (wt%)
HHV	higher heating value
HRE	hygroscopicity reduction extent
$\boldsymbol{ML}$	Mass loss (wt%)
$\boldsymbol{M_i}$	The initial weight of sample (dry basis) (kg)
$\boldsymbol{M_{treated}}$	The instantaneous weight of sample during treatment (kg)
m_{wet}	The weight of humidified wood (g)
m_{dried}	The weight of dried wood (g)
$\boldsymbol{R}$	The universal gas constant (=8.314 J K^{-1} mol^{-1})
SEM	scanning electron microscope

TGA	Thermogravimetric analysis
$\boldsymbol{YS}$	Solid yield (%, in dry basis)
$\boldsymbol{YV}$	Total volatiles yield (%)
$(Y_s)_{exp}$	The experimental solid yield (%)
$(Y_s)_{cal}$	The calculated solid yield (%)
ΔE^*	Total color difference

Chapter 1 Introduction

1.1 Background

In recent years, the promotion of renewable resource-based bioeconomy has garnered much political support because it can contribute to diverse policy aims such as climate change mitigation, environmental protection, energy security, technological progress, growth, employment, and rural value creation (Pätäri et al., 2017; Purkus et al., 2018). The scholars and policy makers broadly understand bioeconomy as the transition from a fossil-based economy to an economy where the basic sources for products, chemicals and energy would be derived from renewable biological resources (Giurca & Späth, 2017). For the greenhouse gas mitigation, the IPCC (Intergovernmental Panel on Climate Change) considering the long-term effect has concluded that producing sustainable wood materials or energy from sustainably managed forests will generate the largest sustained mitigation benefits of GHGs production (Geng et al., 2017).

Mild pyrolysis is a promising process that is performed in an inert atmosphere for upgrading wood materials by thermal modification to produce sustainable materials (e.g. heat treated wood) or solid fuel (e.g. torrefied wood) (Candelier et al., 2016; Chen et al., 2015c). After the treatment, the properties of wood materials are improved, with a higher homogeneity, longer durability, and higher energy density (Chen et al., 2015c; Hakkou et al., 2006). Normally, the mild pyrolysis is carried out in the temperature range of 200-300 °C. Prior to reaching the treatment temperature, different heating rates can be adopted, depending on the purpose of utilization. For example, the typical heat rates for wood heat treatment and torrefaction are in the ranges of 0.1-2 °C min^{-1} and 20-40 °C min^{-1}, respectively (Chen et al., 2015c; Lin et al., 2018).

Nowadays, mild pyrolysis is commonly used in wood industries for construction and building, and this technology has been commercialized (Ferrari et al., 2013b; Sandberg & Kutnar, 2016; Sandberg et al., 2017). Concerning the studies of wood heat treatment (WHT),

they have been carried out since the early 20th century, and the knowledge has been improved quickly in developing countries, especially in Europe (Esteves & Pereira, 2008; Sandberg & Kutnar, 2016). A search for the number of journal papers in Web of Science (Clarivate Analytics) made on January 19, 2019, using the keyword of "wood heat treatment" and restricted to Abstract, Title, Keywords, showed more than 2700 papers published in this subject. Moreover, the annual number of papers regarding wood heat treatment grew rapidly after 2005, as displayed in **Fig. 1-1**.

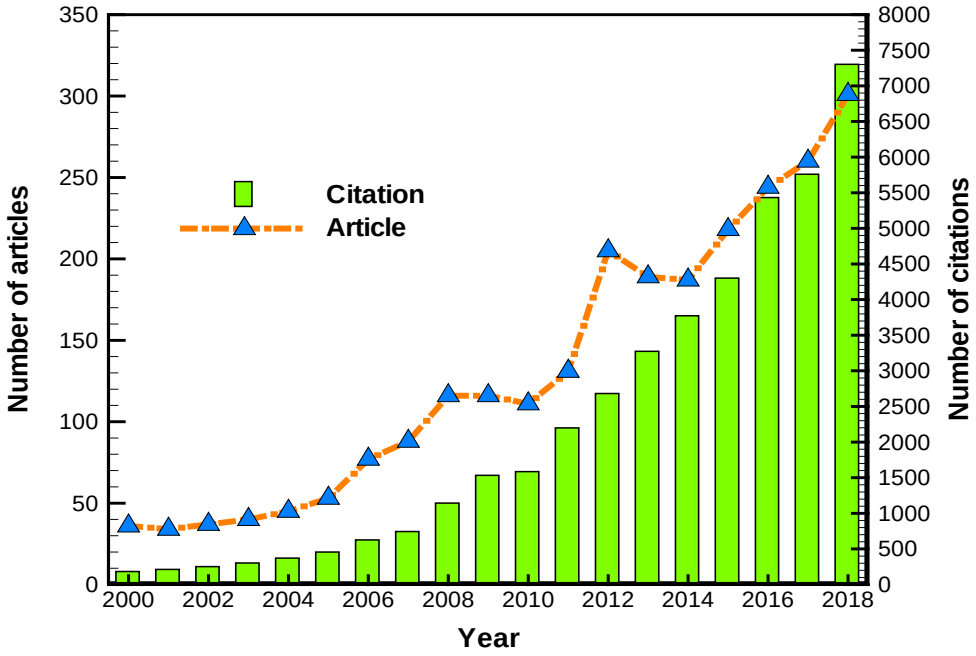

Fig. 1-1. Profile of numbers of articles and citations on wood heat treatment.

In Europe, there are five main different processes that have been commercialized for WHT. They are PLATO, ThermoWood, Le Bois Perdure, Retification, and OHT, respectively (Sandberg & Kutnar, 2016). PLATO (Proving Lasting Advanced Timber Option) process has been developed in Netherlands in 1980s, and is now used by Plato company. The WHT is carried out with two major steps: (1) hydrothermolysis step, and (2) curing step. At the first (hydrothermolysis) step, the green or air dried wood were treated at temperatures between 160 °C-190 °C under increased pressure for 4-5 h. At the second step (curing), the dried intermediate products were heated again at 170 °C-190 °C for 14-16 h to obtain the final

wood products. ThermoWood is the largest producer of heat treated wood, and probably the most successful in Europe. This process has been developed in Finland in 1990. Wood is heated by using steam vapor at a temperature of 185-215 °C. Considering Retification and Le Bois Perdure, both were developed in France. Le Bois Perdure process and reactor were set up by Company BCI-MBS in 1990. They use fresh wood directly, and treat it under steam atmosphere at high temperature. Retification process has been developed by the Ecole des Mines de Saint-Etienne in 1997. In this process, dry wood was put in a specific chamber heated slowly under nitrogen with less than 2 % of oxygen atmosphere. OHT was developed in Germany in 2000. This process was very different, because wood was put inside oil at high temperature in the range of 180-220 °C for heat treatment. This operation was performed in a closed process vessel. The main difference between these processes is the heating medium and the treatment conditions used during WHT. **Table 1-1** summarizes the processing conditions from commercial processes (Sandberg & Kutnar, 2016; Sandberg et al., 2017).

Table 1-1. Summary of the processing conditions from main commercial processes in Europe.

Process	Atmosphere	Operating conditions	Country
PLATO	Saturated steam/ heated air	Temperature: 160-190 °C (hydrothermolysis); 170-190 °C (curing) Process duration: 4-5 h (hydrothermolysis); 14-16 h (curing)	Netherlands
ThermoWood	Steam	Temperature: 130 (drying); 185-215 °C (heat treatment) Process duration:30-70 h	Finland
Le Bois Perdure	Steam	Temperature: 200-300 °C Process duration: 12-36 h	France
Retification	Nitrogen (with less than 2% of O_2)	Temperature: 160-240 °C Process duration: 8-24 h	France
OHT	Vegetable oils	Temperature:180-220 °C Process duration: 24-36 h	Germany

1.2 Objectives

Heat treatment is an eco-friendly and efficient way to improve the defective properties of woods, and to produce sustainable wood materials for construction and buildings (Lin et al., 2018). For example, it has been reported that the heat treated softwood species, such as pine and spruce, are mainly used for outdoor constructions such as garden furniture, windows, doors, and wall or fence boarding. Heat treated hard wood species (e.g., birch and aspen) are widely used for indoor decorations such as kitchen furniture and parquets because of the surface quality (Rapp, 2001; Syrjänen et al., 2000).

The literature stemming from previous works in LERMaB (Laboratoire d'Etudes et de Recherches sur le Matériau Bois) highlighted the correlations between the resulting from curing wood mass loss (ML), treatment intensity (temperature, duration and heating rate) and conferred durability (Chaouch et al., 2010; Hakkou et al., 2006). They indicated that thermal degradation of wood is a complex set of degradation, and the degradation mainly occurs at the wood cell walls, which consisted of hemicelluloses, cellulose, and lignin (Brosse et al., 2010; Candelier et al., 2011; Candelier et al., 2013c). From their results, they found some important relations between conferred properties of woods and wood thermal modifications. For example, the strong relation between the mass loss generated by the thermal degradation and the conferred durability is well known today (Hakkou et al., 2006). The same observations have been published about the correlation between the elemental composition (O/C ratio) and the durability (Candelier et al., 2016).

The literature reviewed above reveals that several studies have been performed the physical, chemical and biological phenomena of woods treated by heat treatment. However, there is still no sufficient information about thermal degradation of wood materials during heat treatment in a pilot-scale reactor, which can provide a more practical approach for industrial applications. Meanwhile, it is also important to evaluate the relations between process parameters, thermal degradation mechanisms, and properties of final wood product in

industry (Candelier et al., 2016). In the study of Silveira et al (2018), they purposed that a modelling of wood thermal modification could become a useful tool for industrial applications, giving the possibility to predict the thermal behavior or properties of heat treated woods in pilot industrial ovens. For these reasons, the main objective in this study is to improve last investigations for a better knowledge about the reaction schemes of thermal degradation in woods heat treated in a pilot-scale reactor, and the obtained results would be further integrated in the mathematical models. To reach the objective, the mild pyrolysis of woods in a semi-industrial scale reactor is evaluated to produce heat treated woods. A comprehensive study on thermal behavior of woods, property changes of treated woods, and kinetic modeling of wood heat treatment is carried out. In this study, a hardwood species (poplar, *Populus nigra*) and a softwood species (fir, *Abies pectinata*) were used, and they have been widely applied in the European wood industry.

The first part of the study aims to investigate the thermal behavior of wood in a semi-industrial scale reactor in which a vacuum environment is adopted to intensify the thermal degradation process. The mass loss dynamics, thermogravimetric analysis (TGA), scanning electron microscope (SEM), proximate analysis, and elemental analysis are performed in untreated and treated woods to evaluate the characteristics of thermal decomposition. The second part of the study examines the property changes, such as changes of chemical structure, crystallinity, color, hygroscopicity and wettability of treated woods. For that A number of analyses such as Fourier-transform infrared spectroscopy (FTIR), X-ray diffraction (XRD), as well as measurement of color changes, equilibrium moisture contents (EMC), and contact angles are performed. The observed phenomena will be discussed in detail. Furthermore, the correlations between elements removals, color changes and hygroscopic transformations are also established.

In the last part of this study, the wood heat treatment kinetics are evaluated based on a two-step kinetic model. This model is used to predict the mass loss dynamics (or solid yield

profiles) according to the experimental results in a semi-industrial scale reactor. An elemental composition model is conducted to predict the C, H and O contents of wood during heat treatment based on the obtained kinetics. Meanwhile, three indices of decarbonization (DC), dehydrogenation (DH) and deoxygenation (DO) are also introduced to evaluate the devolatilization in wood materials during treatment. The obtained models (kinetics and predictions of compositional profiles) give insights into the thermal behavior of wood treated under industrial conditions. The conceptual framework of the thesis is shown in **Fig. 1-2**.

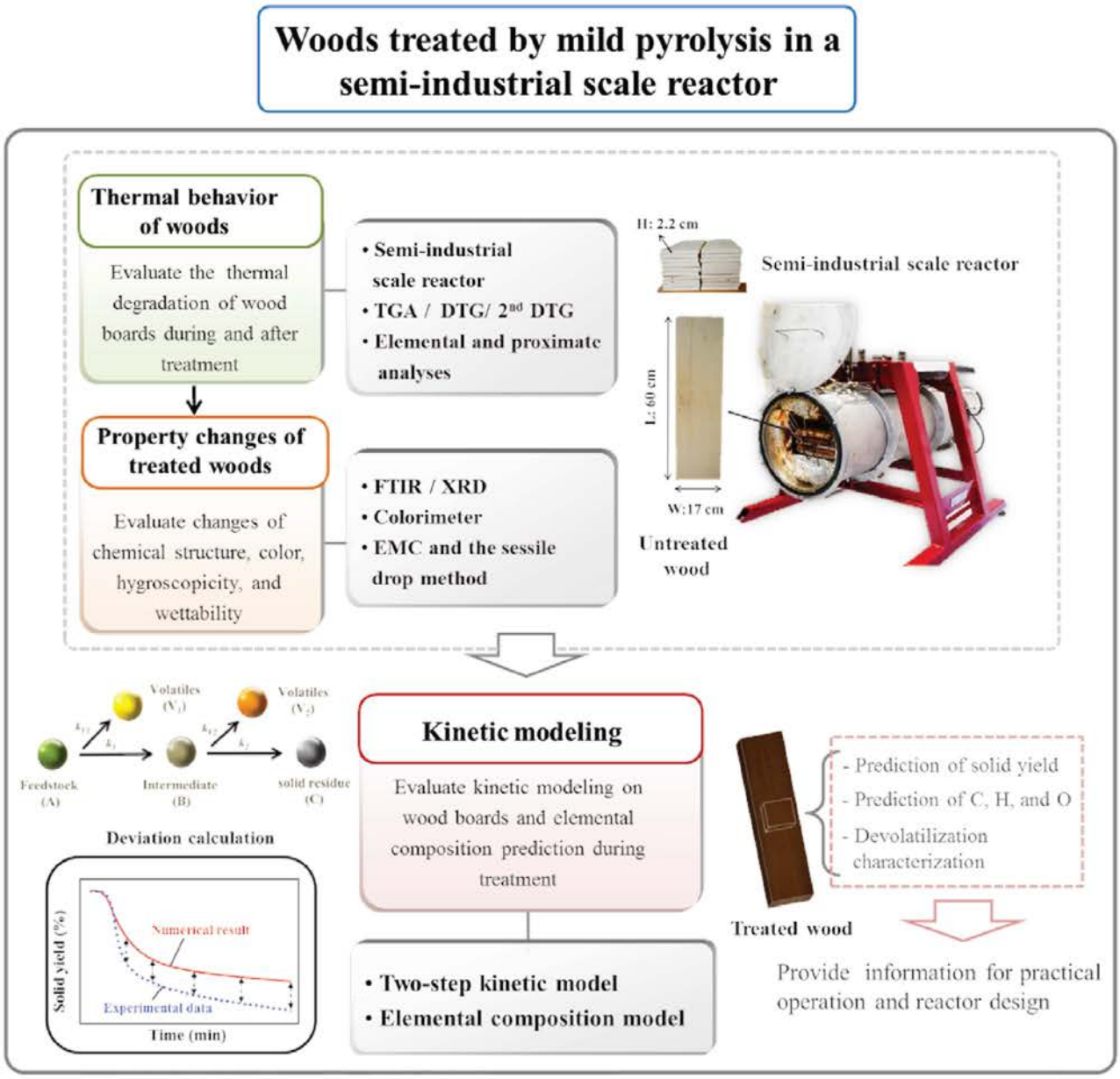

Fig. 1-2. Conceptual framework of the thesis.

1.3 Overview

The content of this thesis includes: (1) Introduction (Chapter 1); (2) State of The Art: a review of wood compositions and preservation processes, wood heat treatment, as well as kinetics of biomass pyrolysis (Chapter 2); (3) Methodology: introduction for the material preparation, experimental setup and procedure, the sample analyses, as well as numerical modeling (Chapter 3); (4) Results and Discussion: Thermal behavior of wood heat treated under industrial conditions (Chapter 4-1), property changes of heat treated wood (Chapter 4-2), and kinetic modeling of wood heat treatment (Chapter 4-3); (5) Conclusions and Perspectives (Chapter 5); (6) References: literature cited in this thesis; (7) Appendix.

Chapter 2 State of the Art

This chapter presents the literature review of the recent advances about (1) wood material (**section 2.1**); (2) wood heat treatment (**section 2.2**); and (3) kinetics of biomass pyrolysis (**section 2.3**) for the preparation work of the thesis.

In **section 2.1**, the current situation of forest and wood utilization, structure and chemical compositions of wood, and the preservation processes are detail descripted to provide a global view of characteristics in wood materials. In **section 2.2**, the characterization of wood heat treatment (such as operating conditions, chemical and physical properties or treated woods, and the related reaction mechanisms), and the different processes (wood heat treated under oil, stem, and vacuum) of heat treatment are illustrated from the recent publication. As mentioned in **Chapter 1**, one part of the study in the thesis is to investigate the kinetic modeling of heat treatment in a pilot scale reactor. For that, the review on recent research activities in kinetics of biomass pyrolysis (non-isothermal and isothermal pyrolysis) is performed in **section 2.3** to find a suitable kinetic model for wood heat treatment. Common kinetic models predicting and evaluating the thermal degradation of biomass are illustrated and summarized. Overall, the review in this chapter is conducive to provide information about heat treated wood production, wood thermal degradation prediction, experiment and reactor designs, as well as the kinetic modeling.

2.1 Wood material

Nowadays, energy shortage and environmental issues have been the biggest challenges facing the world. Accordingly, sustainability, industrial ecology, eco-efficiency, and green chemistry are guiding the development of materials, products, and processes (Mohanty et al., 2002). Forests are the main greenhouse gas sinks in the world, and play an important role in mitigating the climate change. Trees absorb carbon dioxide and utilize water and sunlight to grow and produce oxygen as a byproduct. It is reported that wood is the first choice as a

renewable non-food source of lignocellulosic biomaterial because of its abundance (Karinkanta et al., 2018).

The FAO (Food and Agriculture Organization of the United Nations, FAO) survey reports that around 31% of the total land area of the Earth is covered by forests (**Fig. 2-1**), accounting for about 50% of terrestrial gross primary production i.e. a carbon flux produced by terrestrial plants through photosynthesis, and 80% of total plant biomass (Karinkanta et al., 2018). To date, wood has been widely used as fuel, construction material, and raw material in cellulose and lignocellulose based products. Furthermore, at the end of a product life cycle, the material constituents can be combusted or composted to return the chemical constituents to the grand cycles (Gustavsson et al., 2006; Hill, 2007; Sandberg & Kutnar, 2016).

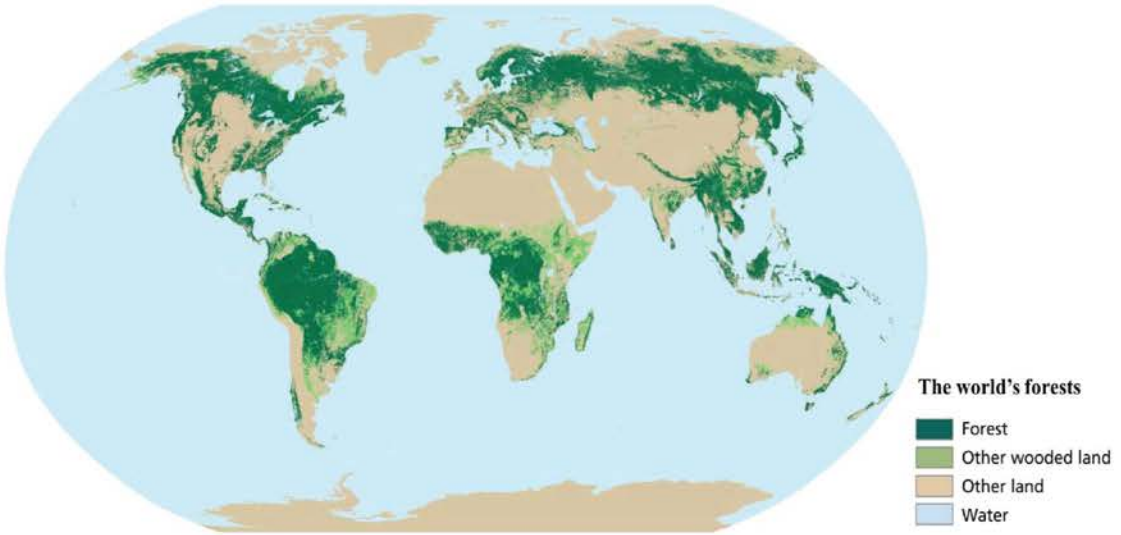

Fig. 2-1. Distribution of forest in world (FAO).

2.1.1 Wood cell wall

The source of wood materials is the plant cell walls, which play important roles in determining the structural integrity of the plant and in defense against pathogens and insects. A wood cell wall is typically composed of three layers, namely, the primary cell wall, the secondary cell wall, and the middle lamella. Cellulose, hemicelluloses, and lignin have different distributions in these layers. Not all types of cells have secondary cell walls. The

mature secondary cell wall accounts for the largest proportion of the lignocellulosic biomass, but its structure and organization begins in the primary cell wall (Davison et al., 2013). The secondary cell wall is the predominant structure in woody biomass, which usually consists of three sublayers; they are S1, S2 and S3. Nevertheless, the integrated structure of cellulose, hemicellulose, and lignin in plant cell walls is still not fully understood (Cheng et al., 2015). The schematic of wood cell wall is shown in **Fig. 2-2**.

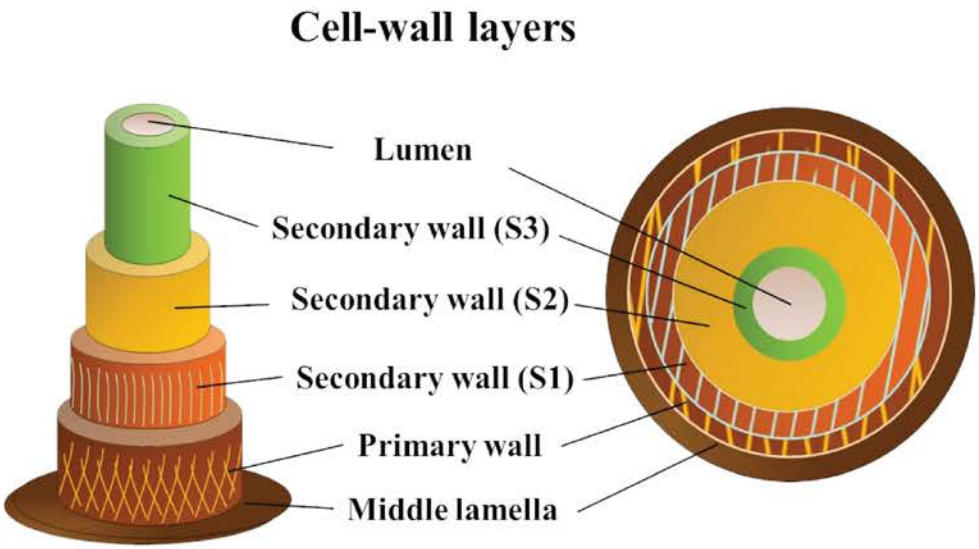

Fig. 2-2. A schematic of cell wall in woody biomass.

The middle lamella contains the highest concentration of lignin. The primary cell wall contains cellulose, hemicellulose, and pectin. The secondary cell wall is divided into three separate parts (S1, S2, S3) based on the structure and composition of polymers present. The exact chemical analysis of each secondary cell wall layer has not been determined for all wood cell wall types. In general, the S1 layer has the greatest concentration of lignin in the secondary cell wall; the S2 layer contains more lignin than the S1 layer. The S2 layer also contains the largest amounts of cellulose and hemicelluloses. Cellulose chains are linked together in the secondary cell wall by hydrogen bonding forming several parallel sheets that constitute the microfibril structure. The S3 layer forms the boundary of the lumen, and has the least amount of lignin (Mathews et al., 2015).

2.1.2 Chemical composition of wood

Wood, as the main representative of lignocellulosic biomass, is mainly constituted by cellulose (a polymer glucosan), hemicelluloses (also called polyose), and lignin (a complex tridimensional phenolic polymer) (Bamdad et al., 2018; Ding et al., 2018; Hernández et al., 2017), as shown in **Fig. 2-3**. In addition to these constituents, wood also contains extractives and inorganic materials (also called ash) (Chen et al., 2015c). The relative contents of these constituents depend on the nature of biomass. For example, cellulose contents (wt%) in softwood, hardwood, and agricultural biomass are 41-50 %, 39-54 %, and 24-50 %, respectively; hemicellulose contents in these materials are 11-27 %, 15-36 %, and 22-35 %, respectively, and lignin contents are 27-30 %, 17-29 %, and 7-29 %, respectively (Kambo & Dutta, 2015). It follows that the relative contents of these constituents in biomass are generally ranked as cellulose > hemicelluloses > lignin. **Table 2-1** is summarized the proportions of compositions (hemicellulose, cellulose, lignin, extractives, and ash) from various biomass (Fuller et al., 2018; Wang et al., 2017).

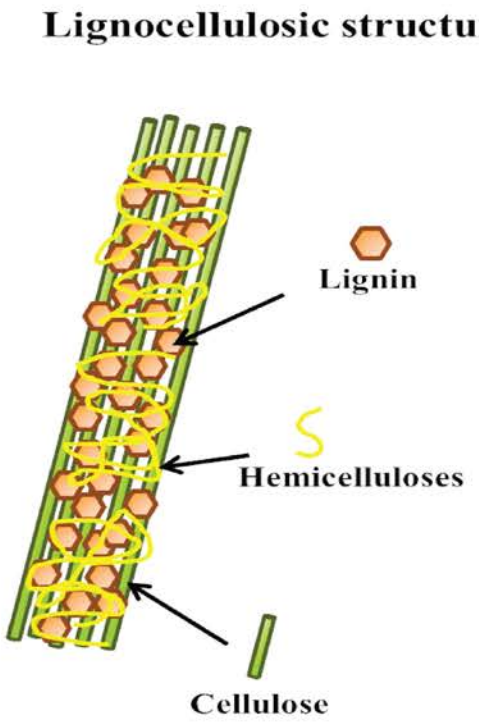

Fig. 2-3. Lignocellulosic structure of lignocellulosic biomass.

Table 2-1. Chemical composition of various biomass types.

	Hardwood biomass	Softwood biomass	Agriculture biomass
Hemicelluloses (wt%)	15-36	11-27	22-35
Cellulose (wt%)	39-54	41-50	24-50
Lignin (wt%)	17-29	27-30	7-29
Extractives (wt%)	2-6	3-10	3-22
Ash (wt%)	0.2-1	0.2-0.6	1-20

2.1.2a Characteristics of hemicelluloses, cellulose, and lignin

The structures and components in hemicelluloses, cellulose, and lignin are very different each other. Hemicelluloses, denoted by $(C_5H_8O_4)_m$ (m: degree of polymerization, 100-200), is a branched mixture of various polymerized monosaccharides such as xylose, glucose, mannose, galactose, arabinose and glucuronic acid. The reactivity of hemicellulose is also higher than that of cellulose (Bach & Skreiberg, 2016). Cellulose, denoted by $(C_6H_{10}O_5)_m$ (m: degree of polymerization, 7,000-12,000), is a linear homopolysaccharide composed of β-D-glucopyranose units linked together by (1→4)-glycosidic bonds (Balat et al., 2008). Cellulose has high amount of carbon compared to the other lignocellulosic components which leads to a significant proportion of energy content in biomass (Mosier et al., 2005). Cellulose molecules have a strong tendency to form intra- and inter-molecule hydrogen bonds which create crystalline micro-fibrils surrounded by amorphous cellulose (Acharya et al., 2015). On account of this special structure, cellulose is more thermally stable than hemicellulose (Bach & Skreiberg, 2016).

Lignin, denoted by $[C_9H_{10}O_3 \cdot (OCH_3)_{0.9\text{-}1.7}]_m$ (Chen et al., 2011), is a three-dimensional, highly branched, and polyphenolic substance which consists of an irregular array of variously

bonded “hydroxy-” and “methoxy-” substituted phenylpropane units (Chen & Kuo, 2011b). Lignin in lignocellulosic biomass acts a binding element for cellulose and hemicellulose structures (Acharya et al., 2015); it also works as a glue in the densification processes (Chen et al., 2015c). The glass transition temperature of lignin is between approximately 135 and 165 °C (Reza et al., 2012). When the temperature during pelletization is higher than the glass transition temperature and the moisture content is between 10% and 15%, lignin in biomass softens and enhances the inter-particles binding.

Overall, cellulose provides a supporting fibrous mesh which is reinforced by lignin polymers (Simoneit, 2002). Cellulose is mainly responsible for the structural strength of wood. Hemicelluloses molecules are less structured than cellulose and their sugar composition varies widely among different tree species. The lignin biopolymers are the fillers in woody tissue making it a complex substance. On account of these inherent differences in structure and composition, the properties among the three constituents are different each other. For example, the hydrophobicity of cellulose is medium, and those of hemicellulose and lignin are low and high, respectively (Kambo & Dutta, 2015). The thermal decomposition characteristics of cellulose, hemicellulose, and lignin demonstrate different reactivities. The thermal decomposition temperature (TDT) of hemicellulose is between 220 °C and 315 °C. Therefore, when biomass is treated by mild pyrolysis, this thermal treatment generally has a drastic impact on hemicelluloses (Chen & Kuo, 2010). The TDT of cellulose is normally between 315 °C and 400 °C (Lu et al., 2012; Yang et al., 2007). The main part of lignin is thermally sable; therefore, its complete degradation requires relatively high temperatures and sufficient time. Although lignin softens at temperature as low as 135 °C (Ciolkosz & Wallace, 2011), its thermal decomposition temperature is in the range of 160-900 °C (Chen et al., 2015c). **Fig. 2-4** shows the thermal decomposition of standard samples, such as cellulose (AlfaAesar, A17730), hemicellulose (SIGMA, X-4252), lignin (Tokyo Chemical Industrial Co., L0045),

xylose (SIGMA, X-1500) and glucose (Panreac Quimica SA, 131341), by the thermogravimetric analysis (TGA) (Chen et al., 2015c).

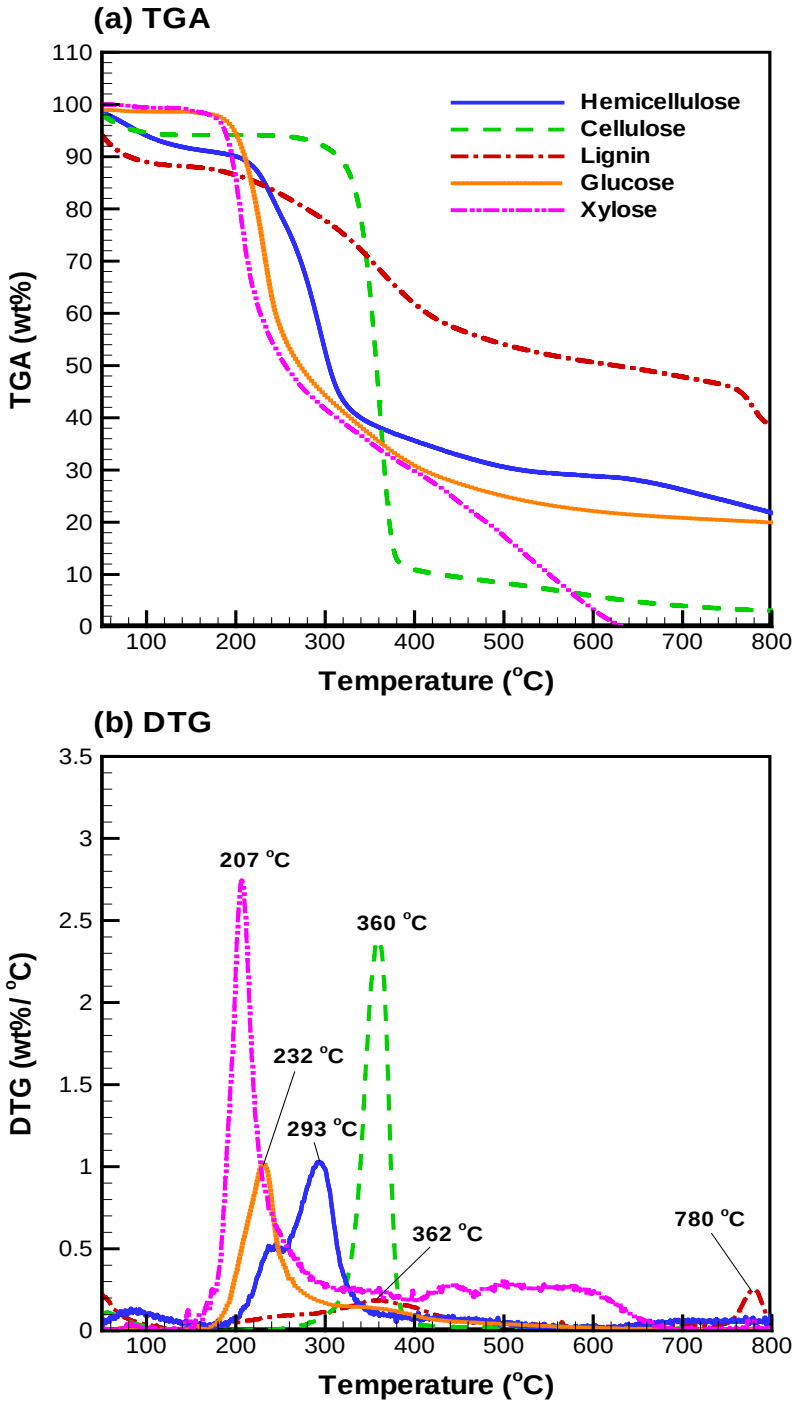

Fig. 2-4. (a) Thermogravimetric analyses (TGA) and (b) derivative thermogravimetric (DTG) analyses of the standards of cellulose, hemicellulose, and lignin (Chen et al., 2015c).

2.1.2b Extractives and ash

Concerning to extractives and ash in wood, extractives are non-structural wood molecules that represent a minor fraction in wood (Valette et al., 2017). The compounds in extractives can be classified in two main groups: (1) aliphatic and alicyclic compounds (terpenes, esters, fatty acids, and alkanes), and (2) phenolic compounds (simple phenols, stilbenes, lignans, isoflavones, flavonoids and hydrolyzable tannins) (Valette et al., 2017). The composition of extractives in wood varies widely from different species, depending on the part of the tree used for isolation, geographical origin, and the season of sampling (Prida & Puech, 2006). The ash content of wood is in the range of 0.2-1 wt% from different wood species (Wang et al., 2017). Because of valuable plant nutrients in wood ash, it can be applied for soil amendment. The major components of wood ash are calcium (Ca), potassium (K), magnesium (Mg) and phosphorus (P). Other macro-elements are aluminum (Al), iron (Fe), sodium (Na), manganese (Mn) and sulfur (S) (Fuller et al., 2018; Wang et al., 2017).

2.1.3. Wood preservation processes

As mentioned above, wood is regarded as a renewable and sustainable material. However, the utilization of wood is limited by its poor resistance to fungal attack (low durability) and the lack of dimensional stability (Candelier et al., 2016; Esteves & Pereira, 2008). Because of that, the material properties, such as dimensional stability, resistance to biological degradation have to be improved before the utilization. The preservation processes of wood normally use one of three strategies: modification of the cell wall, impregnation, and coating to upgrade the defects of wood material (Ramage et al., 2017).

Modification of the cell wall can be further divided into thermal modification and chemical modification. Thermal modification is carried out by heating, and the reactions can be activated within cell walls under high temperature. Chemical modification mainly aims to use hydroxyl groups (OH) in wood to react with other chemical reagents, resulting in the

formation of stable covalent bonds between the reagents and the cell-wall polymers (Ramage et al., 2017; Sandberg et al., 2017). Concerning the other preservation techniques, impregnation of wood is performed with chemicals that diffuse into either the cell wall or the lumen. A coating (or sacrificial layer) can be applied on the surface of wood, supplying a barrier against weathering and degradation and improving the aesthetics of the product (Cogulet et al., 2018; Ramage et al., 2017).

2.2. Wood heat treatment

Among the various techniques of wood treatment mentioned above, wood heat treatment (or thermal modification of wood) is an eco-friendly technology because no chemicals are utilized and added into this process to improve the wood's durability and dimensional stability, whereas toxic chemicals may be used in other chemical modification methods (Candelier et al., 2016; Esteves & Pereira, 2008). In addition, unlike chemically treated woods impregnated by biocidal active compounds, the heat treated wood can be recycled at the end of life cycle without detrimental impact to the environment (Candelier et al., 2016).

2.2.1 Characterization of wood heat treatment

In general, wood heat treatment is conducted in an inert atmosphere (i.e. N_2 atmosphere) where the temperature and heating rate are in the ranges of 180-240 °C and 0.1-2 °C min^{-1}, respectively. The upgraded properties conferred to the wood are the result of thermal degradation of wood cell wall polymers occurring during treatment (Candelier et al., 2016). When wood undergoes heat treatment, hemicelluloses are the most active components compared with cellulose and lignin (Chen et al., 2017). In the study of Chaouch et al. (2010), they examined heat treatment of different softwood and hardwood species at 230 °C under nitrogen. The results revealed that the main modifications occurring during wood heat treatment are due to the degradation of hemicelluloses through depolymerisation reactions to C5 and C6 monosaccharides. In the related study, Chaouch et al.(2013) found that the profiles

of mass loss dynamics were also different between softwood and hardwood species. The mass losses in treated hardwood species were higher than treated softwood species, and it was mainly due to the higher acetyl content present in hemicelluloses of hardwood. Meanwhile, the O/C and H/C ratio of treated woods were also lower than untreated woods because of the thermal degradation. Candelier et al. (2011) investigated the volatile products generated during wood heat treatment between 180 and 230 °C for 15 min by a thermodesorption coupled to gas chromatography coupled to mass spectroscopy (TD-GC–MS). The obtained results suggested that the high amounts of acetic acid generated during thermal degradation of strongly acetylated glucuronoxylan in hardwoods were associated to the formation of numerous degradation products, such as furfural, methylfurfural and vanillin (Candelier et al., 2013c).

After heat treatment, some mechanical properties are reduced, because of the degradation of hemicelluloses, which connects cellulose and lignin in the cell wall (Candelier et al., 2013b). It is reported that the surface hardness of heat treated wood is improved, while other mechanical properties, such as bending strength, compression strengths, cleavage strength and shear strength, are considerably weakened according to the treatment intensities (Candelier et al., 2016; Korkut & Hiziroglu, 2009). Dwianto et al (1996) revealed that the degradation of hemicelluloses causes the cross-linking reactions in the lignocellulosic matrix and the crystallization of microfibrils, as well as the relaxation of stresses stored in microfibrils and matrix. Yildiz et al. (2006) examined the effects of heat treatment on compression strength (CS) of spruce wood, and the results indicated that the CS values of treated wood generally exhibit a decrease when increasing the treatment time and the temperature. Tankut et al. (2014) investigated the mechanical properties of different heat-treated woods (black pine, scotch pine, oriental spruce, iroko, and ash). They pointed out that heat treatment clearly decreased the modulus of rupture (MOR) by 19% and the modulus of elasticity (MOE) by 24%. Although the mechanical performance of treated wood is decreased, it implies that the grindability is

improved. The enhancement of grindability in treated wood is a benefit for fuel application (Chen et al., 2015c; Colin et al., 2017).

Wood is a hygroscopic material in nature, attributing to the cell wall polymers containing hydroxyl (-OH) groups. The groups absorb moisture into the walls and hold water molecules through hydrogen bonding (Chen et al., 2015c). This high hygroscopic nature results in wood are characterized by low dimensional stability and poor durability (Chen et al., 2015c; Pétrissans et al., 2015). Because of that, the decreasing of hygroscopicity or wettability is an important improvement of heat treated wood. The equilibrium moisture content (EMC) is a common indicator to evaluate the hygroscopicity of wood. The EMC of heat treated wood varies from 1 to 6%, depending on the treatment severity, and the treated wood has shown its feature of high hydrophobicity (Iroba et al., 2017). Strandberg et al. (2015) examined the EMC of untreated and treated spruce woods at 20 °C along with 65% relative humidity, and pointed out that the EMC of the torrefied wood was decreased by 50% or more when compared to the EMC of the raw wood. Chen et al. (2015a) conducted the heat treatment of cotton stalk at different temperatures under N_2, and indicated that the EMC decreased obviously with increasing torrefaction temperature.

Concerning the biological degradation of wood, some studies have revealed that the heat treatment can increase its durability (Hakkou et al., 2006; Kymäläinen et al., 2014; Wang et al., 2018b). Overall, the improved durability of torrefied wood against fungi can be explained by four different reasons (Hakkou et al., 2006): (1) an increase of the hydrophobic character of wood, which limited the sorption of water into the material and which is not favorable to the growth of fungi; (2) the generation of new volatile products during treatment that can act as fungicides; (3) the modification of wood polymers leading to a non-recognition of the latter by enzymes involved in fungal degradation; (4) the significant degradation of the hemicelluloses, which constitute one of the main nutritive source for fungi.

In summary, the heat treated woods have longer durability and better dimensional stability, stemming from the reduction in water absorption and biological degradation which are caused from the thermal decomposition of hemicellulose, cellulose, and lignin (Esteves & Pereira, 2008; Hakkou et al., 2006), the property changes of untreated and treated wood is listed in **Table. 2-2**

Table 2-2. Property variation of wood before and afterheat treatment.

Untreated wood	**Heat treated wood**
High moisture content	Low moisture content
High hygroscopicity and wettability	Low hygroscopicity and wettability
Higher O/C and H/C ratio	Lower O/C and H/C ratio
Higher MOR[a] and MOE[b]	Lower MOR[a] and MOE[b]
Poor grindability	Improved grindability
Higher biodegradation	Lower biodegradation
Poor storability and dimensional stability	Higher storability and dimensional stability

[a]: modulus of rupture; [b]: modulus of elasticity

2.2.2 Heat treatment under different atmospheres

2.2.2a Heat treatment under steam / oil

Instead of wood thermal treated in nitrogen condition, different inert mediums, such as steam and oil (Hill, 2007), can also perform heat treatment. In the study of Esteves (2006), t the decreases of hygroscopicity and wettability of wood after steam treatment at 190-210 °C were observed. The equilibrium moisture content of treated samples decreased in the range of 46-61 %, and the radial contact angle of a water drop on wood surface increased from 40 ° to around 80 ° after treatment. Cao et al. (2012) examined dimensional stability of Chinese fir by steam-heat treatment at 170-230 °C for 1-5 h. They indicated that the dimensional stability of treated wood was improved remarkably, and the maximum increase rate of ASE (anti-shrink efficiency) was 72.63 % for heartwood and 70.71 % for sapwood. Moreover, they also

pointed out that the treatment temperature played an important role on the improvement of dimensional stability.

Li et al. (2015a) studied the structural characterization of steam-heat treated wood (*Tectona grandis*) from 120 °C to 220 °C at intervals of 20 °C. The results indicated that the changes of chemical structure become more intense with increasing treatment temperature, and the most significant changes occurred at the treatment temperature of 200 °C. The cleavage of the *β*-O-4 linkages and the splitting of the aliphatic methoxyl chains from the aromatic ring in lignin were also found with increasing treatment temperature. Yin et al. (2017) performed the heat treatment of spruce by compression combined with steam treatment (CS-treatment). They investigated the changes of chemical structure and cellulose crystallinity by Raman microscopy and X-ray diffraction, respectively. The results revealed that the cellulose structure was affected by the treatment and that β-aryl-ether links associated to guaiacyl units of lignin were depolymerized followed by re-condensation reactions. They also reported that the crystallinity index (CrI) and crystallite thickness (*D200*) of cellulose for CS-treated wood were significantly increased owing to crystallization in the semi-crystalline region of cellulose.

Regarding to oil heat treatment (or oleothermal treatment) of wood, this process can improve the properties of wood through synergetic effect of the oil and heat (Lee et al., 2018). The related studies have pointed out that the mechanical properties (such as MOR, MOE, and bending strength) of oil heat treated wood could be better than that treated under nitrogen or steam, and the performance of oil heat treatment is depending on the type of oil (Lee et al., 2018; Li et al., 2015b; Rapp & Sailer, 2000). In the study of Lyon (2007), they evaluated biological resistance of oil heat treated wood (Japanese cedar and beech) by three different vegetable oils (soybean oil, rapeseed oil, and linseed oil) at 130 °C. The results found that linseed oil was the most effective oil to produce durable samples followed by soybean and rapeseed oil. This observation could be attributed to the high content of polyunsaturated fatty

acids in linseed oil, and results in effectively prevented the penetration of water into the wood samples.

Li et al. (2015b) examined the wettability of oil heat-treated bamboo at 180 °C for 2 h, and a significant decrease of the wettability of treated bamboo (*Phyllostachys pubescens*) was observed. The results showed that the contact angle of water drop on the bamboo surface increased from 38 ° to around 60 ° based on the process parameters. Dubey et al. (2011) investigated the heat treatment of pine 180°C and 3 hours by using oil preheated for 0, 3, 9, 15, 21, and 27 h. The results showed that the dimensional stability of treated wood was improved significantly compared to the untreated wood, but the treated wood tended to be darker. They also pointed out that heating aged of oil (up to 27 h) used for heat treatment does not affect dimensional stability and color change of treated wood. As a whole, the characteristics of heat treatment under steam and oil are tabulated in **Table 2-3** (Lee et al., 2018; Okon et al., 2017; Yin et al., 2017; Zhang et al., 2018).

Table 2-3. Characterizations of steam heat treatment and oil heat treatment.

Treatment process	Characterization
Steam heat treatment	- More effective heat transfer than treatment under N_2 - Less severe operating temperature - High stable compressive deformation - Demineralization of alkali and alkaline metals
Oil heat treatment	- Transfer heat within the wood readily and evenly - Higher boiling points allowing higher treatment temperature - Exclude oxygen during treatment resulting in reduction of byproducts - Better mechanical properties

2.2.2b Heat treatment under vacuum

The vacuum process is a novel and promising technology which is suitable for biomass pyrolysis, carbonization, and wood heat treatment (Candelier et al., 2013b; Dewayanto et al., 2014; Ismadji et al., 2005). The applications of the aforementioned thermochemical processes with the vacuum technique are summarized in **Table 2-4**. In a vacuum process, heat is mainly transferred to the sample through conduction, and a vacuum pump is employed to continuously remove volatile compounds released from biomass, thereby accelerating the thermal degradation of polysaccharides in biomass (Hill, 2007).

As far as wood heat treatment in vacuum is concerned, it is an alternative and novel technology for thermal modification of wood where the oxygen content in a reactor is reduced to avoid wood combustion (Sandak et al., 2015). Allegretti et al. (2012) studied thermal modification of spruce and fir under vacuum (150, 210, and 350 mbar) at the temperature range from 160 to 220 °C. There are four different funguses (*P. placenta, C. puteana, T. versicplor,* and *G. trabeum*) were used to examined the durability of heat treated wood. The results indicated that the most aggressive fungus on heat treated wood was brown rot *P. placenta,* and it caused mass loss in the range from 10 to 20 wt%. Based on the results, they reported that heat treated wood at 220 °C for 2.5 h showed a significant improvement of durability. de Oliveira Araújo et al. (2016) investigated heat treatment of three different common wood species (bracitinga, feroba mica, and cumaru) in South America under nitrogen and vacuum at the temperature range from 180 to 220 °C. The results reported that the mass loss were lower for the treatment under nitrogen than under vacuum for all treatment temperatures and species. The equilibrium moisture content (EMC) of treated wood was significantly reduced, and it was more effective to reduce hygroscopicity of wood under vacuum than nitrogen.

Candelier et al. (Candelier et al., 2013a) carried out the heat treatment of beech under nitrogen and vacuum, as well as made the comparison of chemical composition. All

treatments were performed at 220 °C for mass losses resulting from wood thermal degradation of approximately 12 wt%. The results indicated that wood treated under nitrogen present higher Klason lignin and carbon content, lower hemicelluloses and neutral monosaccharides contents comparatively to treated wood under vacuum. Ferrari et al. (2013a, 2013b) investigated heat treatment of Turkey oak under vacuum, steam, and vacuum combined with steam conditions. The temperature for wood treatment was between 100 and 110 °C under steam, as well as 160 °C under vacuum. The results indicated that there was a significant influence on color difference before and after treatment under vacuum. However, the treatment under steam at 110 °C for 24 h can obtain wood products with greater color homogeneity.

Overall, wood thermal modification with vacuum has demonstrated the following advantages: (1) efficient drying and thermal modification with reduced energy consumption and duration (Ferrari et al., 2013a; Ferrari et al., 2013b); (2) easier and cheaper management of volatile wastes produced during heat treatment (Ferrari et al., 2013b); (3) decreasing odor that normally characterizes many thermal treated woods (Ferrari et al., 2013a); (4) higher reactivity of thermal degradation and more effective to reduce hygroscopicity of wood under vacuum than nitrogen (Candelier et al., 2013a; de Oliveira Araújo et al., 2016); and (5) providing greater color homogeneity of wood products (Ferrari et al., 2013a; Ferrari et al., 2013b). Accordingly, thermal modification of wood in vacuum is an attractive and promising technology to improve wood properties and to be applied in wood industry. The comparison of wood treated in vacuum and nitrogen has been carried out in previous works (Candelier et al., 2013a; Candelier et al., 2013b), that revealed that the performance of treatment in a vacuum condition under similar properties of treated wood was higher due to shorter drying and treatment periods.

Table 2-4. Literature review of biomass pyrolysis, carbonization, and heat treatment under vacuum.

Reaction	Material	Experimental condition	Objective	Reference
Pyrolysis	Palm oil decanter cake	Temperature: 400-600 °C Heating rate: 15 °C min $^{-1}$ Pressure: below 300 hPa	Potential of bio-oil production from palm oil decanter cake (PDC) at various temperatures.	(Dewayanto et al., 2014)
	Paper waste sludge	Temperature: 300, 425, 550 °C Heating rate: 30°C min $^{-1}$ Duration: ~ 54 s Pressure: 80 hPa	Comparison of vacuum, slow, and fast pyrolysis processes to transfer energy from paper waste sludge (PWS) to bio-oil and biochar.	(Ridout et al., 2016)
	Chinese fir sawdust	Temperature: 500 °C Duration: 30 min Pressure: 100 hPa	Characteristics of co-pyrolysis from Chinese fir sawdust (CFS) and waste printed circuit boards (WPCBs) at different mass ratios.	(Wu & Qiu, 2014)
	Rape straw	Temperature: 400-600 °C Heating rate: 4-20 °C min $^{-1}$ Duration: 15-75 min Pressure: 50-650 hPa	Optimization of bio-oil yield from vacuum pyrolysis of rape straw by using orthogonal design method.	(Fan et al., 2014)
Carbonization	Teak sawdust	Temperature: 600 °C Heating rate: 20 °C min $^{-1}$ Duration: 60 min Pressure: 50-650 hPa	Preparation of activated carbon from carbonization of teak sawdust, and the investigation of pore structure.	(Ismadji et al., 2005)

	Rice husk and sewage sludge	Temperature: 900 °C Heating rate: 10 °C min $^{-1}$ Duration: 120 min Pressure: 50 hPa	Synergetic effect on gas production during co-pyrolysis of rice husk and sewage sludge.	(Zhang et al., 2015)
	Sugar cane bagasse	Temperature: 460 °C Heating rate: 17 °C min $^{-1}$ Duration: 60 min Pressure: 80 hPa	Production of biochar/activated carbon from carbonization of sugar cane bagasse.	(Carrier et al., 2012)
Heat treatment of wood	Norway spruce, silver fir, European larch, European beech, oak, European ash, wild cherry, and black locust	Temperature: 160-230 °C Pressure: 250 hPa	Potential application of near infrared spectroscopy for quality control of heat treated wood from softwood and hard wood	(Sandak et al., 2015)
	Spruce and fir	Temperature: 160-220 °C Duration: 240-900 min Pressure: 210 hPa	Investigation of properties (EMC, color, anti- swelling efficiency and durability) changes after heat treatment.	(Allegretti et al., 2012)
	Bracitinga, feroba mica, and cumaru	Temperature: 180-220 °C Duration: 60 min Pressure: 600 hPa	Examination of physical and technical properties of heat treated wood from common South America wood species.	(de Oliveira Araújo et al., 2016)
	Beech	Temperature: 230 °C Heating rate: 0.2 °C min $^{-1}$ Pressure: 200 hPa	Comparison of chemical composition and durability of beech under vacuum and nitrogen.	(Candelier et al., 2013a)
	Turkey oak	Temperature: 160 °C Duration: 180 min Pressure: 200-230 hPa	Evaluation of wood thermal modification through combined steam and vacuum process.	(Ferrari et al., 2013b)

2.3 Kinetics of biomass pyrolysis

Thermal degradation of biomass during mild pyrolysis is a complex set of decomposition and polymerization reactions. For lignocellulosic biomass, the degradation mainly occurs at biomass cell walls in which hemicelluloses, cellulose, and lignin are the prime constituents (Brosse et al., 2010; Candelier et al., 2013c; Lin et al., 2018). For microalgal biomass, the degradation involves the decomposition of carbohydrates, proteins and lipids (Bach & Chen, 2017b; Chen et al., 2015b). The kinetic analysis is regarded as an efficient method to characterize the thermal decomposition behavior of wood during pyrolysis (Bach & Chen, 2017c; Wang et al., 2016). As a whole, there are two basic modes of biomass pyrolysis kinetics: non-isothermal and isothermal kinetics. Based on the two modes, some different models such as one-step model (or called model-free) (Chen et al., 2014a), two-step model (Chen et al., 2015c), multi-step model (Cavagnol et al., 2013), and multi-components model (Bach & Chen, 2017a; Wang et al., 2017) have been developed, as demonstrated in **Fig 2-5**.

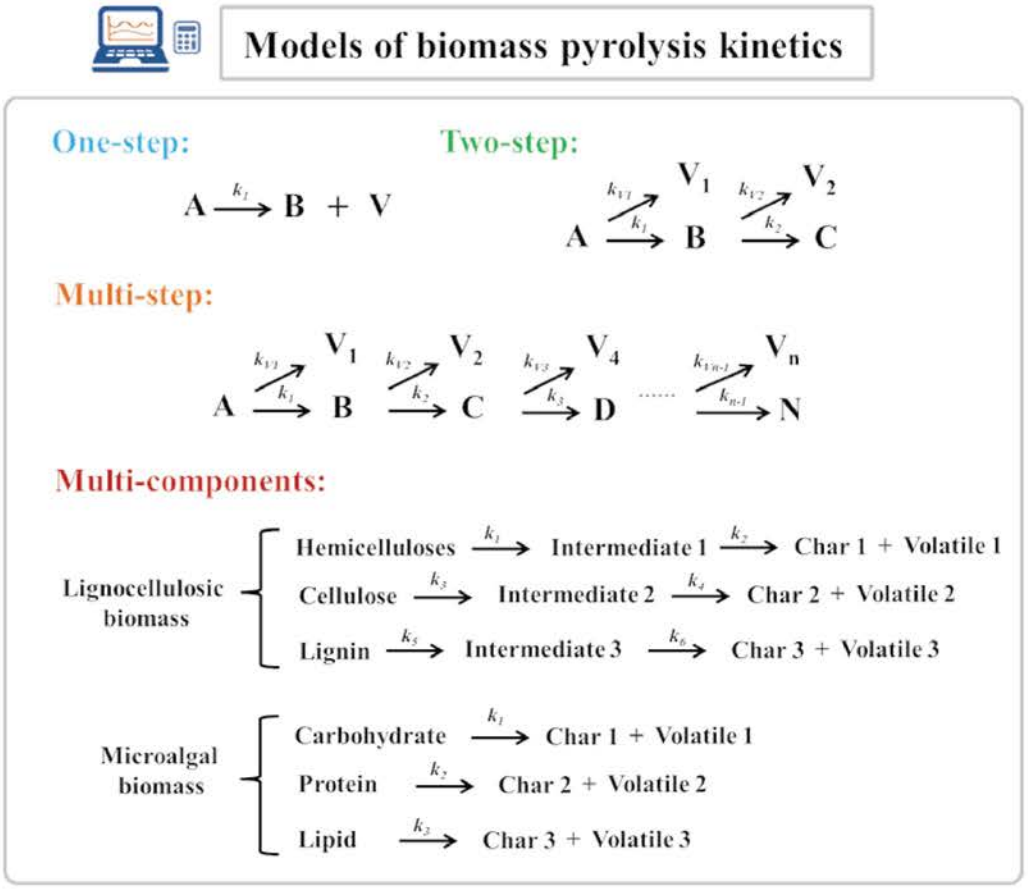

Fig. 2-5. Various models for biomass pyrolysis kinetics.

2.3.1 Non-isothermal pyrolysis

The non-isothermal pyrolysis kinetics of biomass is generally calculated from 100-800 °C to predict the reaction rates, substance conversion, and product formation based on the experimental results of TGA (Bach & Chen, 2017b; Chen et al., 2015c). Chen et al. (2014a) studied the effects of heating rate on pyrolysis behavior and kinetic parameters of moso bamboo. The kinetics of bamboo pyrolysis were obtained from a one-step model, and the results showed that the increasing of heating rate (from 5 to 30 °C min^{-1}) increased the temperature range of devolatilization stage and the activation energy values. Burra and Gupta (2019) investigated the calculation of biomass pyrolysis kinetics by using multi-step reaction model, and six different biomasses (cardboard, dry-paper waste, pinewood, rice husk and chicken manure) were examined. They reported that multi-step pyrolysis model was fitted to the pyrolysis results of these feedstocks, which revealed that lignocellulosic biomass required at least three-step sequential model for accurate pyrolysis modeling.

Weerachanchai et al. (2010) investigated the effects of biomass type (cassava pulp residue, palm kernel cake, palm shell, coconut shell and longan fruit seed), particle size (106-1325 μm), and heating rate (5-40 °C min^{-1}) on the behavior of thermal decomposition and examined the pyrolysis kinetics with different models (one-step, two-step consecutive-reaction, two-component parallel reaction). They found that the greatest fitting was reached with the two-component parallel reaction, while the other models provided satisfactory results with assuming n^{th} order reactions and providing stoichiometric coefficients, respectively. Bach and Chen (2017a) tested a single reaction, two to four parallel reactions, as well as seven parallel reactions models, and compared the results with the experimental data to obtain the optimal model for pyrolysis of microalgal biomass. The results pointed out that the fit quality of the model was improved with the increasing of the number of reactions and that the four reactions model was suitable for simulating the thermal degradation of microalgae. Din et al. (2018) evaluated the pyrolysis kinetics of beech wood under a bench-scale reactor

according to a three-component parallel reaction scheme. The predicted results agreed well with the experimental data, and the degree of deviation on predicted mass fraction was larger than that based on the optimized parameters with R^2=0.9041.

Because of the development of artificial intelligence, some studies evaluated the pyrolysis kinetics coupled with evolutionary computation in recent years (Chen et al., 2018a). Sheth and Babu (2008) estimated the kinetic parameters for pyrolysis of hazelnut shell by differential evolution. The presented results by differential evolution were better than the traditional techniques for optimization. Li et al. (2014) optimized the kinetic parameters of the medium-density fiberboard (MDF) pyrolysis via a genetic algorithm. It was found that as the combination of genetic algorithm and Kissinger's method, the predicted results provided better accuracy than using the genetic algorithm or Kissinger's method alone. Ding et al (2016) calculated the kinetics of beech wood by applying the three parallel reactions model and using the Shuffled Complex Evolution. The simulated results show stronger fits to the experimental data for different heating rates than those proposed from the previous literature. Chen et al. (2018a) evaluated the pyrolysis kinetics of different microalgae by particle swarm optimization (PSO). The pyrolysis of microalgae (*Chlorella vulgaris* ESP-31, *Nannochloropsis oceanica* CY2, and *Chlamydomonas* sp. JSC4) were examined by thermogravimetric analysis (TGA). The results suggested that the thermal degradation curves of the three microalgae could be predicted with a fit quality of at least 97.9%.

2.3.2 Isothermal pyrolysis

The isothermal pyrolysis kinetics have been applied in biomass torrefaction and heat treatment processes to describe the thermal degradation mechanisms of biomass (Gul et al., 2017; Pétrissans et al., 2014). Chen and Kuo (2011a) developed the isothermal pyrolysis kinetics by a one-step model to predict the thermal decompositions of hemicellulose, cellulose, lignin and xylan at 200-300 °C. The recommended values of the reaction order on cellulose, and lignin and xylan are 3, 1, and 1, whereas their activation energies are 187.06, 124.42, and

37.58 kJ mol^{-1}, respectively. Chen et al. (2014a) carried out the isothermal and non-isothermal torrefaction of a microalga (*Scenedesmus obliquus* CNW-N) using TGA and investigated the torrefaction kinetics. They found that the activation energy under isothermal torrefaction. The comparison between the two different heating modes indicated that, under the same average temperature, the non-isothermal torrefaction is more severe than the isothermal torrefaction.

Oluoti et al. (2018) examined the torrefaction kinetics of *Alstonia congensis* (Ahun) and *Ceiba pentandra* (Araba) based on a one-step model, and the kinetic parameters were obtained by non-linear regression method. The results found that the activation energies of Araba and Ahun were 134.45 kJ mol^{-1} and 143.38 kJ mol^{-1}, while the corresponding reaction orders were 2.15 and 2.28, respectively. Klinger et al. (2014) studied the kinetics of aspen torrefaction by a multi-step model. The model was used to predict the amount of various chemical species evolved during torrefaction based on the degradation of hemicelluloses, and the obtained kinetics could accurately predict the dynamic profiles of gas-phase product over the initial stages of torrefaction (up to 30% mass loss) from 260 to 300 °C. Cavagnol et al. (2013) investigated the kinetics of wood (locust, spruce and eucalyptus) torrefaction with long residence time in the temperature range of 210-290 °C. The kinetic parameters were determined for various multi-step series reaction mechanisms developed from the literature (one, two and three-step models). The results revealed that the two-step model provides acceptable accuracy for the prediction of the mass loss during torrefaction.

The two-step model is well known for determining the isothermal pyrolysis kinetics of biomass, which considers a completive volatile and solid formation (Di Blasi & Lanzetta, 1997). In the study of Branca and Di Blasi (2003), the results from isothermal degradation of beech indicated that the first step of reaction was attributed to the removal of extractives and the degradation of hemicelluloses, while the second step reaction was ascribed to the degradation of hemicelluloses, cellulose, and part of lignin. Bates and Ghoniem (2012) determined the evolution of volatile and solid products during willow torrefaction between

200 and 300 °C based on the two-step kinetic model. The predicted the composition of volatiles and their results were validated with the experiments of Prins (2006). Sheng et al (2014) adopted the two-step model to evaluate the torrefaction kinetics of wood chips in a pilot-scale reactor and to predict the mass yield during torrefaction, and established the correlation between the mass yield and the higher heating value to estimate the energy yield of torrefied chips. Shoulaifar et al. (2016) investigated the mass loss dynamics during spruce torrefaction with different contents of potassium (K) based on the two-step kinetic model. Depending on the contents of impregnated potassium, they used the same activation energy but different pre-exponential factors for the rate constants. Their results were in a good agreement with the experiments. Silveira et al. (2018) investigated kinetics of wood (poplar wood boards) heat treatment based on the two-step kinetic scheme with three-stage approach. The calculated deviation values from the direct approach and the three-stage approach were 0.363 and 0.235, respectively, accounting for 35% improvement from the proposed three-stage approach. They also suggested that the two-step model could be regarded as a promising approach to directly apply for solid yield prediction during the heat treatment of wood boards in a pilot scale reactor. In summary, the related studies on the kinetics of biomass non-isothermal and isothermal pyrolysis are listed in **Table 2-5**.

Table 2-5. Summary of studies on non-isothermal and isothermal pyrolysis of biomass.

Mode	Material	Kinetic model	Experimental condition	Objective	Reference
Non-isothermal	Moso bamboo	One-step	Temperature: 100-700 °C Heating rate: 5-30 °C min^{-1} Flow rate of gas: 100 mL min^{-1}	Effects of heating rates on slow pyrolysis and the kinetic parameters.	(Chen et al., 2014a)
	Eucalyptus	One-step	Temperature: 100-700 °C Heating rate: 5-20 °C min^{-1} Flow rate of gas: 80 mL min^{-1}	Pyrolysis kinetics of torrefied wood with different approach	(Doddapaneni et al., 2016)
	Cardboard, dry-paper waste, pinewood, rice husk and chicken manure	Multi-step	Temperature: 50-1000 °C Heating rate: 10 °C min^{-1} Flow rate of gas: 100 mL min^{-1}	Simultaneous thermal analysis (TGA-DSC) of biomass pyrolysis and modeling of pyrolysis kinetics.	(Burra & Gupta, 2019)
	C. vulgaris ESP-31	Multi-components	Temperature: 100-700 °C Heating rate: 10 °C min^{-1} Flow rate of gas: 100 mL min^{-1}	Comparison of microalga pyrolysis kinetics from a single reaction to seven parallel reactions.	(Bach & Chen, 2017a)
	Poplar	Multi-components	Temperature: 300-973 K Heating rate: 5-30 K min^{-1} Flow rate of gas: 20 mL min^{-1}	Determination of kinetics parameters for the prediction of product distributions	(Vo et al., 2017)
Isothermal	Hemicellulose, cellulose, lignin ,and xylan	One-step	Temperature: 200-300 °C Heating rate: 20 °C min^{-1} Flow rate of gas: 200 mL min^{-1} Duration: 60 min	Thermal degradation of hemicellulose, cellulose, lignin ,and xylan, and its kinetics during torrefaction	(Chen & Kuo, 2011a)

S. obliquus CNW-N	One-step	Temperature: 205-295 °C Heating rate: 0.5-1.5 °C min^{-1} Flow rate of gas: 100 mL min^{-1} Duration: 100 min	Effects of non-isothermal torrefaction characteristics on microalga.	(Chen et al., 2014b)
Fir, pine, and poplar	Two-step	Temperature: 230 °C Heating rate: 1 °C min^{-1} Duration: 600 min	Investigation of thermal degradation on different wood species during mild pyrolysis.	(Pétrissans et al., 2014)
Beech, pine, wheat straw, and willow	Two-step	Temperature: 220-300 °C Duration: 300 min	Modeling of volatile release during torrefaction and the optimization.	(Gul et al., 2017)
Beech	Multi-step	Temperature: 528-708 K Heating rate: 1000 K min^{-1} Duration: 100 min	Kinetics of wood thermal degradation with a three-step model.	(Branca & Di Blasi, 2003)
Locust, spruce, and eucalyptus	Multi-step	Temperature: 210-290°C Heating rate: 20 °C min^{-1} Flow rate of gas: 15 mL min^{-1} Duration: 600 min	Evaluation of different multi-step kinetic models on wood heat treatment.	(Cavagnol et al., 2013)
Aspen	Multi-step	Temperature: 260-300°C Heating rate: 1000 °C s^{-1} Duration: 90 min	Effects of temperatures on torrefaction kinetics and the prediction of volatile products.	(Klinger et al., 2014)
Beech	Multi-components	Temperature: 200-260°C Duration: 420 min	The validation of kinetics model on wood heat treatment, and the behavior of heat and mass transfer.	(Turner et al., 2010)

Chapter 3 Methodology

3.1 Material preparation

In this study, a hardwood species (poplar, *Populus nigra*) and a softwood species (fir, *Abies pectinata*) were studied. They have been widely used in the European wood industry but have lower economic values. This can be solved through heat treatment that improves the wood properties and increases its potential applications. The wood boards were cut to the dimensions 60 cm × 17 cm × 2.2 cm for heat treatment. Prior to the experiments, the boards were dried in an oven at 103 °C until mass stabilization. The densities of the wood species were measured after drying, and the average densities of poplar and fir were 324 and 349 kg m^{-3}, respectively. The basic properties of untreated poplar and fir such as proximate and fiber analyses are listed in **Table 3-1**.

Table 3-1. Basic properties of poplar and fir.

Wood material	**Poplar (*Populus nigra*)**	**Fir (*Abies pectinata*)**
Density (kg m^{-3}) [*a]	324	349
Proximate analysis (wt%) [*a]		
Volatile matter (VM)	84.74	85.53
Fixed carbon (FC)	14.70	14.28
Ash	0.56	0.19
Fiber analysis (wt%) [*b]		
Hemicelluloses	22.54	19.28
Cellulose	50.11	46.78
Lignin	24.71	30.15
Extractives	2.63	3.80

[a]: dry-basis; [b]: dry-ash free-basis

3.2. Experimental system and procedure

The experimental system for wood heat treatment in vacuum was composed of three units which included a wood heat treatment unit, a vacuum unit, as well as a control and recording unit, as demonstrated in **Fig. 3-1**.

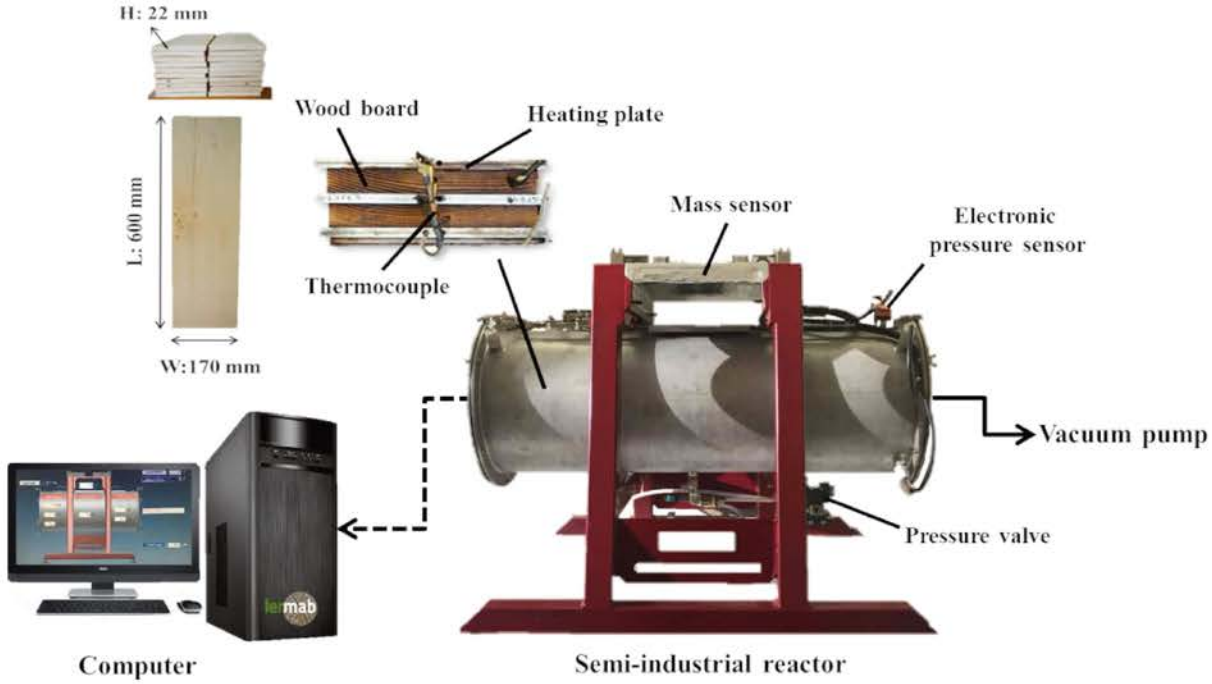

Fig. 3-1. A schematic of the system for wood heat treatment under vacuum.

In the wood heat treatment unit, a semi-industrial scale reactor made of stainless steel (outside diameter: 32 cm; length: 86.5 cm) contains three heating plates (length=65 cm and width=18 cm) and a mass sensor was used to record the mass of the whole reactor including wood boards. The resolution of the mass sensor in the system was 0.1 g, and a calibration curve between 0 and 4 kg was established by the standard weight. In each run of experiment, two boards with the same wood species and size were put inside the reactor. Each wood board was placed between two heating plates, and K type thermocouples were installed inside the heating plates. The mass sensor was connected to a computer to record the instantaneous mass of wood boards during the heat treatment. In the vacuum unit, a vacuum pump (ElmoRietschle L-BV3) and a pressure valve were used to control the pressure in the reactor at a vacuum condition where the pressure was fixed at 200 hPa (≈ 0.2 atm) during the

treatment. An electric pressure sensor (iFM 45128 Essen) was installed to control and measure the pressure of the whole system. As for the control and recording unit, a computer along with a monitoring software was adopted to control and record temperature, pressure, and sample mass during the treatment. The mass loss (*ML*) of a wood sample is expressed as

$$ML\ (\%) = \frac{M_i - M_{treated}}{M_i} \times 100 \quad \textbf{(3-1)}$$

where M_i is the initial weight of sample (dry basis), and $M_{treated}$ is the instantaneous weight of sample during treatment.

The mass loss of treated wood for the industry in Europe is normally controlled at 8-10 wt%, and the temperature range of 200-240 °C has been widely applied for wood heat treatment (Candelier et al., 2016). For these reasons, the wood materials were treated at 200, 210, 220, and 230 °C in this study. The temperature in the reactor increased from room temperature to 103 °C at a heating rate of 0.2 °C min^{-1}, followed by keeping that temperature for 120 min to completely remove moisture. Subsequently, the temperature was lifted to 170 °C at the same heating rate. Then, the temperature was held for 120 min for the thermal homogenization of the wood boards to avoid the cracking of wood boards during treatment (Pétrissans et al., 2014). After that, the temperature in the reactor was increased to the target temperature which was kept for 1,000 min. The heating program during heat treatment is illustrated in **Fig. 3-2**. This treatment time was longer than that in industrial practice to observe detailed mass loss dynamics of the wood samples. The initial recorded point of all the experimental began at 50 °C to provide the basis of heat treatment and the entire process took 2,130 min.

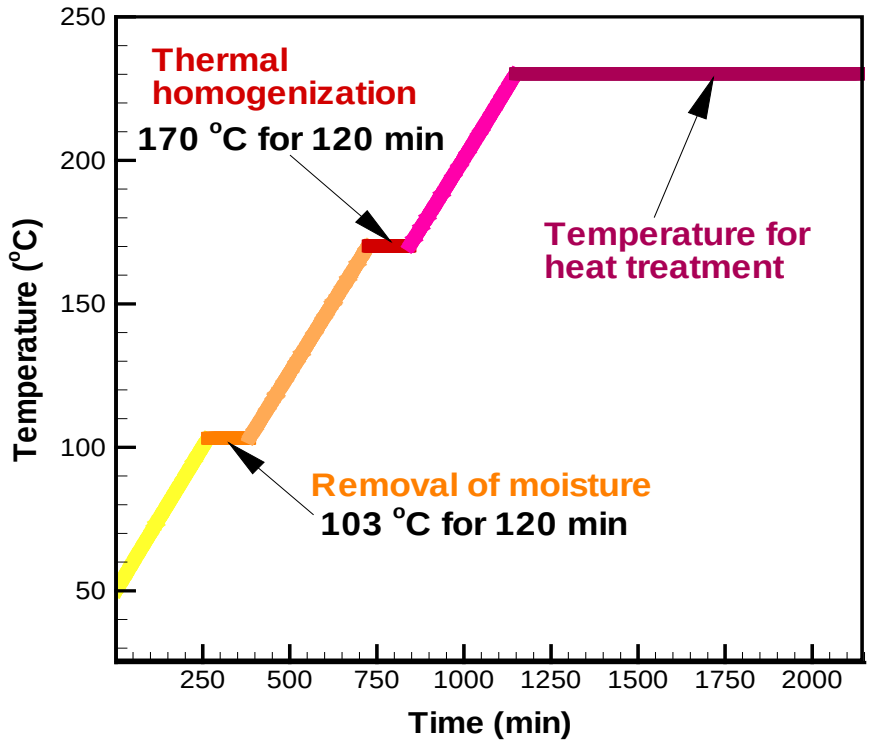

Fig. 3-2. Illustration of heating program during heat treatment.

To ensure the experimental quality, prior to performing experiments the adopted instruments were periodically calibrated by clean and blank process, as shown in the **Appendix**. Moreover, the experiments of the present work were repeated at least twice. The mass loss data displayed were the average values, and the relative error of the mass loss between the two experiments are controlled below 5 %.

3.3 Analysis of wood samples

Before the analyses, the wood samples were crushed with a grinder and sieved to the particle sizes ranging from 0.36 to 1.7 mm (i.e. 12-45 mesh). The sieved wood samples were dried in an oven at 105 °C for 24 h to provide a basis for analysis. Subsequently, the samples were placed in sealed plastic bags and stored in electronic cabinet at room temperature until experiments were carried out.

3.3.1 Proximate analysis

The proximate analysis was performed according to the ASTM standard procedures (i.e., moisture: E871; volatile matter: E872; fixed carbon: E870; and ash: D1102) (Lin et al., 2018). The moisture is obtained from the mass loss percentage of sample placed in a drying oven at the temperature of 103°C for 16 h. The examination of volatile matter (VM) is based on the mass loss percentage of the dried sample which is placed in a high-temperature furnace at 950 °C for 7 min. The ash content is the retained weight percentage of a sample, which is placed in a furnace and heated to temperatures between 580 °C and 600 °C with 20 °C min^{-1} of heating rate. The fixed carbon (FC) is determined is by difference, namely, FC (%)=100-Moisture-VM-Ash).

3.3.2 Elemental analysis

The elemental analysis was carried out using an elemental analyzer (2400 Series II CHNS/O Elemental Analyzer, PerkinElmer). In each run, around 0.15-0.30 mg of sample was put into the sampling subsystem. The weight percentages of C, H, and N in samples were measured, while the weight percentage of O was calculated by difference, that is, O (wt%) = 100-C–H–N.

3.3.3 Fiber analysis

In the fiber analysis, hemicellulose, cellulose, and lignin were examined by determining the neutral detergent fiber (NDF), acid detergent fiber (ADF), and acid detergent lignin (ADL) (Chen et al., 2010). In brief, the NDF was determined first, and followed by the ADF was examined. The extractives is obtained when the NDF was examined (Extractives =100- NDF) (Colin et al., 2017). From the results of NDF and ADF, hemicellulose could be obtained (hemicelluloses = NDF-ADF). Furthermore, the cellulose was acquired after the ADL treated by concentrated H_2SO_4 (cellulose = ADF-ADL). Eventually, the content of lignin was obtained once the ash was measured.

3.3.4 Thermogravimetric analysis

The pyrolysis characteristics of biomass samples were analyzed by a thermogravimetric analyzer (TG, SDT Q600 TGA, TA Instruments). In each run, around 5 mg of sample were loaded into an Al_2O_3 crucible, and then the crucible was sent into the TG furnace. The N_2 at a flow rate of 100 mL min^{-1} was used as the carrier gas. In TGA, the raw or biochar samples were heated from 50 °C at a heating rate of 20 °C min^{-1} to 105 °C, followed by keeping this temperature for 10 min to provide a dry-basis sample for the TGA. The samples were then heated from 105 °C to 800 °C at the heating rate of 20 °C min^{-1}.

The instantaneous weight of the sample in the course of analysis was detected and recorded at a frequency of 2 Hz. To ensure the quality of measurements and analyses, the temperature and weight in the TG were periodically calibrated using zinc (Zn), calibration weights, and sapphire glass, respectively.

3.3.5 Scanning electron microscope

The microstructures of all the samples (raw and treated samples) were examined by using a scanning electron microscope (SEM, Hitachi S-3000N). Before the analysis, the goal was coated on the wood sample by a sputter in order to increase the electrical conductivity of sample to have a better observation.

3.3.6 FTIR and XRD analyses

The chemical structures in untreated and treated wood samples were analyzed by means of a FTIR spectrometer (Spectrum 100, PerkinElmer) with the attenuated total reflection (ATR) and an X-ray diffractometer (D8 Discover with GADDS, Bruker AXS GmbH) with monochromatic Cu $K\alpha_{1+2}$ radiation (λ = 0.1542 nm). The FTIR spectra were recorded for the wavenumber in the region of 4000-650 cm^{-1}, and 16 scans were collected per run with a spectral resolution of 4 cm^{-1} at room temperature. In the XRD analysis, the samples were measured for the diffraction angle (2θ) between 7 and 40 °.with an exposure time of 300 s $frame^{-1}$.

3.3.7 Color measurement

In this study, the colors of the untreated and treated woods were measured by a colorimeter (Chroma meter CR-410, Konica Minolta) based on the three dimensional CIELAB color space, which has been adopted to quantify the color change of treated biomass (González-Peña Marcos & Hale Michael, 2009; Tooyserkani et al., 2013). In the CIELAB color space, the vertical coordinate for lightness L^* represents the position on the black-white axis (L^*=0 for total black and L^*=100 for pure white). The chromatic coordinates a* and b* are characterized by the position of horizontal plane. The chrome value of a^* stands for the position on the green-red axis (+a^* for red and -a^* for green), while the chrome value of b^* responds the position on the blue-yellow axis (+b^* for yellow and -b^* for blue) (Agudo et al., 2014). The total color difference ΔE^* is expressed by (Tooyserkani et al., 2013):

$$\Delta E^* = \sqrt{(L_2^* - L_1^*)^2 + (a_2^* - a_1^*)^2 + (b_2^* - b_1^*)^2} \quad \textbf{(3-2)}$$

where subscripts 1 and 2 represent raw and treated samples, respectively.

3.3.8 EMC and contact angle examinations

For the measurements of EMC and contact angle, the samples were cut to the dimensions of 20 mm × 20 mm × 20 mm. The sieved and cut wood samples were dried in an oven at 105

°C for 24 h to provide a dry basis for examinations. Prior to testing EMC, the dried block samples were placed in a humidity chamber at 25 °C with 55 % relative humidity until mass stabilization. The EMC is defined as follows:

$$\text{EMC}\ (\%) = \frac{m_{wet} - m_{dried}}{m_{dried}} \times 100 \qquad \textbf{(3-3)}$$

where m_{wet} is the weight of humidified wood and m_{dried} is the weight of dried wood. The measurement of the contact angle was based on the sessile drop method (Pétrissans et al., 2003) to observe the profile of a deposited drop on a solid surface (**Fig. 3-3**). The observation was performed using an optical contact angle apparatus, which consisted of a video measuring system and a high-resolution CCD camera (1/3'' CCD B/W Camera). A commercial software (FTA32) was connected with the system to measure and record the drop shape.

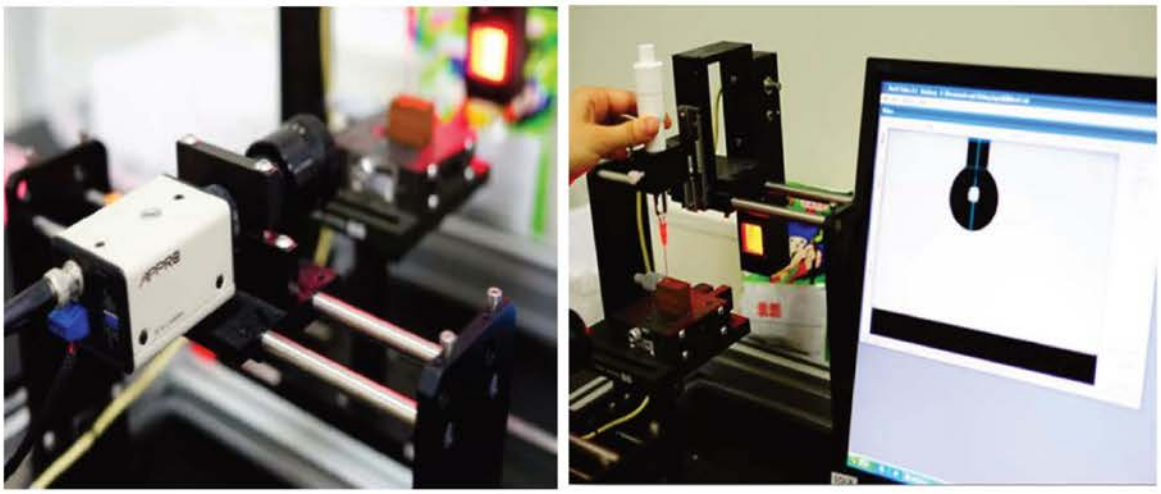

Fig. 3-3. Illustration of the sessile drop method.

3.4 Numerical modeling

3.4.1 Kinetic model

The two-step kinetic model developed by Di Blasi and Lanzetta (1997) is applied to obtain the kinetics of wood heat treatment in the pilot-scale reactor. The two-step reaction in series model is demonstrated in **Fig. 3-4**. The feedstock (raw material), denoted by "A", is converted to a solid intermediate B and volatiles V_1. The intermediate B further decomposes into solid residue C and volatiles V_2. At any moment, the mass of solid product is identified by the sum of masses of A, B, and C, while the total mass of volatiles is described by the sum of V_1 and V_2 (Bach et al., 2016; Bates & Ghoniem, 2012). The four reaction rate constants (k_1, k_{V1}, k_2, and k_{V2}) are determined by fitting predicted curves to dynamic mass loss curves from experiments.

Assuming that the two steps of the reactions are first order, the rate equations for solids (A, B, and C) and volatiles (V_1 and V_2) are expressed as (Bates & Ghoniem, 2012):

$$\frac{dm_A}{dt} = -m_A \times (k_1 + k_{v1}) \quad \textbf{(3-4)}$$

$$\frac{dm_B}{dt} = k_1 \times m_A - m_B \times (k_2 + k_{v2}) \quad \textbf{(3-5)}$$

$$\frac{dm_C}{dt} = k_2 \times m_B \quad \textbf{(3-6)}$$

$$\frac{dm_{V1}}{dt} = k_{v1} \times m_A \quad \textbf{(3-7)}$$

$$\frac{dm_{V2}}{dt} = k_{v2} \times m_B \quad \textbf{(3-8)}$$

In these equations, m_i is the mass of any pseudo-component (i= A, B, C, V_1, and V_2). The rate constants obey the Arrhenius law: $k_i(T) = A_i exp\left(\frac{-Ea_i}{RT}\right)$, in which A, Ea, R, and T are the pre-exponential factor (s^{-1}), the activation energy (J mol^{-1}), the universal gas constant (R=8.314 J K^{-1} mol^{-1}), and the absolute temperature (K), respectively. The formation of components can be obtained by integrating **Eqs. (3-4)-(3-8)** (Prins et al., 2006; Shang et al., 2014). The cumulative mass yield of the components can be calculated as a function of time,

from which the total solid proportion (Y_S)and the total volatiles yield (Y_V) are the sums of appropriate components, that is, $Y_S=Y_A+Y_B+Y_C$ and $Y_V=Y_{V1}+Y_{V2}$. Ys is the ratio between the mass of treated wood and untreated wood in dry basis.

A numerical approach using Matlab® is conducted to determine all kinetic parameters, and the numerical solid yield are obtained based on the kinetic parameters and temperature profiles from the experiments. The calculation flowchart is demonstrated in **Fig. 3-4**. In the beginning, it is assumed that the entire solid is A, without B and C. According to this assumption, the initial k_1, k_{V1}, k_2, k_{V2} are adopt from the literature (Bach et al., 2016). The numerical solver will determine the new solid yield from the new kinetic parameters after iteration, and obtain the most suitable results. The solver (function fminsearch of Matlab® software) is based on the Nelder-Mead optimization algorithm (Prins et al., 2006; Shang et al., 2014; Silveira et al., 2018), which is applied to minimize the root mean square of the difference between experimental and calculated solid yields, as expressed in the following:

$$diff^{(T)} = \sqrt{\sum_{t}\left(\frac{(Y_{s,j}^{(T)})_{exp} - (Y_{s,j}^{(T)})_{cal}}{(Y_{s,j}^{(T)})_{cal}}\right)^2} \quad \textbf{(3-9)}$$

where $(Y_{s,j}^{(T)})_{exp}$ and $(Y_{s,j}^{(T)})_{cal}$ are the experimental and calculated solid yield at the data point j and temperatures T. The temperatures applied for the kinetics calculation are corresponding to the temperatures of heating plates. In the developed model, both the isothermal and non-isothermal heating environments are taken into account. When the absolute difference of $diff^{(T)}$ value between two iterations is smaller than 10^{-4}, it is presumed that the calculation is convergent and thus the optimization is stopped**..**

The initial temperature for kinetic calculations began at 105 °C after drying to provide a basis of pyrolysis, and the entire process took 1,740 min. The measurements of temperature profiles of the heating plates as well as wood board's surface and center suggested that the temperature difference was smaller than 4 °C. This confirmed the temperature uniformity in

the samples. This implied, in turn, that the temperature gradient inside the wood board was negligible. The length (60 cm) and width (17 cm) of the wood boards were much greater than the thickness (2.2 cm), so the lateral heat transfer could be ignored. The wood boards could be conceived as homogeneous boards in terms of composition and temperature distribution. Consequently, the kinetic model could directly be applied to predict the thermal degradation dynamics of the heat treated wood in the pilot-scale reactor.

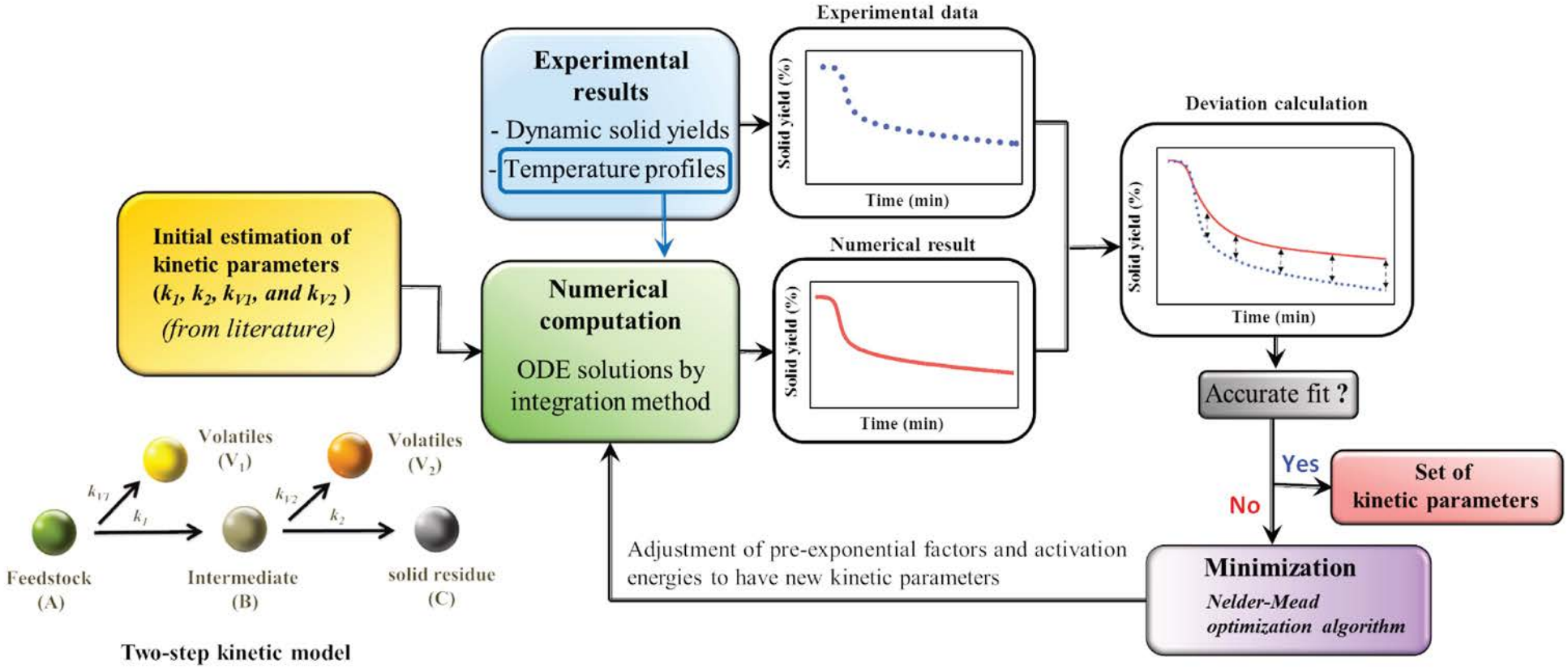

Fig. 3-4. A schematics of two-step kinetic model and calculation flowchart for the kinetics.

3.4.2 Elemental composition model

In this study, a direct method is conducted to predict the C, H and O contents based on the pseudo-components evolutions (A, B, and C) as well as the raw (initial) and treated wood (final) elemental analysis (Bach et al., 2016). In this model, the content of N in wood material is neglected because of very small amount (less than 1 wt%) and much lower than the other elements (Bach et al., 2016; Gul et al., 2017). The raw biomass is assumed to be composed only of C, H and O. The raw material ($t = 0$) and the treated wood ($t = \mathrm{f}$) yields can be written in terms of elemental composition as the following:

$$Y_A\ (t = 0) = Y_{A,0} \times C_{A\%} + Y_{A,0} \times H_{A\%} + Y_{A,0} \times O_{A\%} \quad \textbf{(3-10)}$$

$$Y_{cal,f}\ (t = f) = Y_{cal,f} \times C_{S\%} + Y_{cal,f} \times H_{S\%} + + Y_{cal,f} \times O_{S\%} \quad \textbf{(3-11)}$$

where $\mathrm{C_{A\%}}, H_{A\%},$ and $\mathrm{O_{A\%}}$ are based on the elemental analysis of the raw material, and $Y_A(t)$ is the mass yield evolution of A. Appling the simplification $Y_{cal,f} \times C_{S\%} = Y_{S,C}$ (subscript S designates total solid product) to the other elements (H and O), **Eq. (3-12)** assumes the form:

$$Y_{cal,f}\ (t = f) = Y_{S,C} + Y_{S,H} + Y_{S,O} \quad \textbf{(3-12)}$$

A linear system for the pseudo-component evolutions can be established for A, B and C:

$$Y_A(t) \times C_{A\%} + Y_B(t) \times C_{B\%} + Y_C(t) \times C_{C\%} = Y_{S,C} \quad \textbf{(3-13)}$$

$$Y_A(t) \times H_{A\%} + Y_B(t) \times H_{B\%} + Y_C(t) \times H_{C\%} = Y_{S,H} \quad \textbf{(3-14)}$$

$$Y_A(t) \times O_{A\%} + Y_B(t) \times O_{B\%} + Y_C(t) \times O_{C\%} = Y_{S,O} \quad \textbf{(3-15)}$$

Meanwhile, the elemental composition for each pseudo component must correspond to 100%:

$$C_{B\%} + H_{B\%} + O_{B\%} = 100 \quad \textbf{(3-16)}$$

$$C_{C\%} + H_{C\%} + O_{C\%} = 100 \quad \textbf{(3-17)}$$

According to **Eqs. (3-13)-(3-17)**, the elemental compositions ($C_{i\%}, H_{i\%},$ and $O_{i\%}$) of pseudo-components ($i = \mathrm{B}$ and C) can be obtained by the solver (function fmincon implemented in MATLAB® software) when the evolutions of Y_A, Y_B, and Y_C as well as the initial and final elemental composition of samples are known. With this procedure, the composition of the treated wood at any temperature and time can be obtained.

Chapter 4 Results and Discussion

In this chapter, the results from the first part, wood heat treatment under industrial conditions, the second part, property changes of heat treated wood, and the third part, kinetic modeling of wood heat treatment, are described in detail in **section 4.1**, **4.2** and **4.3**, respectively.

4.1 Thermal behavior of wood heat treated under industrial conditions

4.1.1 Mass loss dynamics during heat treatment

The distributions of mass loss are presented in **Fig. 4-1a** and **4-2a** to evaluate the thermal degradation dynamics of the woods during treatment. In order to identify the intensity of thermal degradation, an index called differential mass loss (*DML*) is introduced and expressed as $DML=dML/dt$ where *ML* is the mass loss (%) of wood boards during treatment and t is the treatment time. The profiles of *DML* are also plotted in **Fig. 4-1b** and **4-2b**. Wood species are made up of hemicelluloses (11-36 wt%), cellulose (39-54 wt%), and lignin (17-30 wt%) (Wang et al., 2017). The curves shown in **Fig. 4-1** and **4-2** suggest that the entire heat treatment process can be divided into four stages. In the first stage (50-103 °C), called drying process, the weight loss of the woods is a consequence of water removal (Chen & Kuo, 2010). In the present study, the wood boards have been dried prior to heat treatment. This is the reason why there is no significant mass loss in this stage. In the second stage (103-175 °C), the devolatilization of light volatile matters and the removal of extractives inside the wood occur (Chaouch et al., 2010; Chen & Kuo, 2010). However, it can be observed that the mass loss, ranging from 0.21 to 0.52 %, and *DML* peaks are not pronounced.

Some studies have pointed out that the thermal degradation of wood started at temperatures of 180-200 °C (Candelier et al., 2016; Esteves & Pereira, 2008). In **Fig. 4-1b** and **4-2b**, *DML* curves depict that the degradation of the woods starts at around 175-180 °C, and the end of main degradation is close to 1800 min. Consequently, the third stage is defined from 175 °C to 1800 min, which constitutes the main thermal degradation process. The maximum

decomposition rates of poplar in this stage are in the range of 0.014-0.050 % min^{-1} at temperatures of 200-230 °C, while those of fir are in the range of 0.0057-0.029 % min^{-1}. These results reflect that intensity of thermal degradation of poplar is greater than that of fir. Dehydration, deacetylation, depolymerization, and oxidation of the wood materials take place in this stage, mainly due to the decomposition of hemicelluloses (Collard & Blin, 2014; Esteves & Pereira, 2008). Compared to cellulose and lignin, hemicelluloses are the easiest components to be decomposed during heat treatment. The degradation starts by deacetylation where the acetyl groups (-$COCH_3$) of hemicelluloses are broken and acetic acid is generated. After deacetylation, the produced acetic acid is regarded as a catalyst of depolymerization which further increases the decomposition of polysaccharides (Collard & Blin, 2014; Esteves & Pereira, 2008). The acid catalyzed degradation leads to the formation of formaldehyde, furfural, and aldehydes. At the same time, the dehydration of hemicelluloses progresses, decreasing the number of hydroxyl groups (Candelier et al., 2013c; Chaouch et al., 2010).

The significant difference of thermal sensitivity between poplar and fir is mainly due to different hemicelluloses compositions in hardwood (poplar) and softwood (fir). In hardwood species, the major components of hemicelluloses are glucuronoxylan (15-30 wt%) and glucomannan (2-5 wt%), whereas they are galacto- glucomannan (5-8 wt%), glucomannan (10-15 wt%), and arabino-glucuronoxylan (7-10 wt%) (Pettersen, 1984; Zhou et al., 2017) in softwood species. The higher thermal sensitivity of hardwoods compared to softwoods is attributed to their higher content in acetyl groups from acetylated glucuronoxylan, which leads to the formation of considerable amounts of acetic acid. Furthermore, the high liberation of acetic acid accelerates the thermal degradation of woods (Chaouch et al., 2010). The fourth stage is located between 1800 min of treatment to the end of the process where low level and oscillating *DML* curves are exhibited. This is attributed to the continuous and slow weight loss of carbonaceous matters in the wood (Chen & Kuo, 2010).

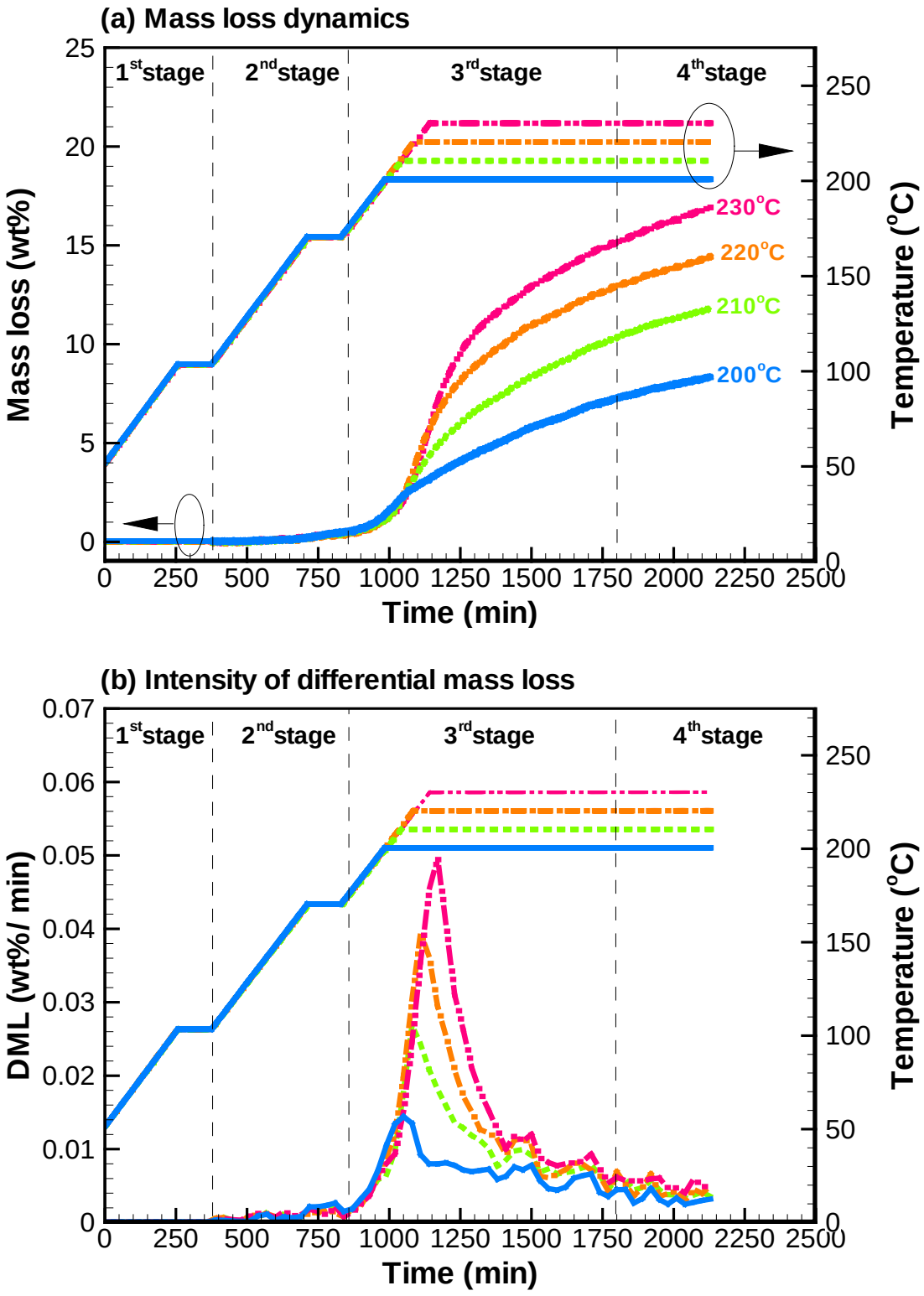

Fig. 4-1. Profiles of (a) mass loss dynamics, and (b)intensity of differential mass loss (*DML*) during heat treatment of poplar.

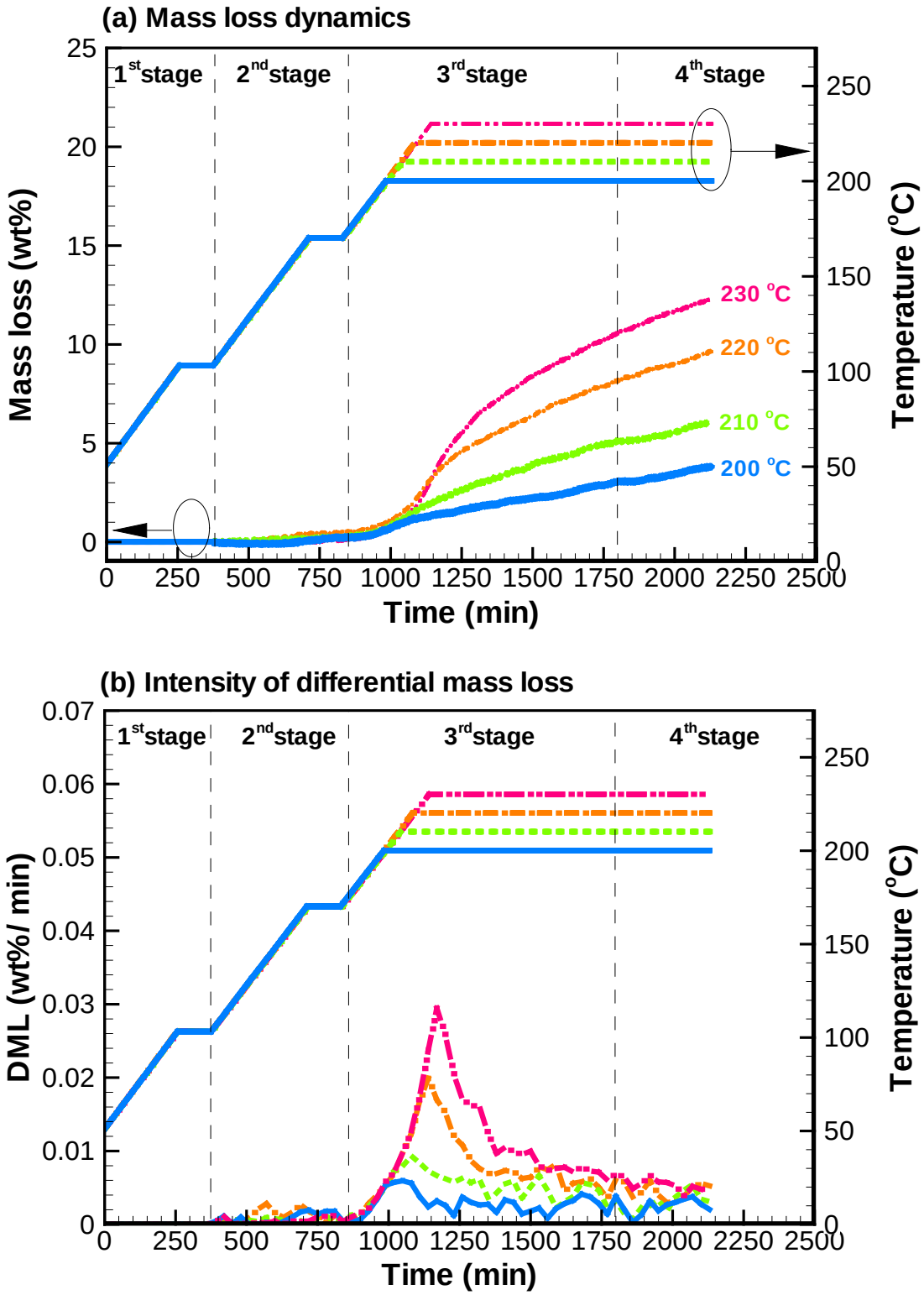

Fig. 4-2. Profiles of (a) mass loss dynamics, and (b) intensity of differential mass loss (*DML*) during heat treatment of fir.

4.1.2 Thermogravimetric analysis of treated wood

Thermogravimetric analysis as well as derivative thermogravimetric (DTG) and second derivative thermogravimetric (2nd DTG) analyses of untreated and treated poplar and fir are displayed in **Fig. 4-3** and **Fig. 4-4,** respectively. The TGA curves (**Fig. 4-3a** and **Fig. 4-4a**) reveal that the thermal degradation of the woods mainly occurs at temperatures of 200-400 °C, while the DTG curves (**Fig. 4-3b** and **Fig. 4-4b**) indicate that the maximum degradation rates of untreated poplar and fir occur at 361 and 372 °C, respectively. These peaks are attributed to the thermal decomposition of cellulose (Chen & Kuo, 2010). For the untreated poplar and fir, shoulders before the cellulose peaks, corresponding to the thermal degradation of hemicelluloses, can be observed. The curves behind the peaks account for the pyrolysis of lignin whose levels are by far smaller than those of the shoulders and peaks. When the temperature is higher than around 600 °C, the curves are nearly characterized by a flat region and approach zero, implying that lignin is almost completely depleted.

Though the shoulders stemming from the hemicellulose decomposition are observed, it is difficult to point out their exact locations. The 2nd DTG analysis can be used to identify the shoulder (Grønli et al., 2002). According to the 2nd DTG curves shown in **Fig. 4-3c** and **Fig. 4-4c**, two upward peaks and one downward peak are found in the curves of the untreated poplar and fir as well as the fir treated at 200 and 210 °C. The temperatures of shoulders are identified at the trough between the two upward peaks. The shoulder temperatures of the untreated poplar and fir are 315 and 329°C, respectively. These observations are consistent with the study of Chen et al. (2015c) where it was reported that the thermal decomposition of hemicelluloses mainly occurred in the temperature range of 200-315 °C, whereas the decomposition temperature of cellulose was between 315 and 400 °C. Lignin decomposed over a large temperature range of 160-900 °C, with a higher decomposition rate between approximately 360 and 400 °C (Chen et al., 2015c). For the treated poplar and the fir treated at 220 and 230 °C, the 2nd DTG curves just have an upward peak. This reflects that hemicelluloses in these

samples have been destroyed severely during the heat treatment. Based on the obtained results, the DTG and 2nd DTG curves are able to provide a strong evidence to show the profound impact of heat treatment upon hemicellulose structure.

The peaks of the treated biomass materials are higher than those of the untreated counterparts (**Fig. 4-3b and 4-4b**), regardless of the temperature, whereas their width decreases after treatment. This can be explained by the degradation of amorphous cellulose after treatment (Esteves & Pereira, 2008) where the reactivity of the amorphous cellulose is higher than that of crystalline one, resulting from lower cohesive energy density (Mazeau & Heux, 2003). The DTG curves corresponding to lignin degradation increases slightly with increasing treatment temperature, as a consequence of relatively more lignin retained after treatment. This behavior was also observed in other works (Candelier et al., 2013c). Yildiz et al. (2006) underlined that the relative mass proportion of lignin increased when the treatment temperature and time increased, whereas the mass proportions of carbohydrates were lessened.

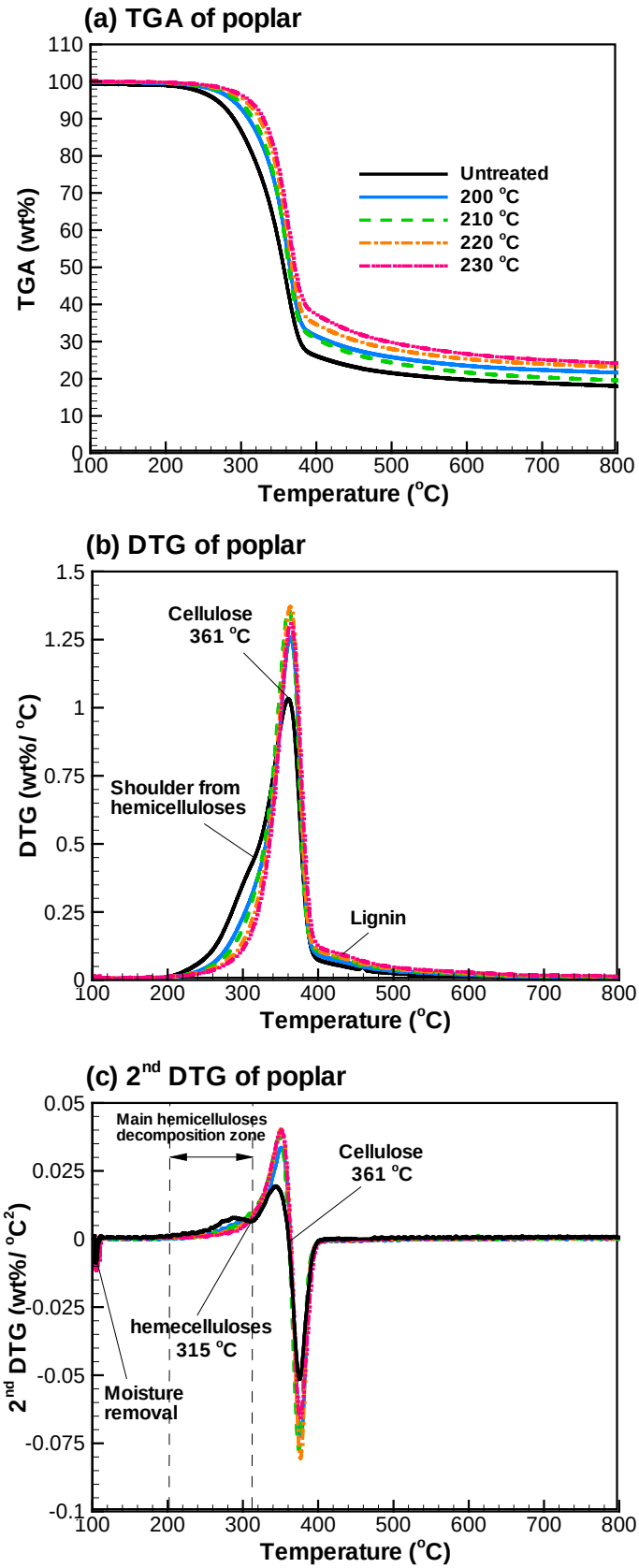

Fig. 4-3. Distribution of (a) TGA and (b) DTG and (c) 2nd DTG of poplar before and after treatment.

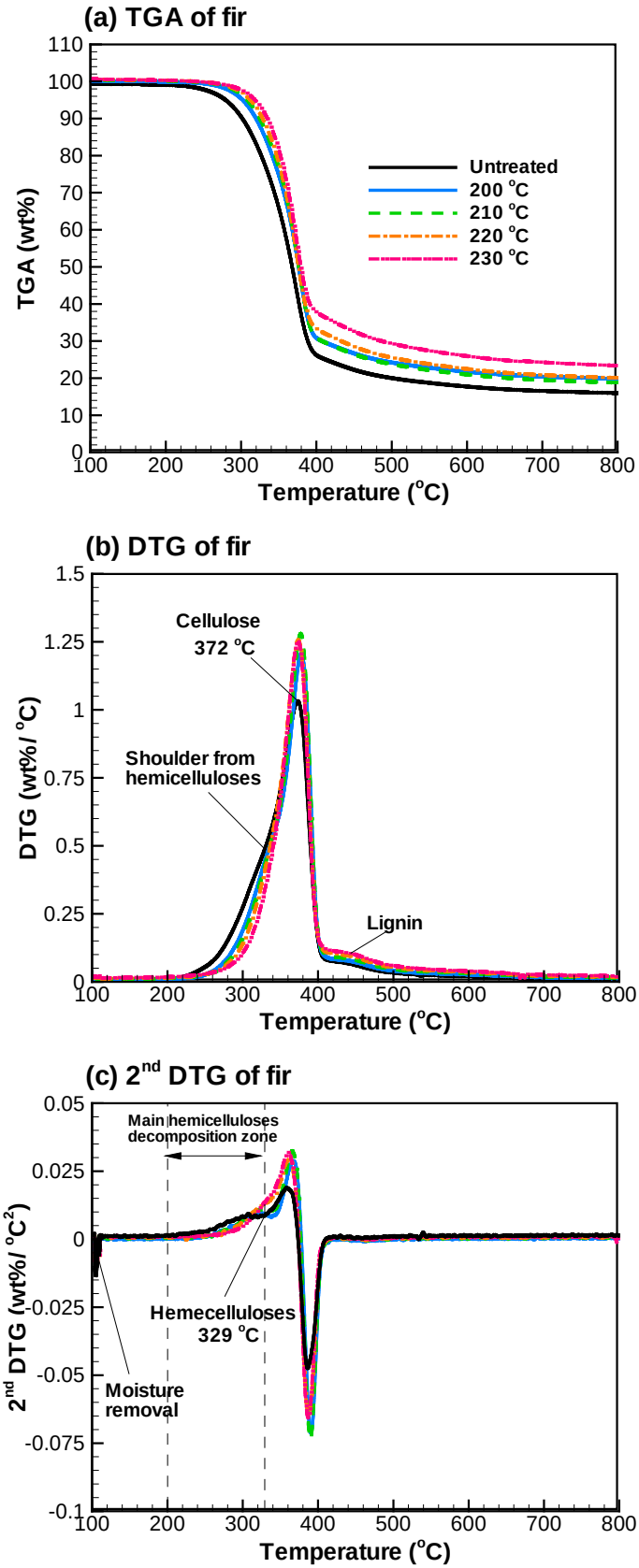

Fig. 4-4. Distribution of (a) TGA and (b) DTG and (c) 2nd DTG of poplar before and after treatment.

4.1.3 SEM of treated wood

In order to provide a deeper insight into the impact of heat treatment upon wood structure, the SEM is applied to observe the surface morphology of the raw and torrefied woods. The SEM images of the samples at a 1000 magnification are shown in **Fig. 4-5 and Fig. 4-6**. In the poplar (**Fig. 4-5**), the well-defined porous ovals are observed in raw material (Granados et al., 2017). When the treatment temperature is higher, the ovals start to crack. The damaged fibre structure is also observed. For the treatment temperature of 230 °C, the ovals are significantly destroyed, attributing to the severe degradation. For the raw fir (**Fig. 4-6**), a homogeneous fibrillary organization in the external surface with tiny pores can be observed. After heat treatment, the cell-wall structures are characterized by bigger and destroyed pores, elucidating the profound collapse of the cell walls. This is assigned to the release of VM, namely, the devolatilization mechanism, in the course of heat treatment (Ramos-Carmona et al., 2018). The change in the surface morphology of the wood materials from wood heat treatment such as destroyed cell walls and increased porosity can decrease the mechanical properties. However, the improvement of their grindability and the reactivity can be applied in solid-gas reactions for energy production, such as gasification and combustion (Chen et al., 2011; Ramos-Carmona et al., 2018).

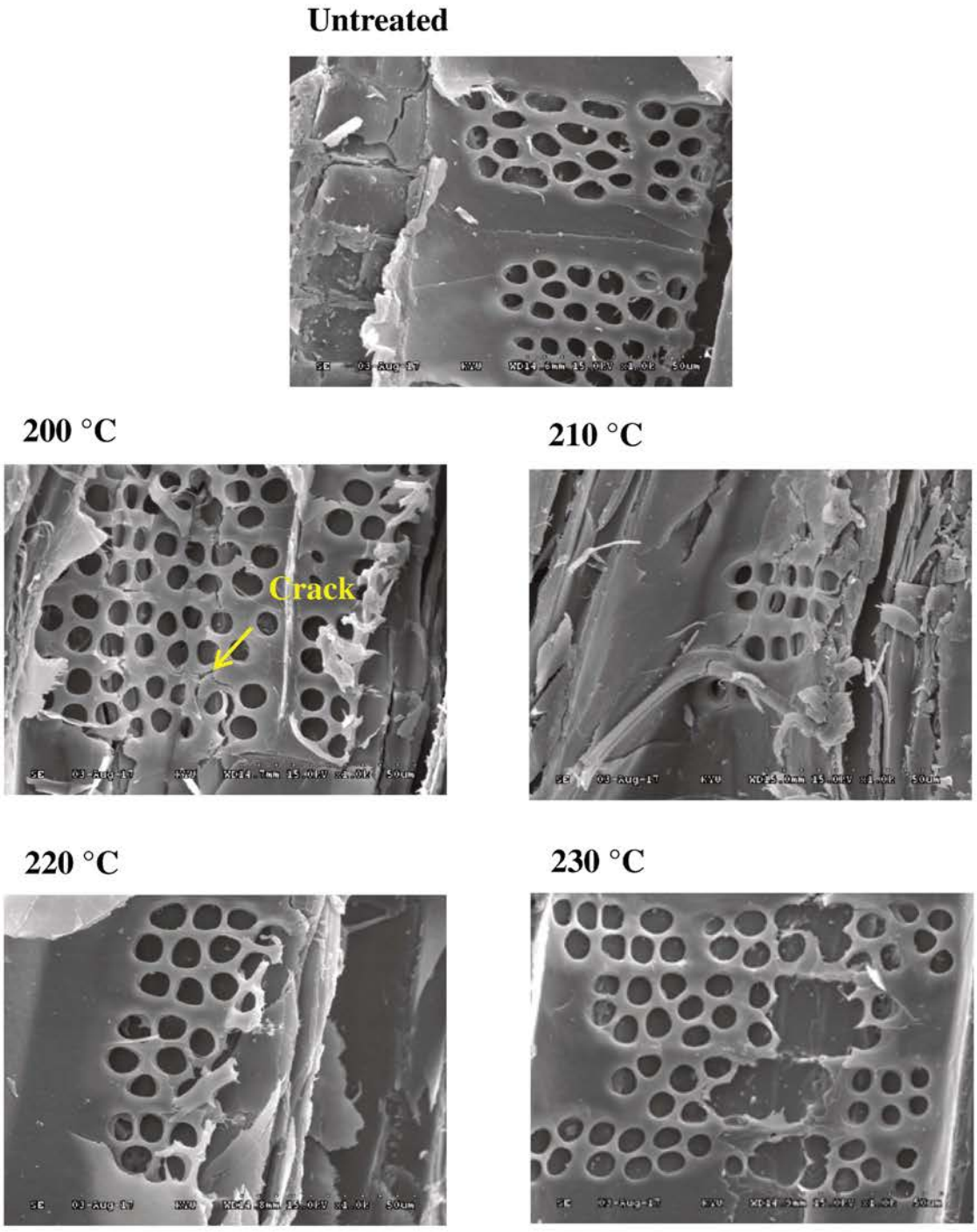

Fig. 4-5. SEM images (1000X magnification)of poplar before and after heat treatment.

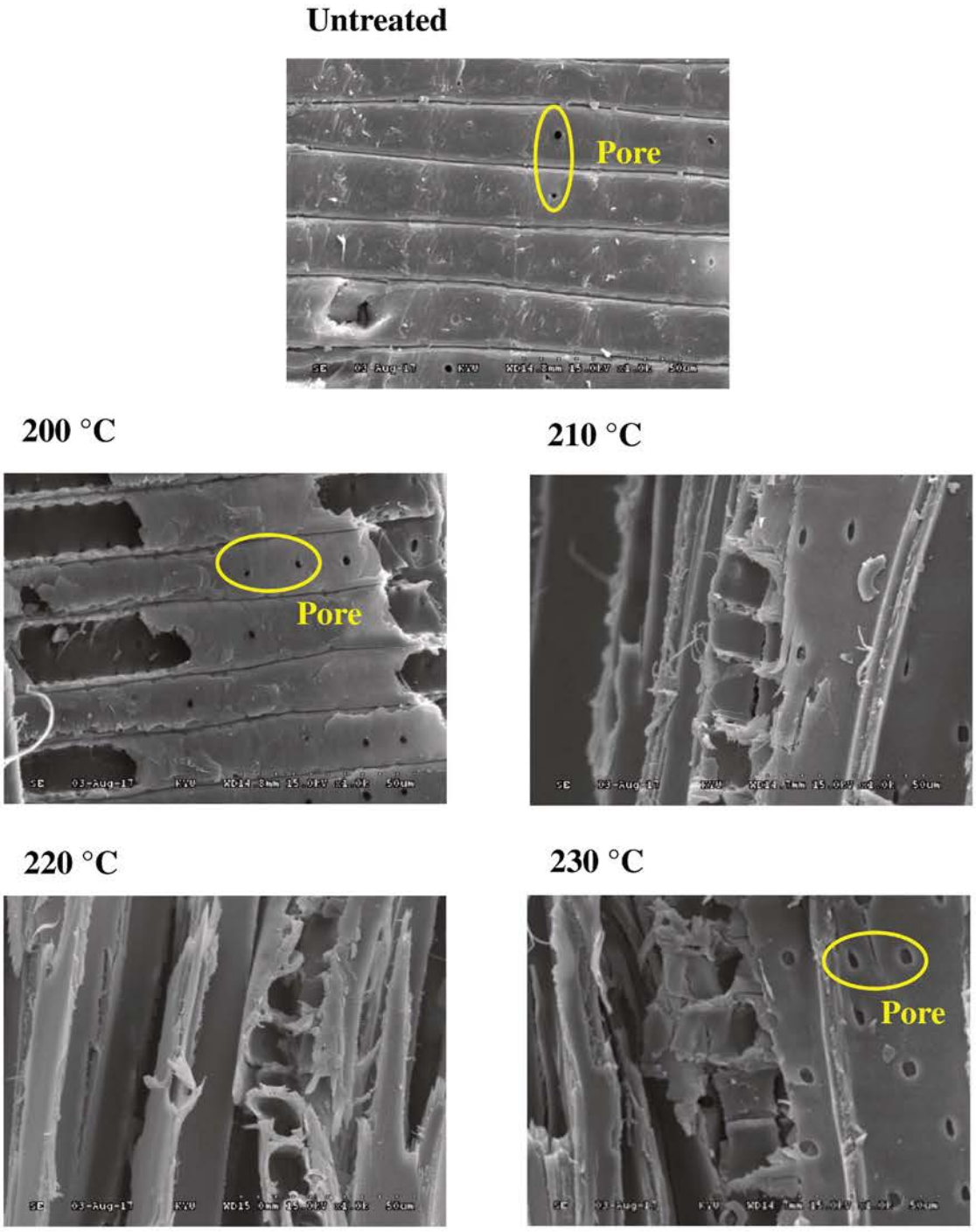

Fig. 4-6. SEM images (1000X magnification) of fir before and after heat treatment.

.

4.1.4 Proximate and elemental analyses of treated wood

The proximate and elemental analyses of untreated and treated woods are tabulated in **Table 4-1**. The results indicate that the volatile matter (*VM*) in the samples decreases after heat treatment, whereas the fixed carbon (*FC*) increases, resulting from the devolatilization reaction during treatment (Chen et al., 2015c). In regard to the elemental analysis, the carbon content increases dramatically with increasing treatment severity. This arises from the fact that carbonaceous materials are formed during heat treatment due to thermal reticulation reactions (Chaouch et al., 2013).

The results of elemental analysis indicate that the carbon content of treated wood increases significantly with increasing temperature, while hydrogen and oxygen contents decrease. The observation is consistent with other related literature. Šušteršic et al. (2010) investigated the heat treatment of pine wood at the temperature of 220-250 °C. The carbon content increased from 49.5 to 54.6 wt%. In contrast, the contents of hydrogen and oxygen decreased after treatment, and they were in the range of 5.7-6.0 wt% and 39.9-43.7 wt%, respectively. Furthermore, based on the weight percentage of C, H, and O of wood samples, the atomic H/C and O/C ratios have been calculated. The atomic H/C ratios of the two raw materials are approximately 1.63, and their atomic O/C ratios range from 0.73 to 0.75. It is found that the O/C ratio of untreated poplar is higher than that of untreated fir. This is attributed to the lignin of hardwood species with higher syringyl content compared to softwood species, which contain mainly guaiacyl units (Chaouch et al., 2013). When the wood materials undergo heat treatment, the atomic H/C and O/C ratios are in the ranges of 1.35 - 1.53 and 0.59-0.70, respectively. The van Krevelen diagram for the woody biomass species from literature and this study is demonstrated in **Fig. 4-7** (Chaouch et al., 2013; Chen et al., 2015c)

Table 4-1. Proximate analysis and elemental analysis of untreated and heat treated woods.

Wood sample	Mass loss (%)	Proximate analysis (wt%, db [a])			Elemental analysis (wt%, daf [b])				Atomic O/C ratio	Atomic H/C ratio
		VM	FC	Ash	C	H	N	O [c]		
Poplar										
Untreated	0	84.74	14.70	0.56	46.61	6.32	0.28	46.79	0.75	1.63
200 °C	8.27	81.40	18.04	0.57	49.44	6.27	0.28	44.01	0.67	1.52
210 °C	11.75	79.59	19.68	0.73	50.54	6.12	0.36	42.98	0.64	1.45
220 °C	14.39	78.27	20.93	0.80	51.02	5.95	0.38	42.65	0.63	1.40
230 °C	16.92	76.46	22.70	0.84	52.25	5.88	0.45	41.42	0.59	1.35
Fir										
Untreated	0	85.53	14.28	0.19	47.16	6.41	0.23	46.20	0.73	1.63
200 °C	3.82	83.31	16.49	0.20	48.36	6.17	0.24	45.23	0.70	1.53
210 °C	6.08	82.59	17.18	0.23	49.35	6.05	0.27	44.33	0.67	1.47
220 °C	9.64	80.88	18.87	0.24	50.73	5.98	0.34	42.95	0.63	1.41
230 °C	12.29	79.72	20.03	0.25	51.83	5.94	0.38	41.86	0.61	1.38

[a]: dry basis; [b]: dry-ash-free; [c]: by difference.

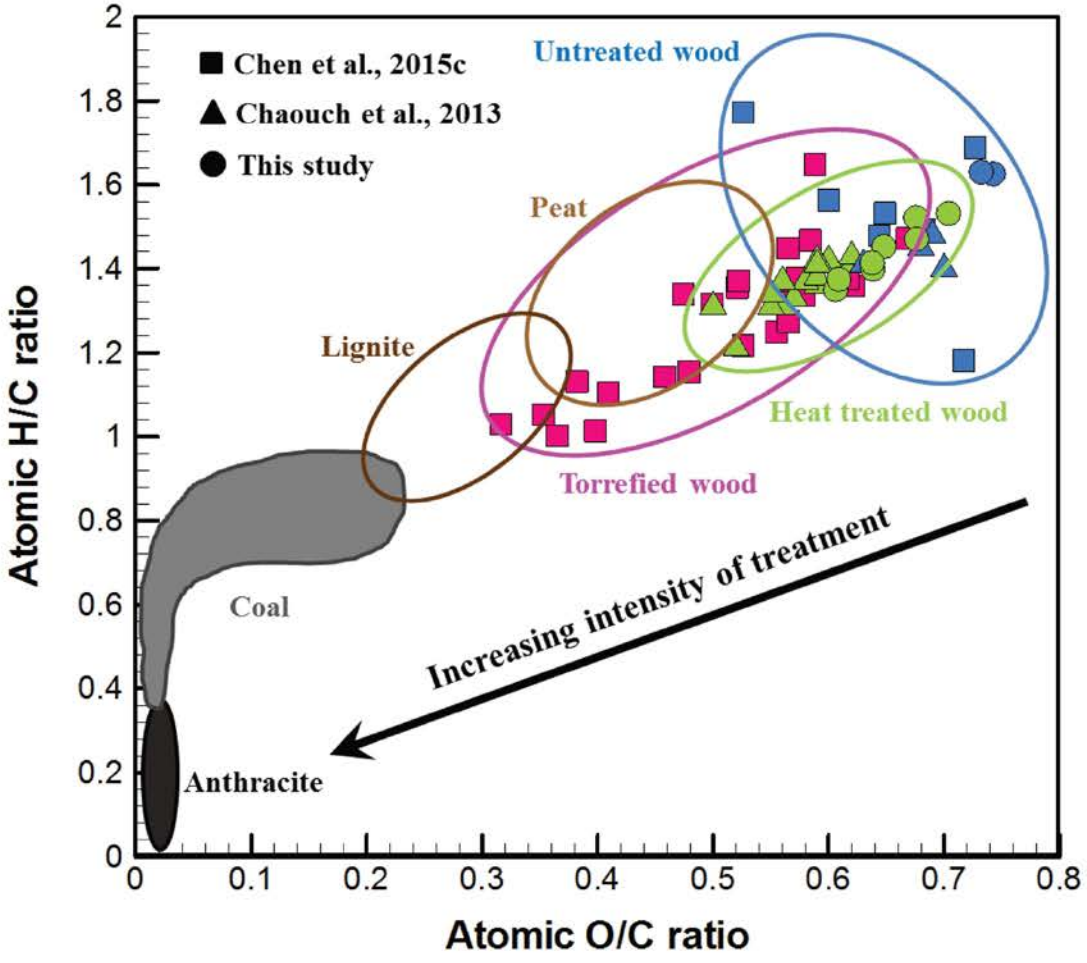

Fig. 4-7. The plots of van Krevelen diagram of woody biomass species

According to the results in **Table 4-1**, the linear regressions of atomic H/C ratio, atomic O/C ratio, and devolatilization index (*DI*) with respect to mass loss are shown in **Fig. 4-8** where their coefficients of determination (i.e., R^2) are also given. The *DI* is expressed as

$$DI = \frac{VM_{untreated} - VM_{treated}}{VM_{untreated}} \quad \textbf{(4-1)}$$

where $VM_{untreated}$ and $VM_{treated}$ designate the weight percentages of *VM* in untreated and treated woods, respectively. As a whole, the three quantities are correlated well by mass loss in that the value of R^2 is in the range of 0.980-0.997, yielding strong correlations. The slopes

of fir in **Figs. 4-8a** and **Fig. 4-8b** are steeper than those of poplar. This implies, in turn, that the extents of dehydrogenation and deoxygenation in fir (softwood species) undergoing heat treatment are stronger than those in poplar (hardwood species). Similar results have been observed in other studies (Chaouch et al., 2013). It arises mainly because of the stronger dehydration and removal of methoxyl groups from lignin condensation and stronger deoxygenation from hemicelluloses degradation in softwood species during treatment (Chen et al., 2015a; Wang et al., 2017; Wikberg & Liisa Maunu, 2004), despite lower thermal sensitivity of softwood species.

The regression lines of *DI* of versus mass loss displayed in **Fig. 4-8c** are close to each other. Based on this characteristic, the *DI* of seven different wood species (Norway spruce, beech, pitch pine, pine, eucalyptus, poplar, and fir) versus different thermal treatment severity or mass loss, due to altered treatment time, heating rate, temperature, or atmosphere from the literature (Broström et al., 2012; Chen et al., 2015c; Li et al., 2016; Na et al., 2015; Park et al., 2012; Wang et al., 2018a) and this study are plotted in **Fig. 4-9**.

It is apparent that the profile is characterized by a strong linear correlation inasmuch as R^2 is equal to 0.9232. The correlation can be rearranged as:

$$ML\ (\%) = \frac{DI + 0.0261}{0.0076} \qquad \textbf{(4-2)}$$

Furthermore, based on the mass loss level, the plot of *DI* versus mass loss can be partitioned into 3 different zones: (1) wood heat treatment and light torrefaction for mass loss below 15 %, (2) mild and severe torrefaction for mass loss between 15 and 40 %, and (3) carbonization for mass loss beyond 40 %. The experimental data in the 1st zone is characterized by a strongly linear distribution. In contrast, the points in the 3rd zone are relatively more scattered, as a result of severer degradation and more complicated reactions with large amounts of intermediates produced during carbonization (Lohri et al., 2016). It should be addressed that this linear correlation covers different operating atmospheres (i.e., N_2, air, and vacuum). In Europe, wood heat treatment is normally controlled at a mass loss of 8-10 %.

In practice, treated woods can be sampled and analyzed from proximate analysis to identify their values of the *DI*. Then, the mass loss can be estimated easily from the correlation. It is thus concluded that the correlation provides a simple tool to evaluate the performance of wood heat treatment.

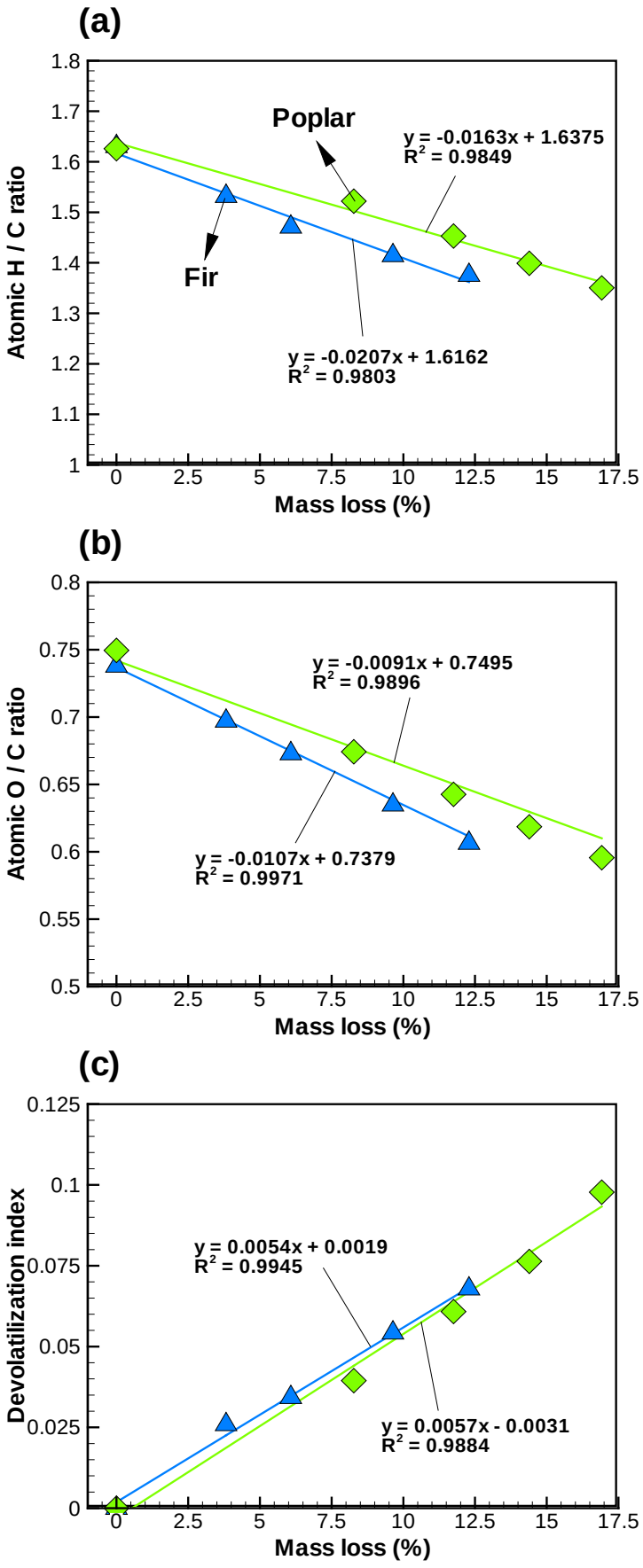

Fig. 4-8. Profiles and linear regressions of mass loss versus (a) atomic H/C ratio, (b) atomic O/C ratio, and (c) devolatilization index.

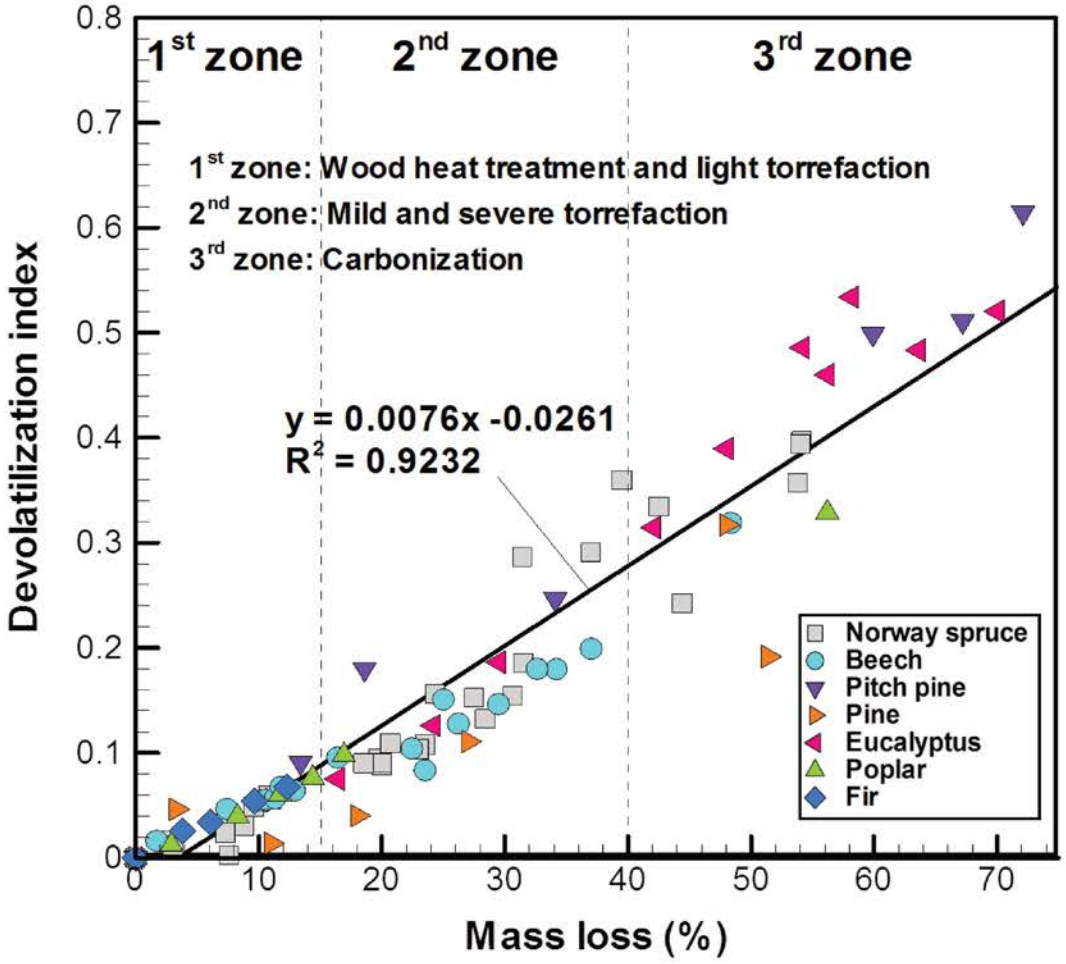

Fig. 4-9. Profile and linear regression of mass loss versus devolatilization index from various wood species with different thermal intensities of treatment.

4.2 Property changes of heat treated wood

4.2.1 Changes of chemical structure

The chemical structures in untreated and treated wood samples were evaluated by means of a FTIR spectrometer an X-ray diffractometer. In the FTIR spectra of wood materials, the absorption bands are normally in the region of 800-1800 cm^{-1} (Lin et al., 2018). **Fig. 4-10** shows the FTIR spectra of poplar and fir before and after treatment. Meanwhile, the remarks and band assignment of the FTIR spectra are summarized in **Table 4-2**. The absorption bands at

1730-1740 cm^{-1}, attributed to C=O stretching vibrations of acetyl, carbonyl and carboxyl groups, decrease with increasing treatment temperature. This is due to the cleavage of acetyl side chains from hemicelluloses after treatment (Emmanuel et al., 2015; Özgenç et al., 2017). A decrease in the absorption band at 1663 cm^{-1}, assigned to conjugated C=O in quinines coupled with C-O stretching of various groups, is due to: (1) deacetylation reactions from hemicelluloses, leading to the release of acetic acid, which further catalyzes depolymerization of less ordered carbohydrates, and (2) lignin condensation and degradation reactions (Özgenç et al., 2017; Popescu et al., 2013) during heat treatment. The removal of acetyl groups can also be evidenced by the decrease of the intensity at the absorption bands of 1263-1269 cm^{-1} and 1240-1245 cm^{-1}, which stem from to C-O stretching vibration of Ph-O-C (Ph: p-hydroxyphenyl) coupled with aromatic ring vibration in lignin, C-O stretching vibration of xyloglucan in hemicellulose (Emmanuel et al., 2015; Popescu et al., 2013).

The absorption bands at 1594-1597, 1507-1514, 1452-1459, and 1421-1427 cm^{-1} are considered as the characteristic bands of C=C stretching of the aromatic skeletal vibrations, representing the change of lignin in wood materials(Özgenç et al., 2017; Popescu et al., 2013). The intensity of absorption bands at 1594-1597 cm^{-1} increases after treatment, and a gradual overlapping of characteristic bands in the range of 1421-1514 cm^{-1} at higher temperatures ($\geq$ 220 °C) can be observed. These changes are owing to the condensation from the cleavage of β-O-4 linkages, and the splitting of aliphatic side chains in lignin during treatment (Emmanuel et al., 2015; Popescu et al., 2013). The absorption bands at 1368-1370 cm^{-1} represent lignin carbohydrate complexes, which mainly are $-CH_3$ (lignin) and $-CH_2$ (carbohydrates) groups (Popescu et al., 2013; Zheng et al., 2015). The bands at 1319-1333 cm^{-1} demonstrates the presence of phenol groups and syringyl and guaiacyl rings (Hakkou et al., 2006; Özgenç et al., 2017). The intensity of 1368-1370 cm^{-1} and 1319-1333 cm^{-1} decreases with increasing treatment temperature, resulting from the stronger degradation of wood. The bands at 1203-1210 and 1104-1113 cm^{-1} are assigned to glucose ring stretching vibration, C-O-C bridges stretching

vibrations, C-O stretching vibrations in cellulose and hemicelluloses, and OH- bending and association in cellulose (Esteves et al., 2013; Popescu et al., 2013). Their intensity increases with increasing treatment temperature. It has been reported (Özgenç et al., 2017; Popescu et al., 2013) that the increasing intensity in these bands can be regarded as a consequence of increase in the relative crystallinity of cellulose, which is due to the cleavage and dehydration of amorphous carbohydrates in cellulose. It is thus figured out that the amorphous part in cellulose is significantly affected with increasing intensity of heat treatment.

There is an obvious absorption band in the range of 1032-1051cm^{-1} in the spectra of poplar and fir, and the intensity decreases drastically with increasing treatment temperature. It is an overlap between cellulose and lignin, and these bands are attributed to symmetric C-O-C stretching of dialkyl ethers, C-O ester stretching vibrations in methoxy groups, C=O deformation in cellulose, aromatic C-H deformation in lignin, and β-O-4 linkages in lignin (Emmanuel et al., 2015; Özgenç et al., 2017; Zheng et al., 2015). The bands located at 895-897 and 807-809 cm^{-1} in the fingerprint region display a slight reduction in intensity after treatment, and they are assigned to C-H out-of-plane bending vibration in lignin, and C-H out-of-plane distortion in cellulose and hemicelluloses (Özgenç et al., 2017; Zheng et al., 2015). The reduction in intensity can be explained by releasing organic acids during heat treatment, which further promotes the hydrolysis of hemicellulose and cellulose chains (Özgenç et al., 2017).

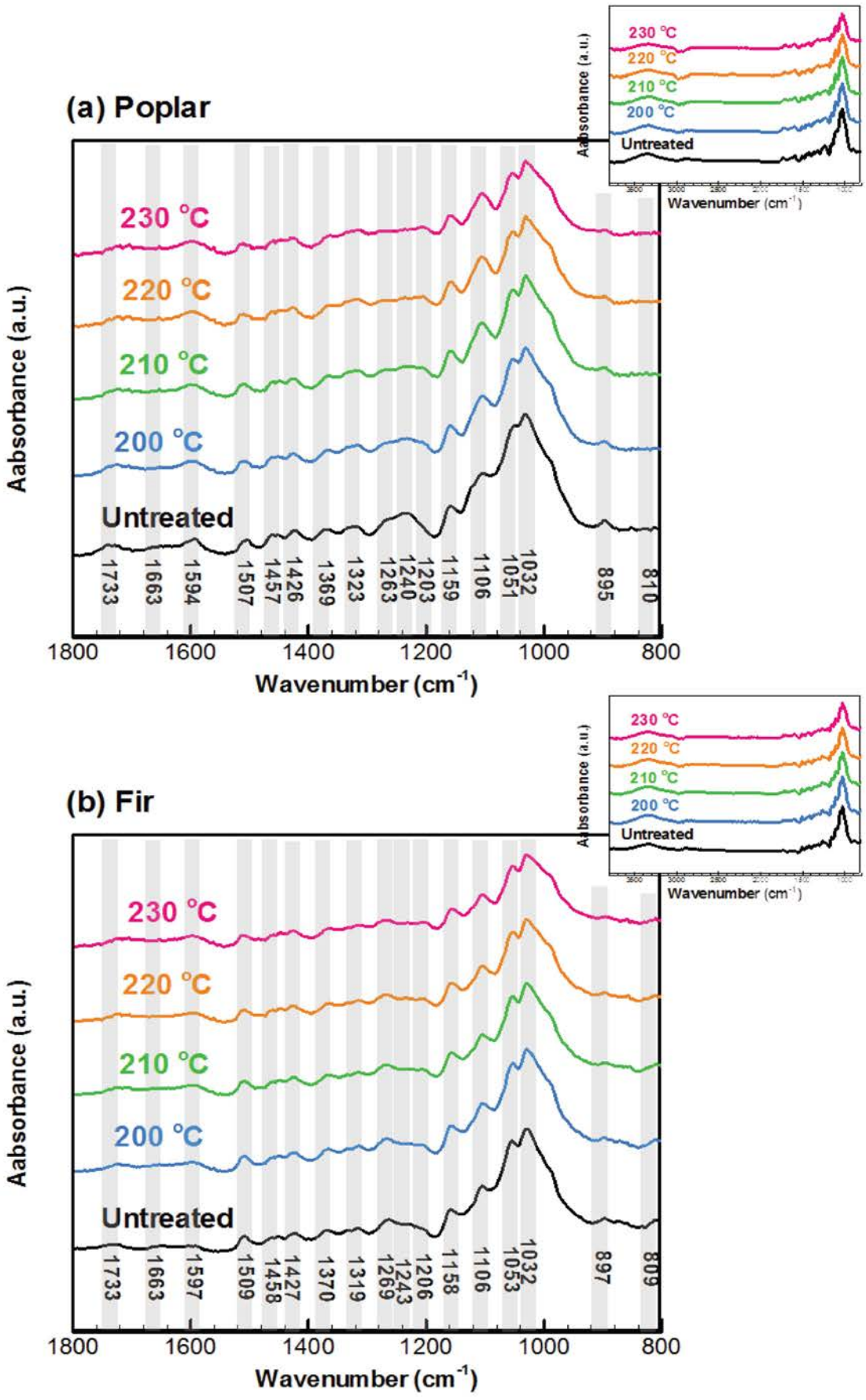

Fig. 4-10. FTIR spectra of untreated and treated wood: (a) poplar and (b) fir.

Table 4-2. Main bands of FTIR in wood materials and assignment.

Wave number (cm^{-1})	Remarks and band assignment
3200-3500	O-H stretching of water, alcohols, phenols, acids (Emmanuel et al., 2015)
2970-2850	C-H stretching (Esteves et al., 2013)
1730-1740	C=O carbonyl band, C-O stretching vibrations of acetyl groups of galactoglucomannan, carboxyl- and aldehydes, aromatic/conjugated aldehydes and esters (Emmanuel et al., 2015; Hakkou et al., 2006; Özgenç et al., 2017)
1663	Conjugated C-O in quinines coupled with C=O stretching of various groups (Popescu et al., 2013)
1650-1655	C=O stretching of the aromatic structures, absorbed water (Özgenç et al., 2017; Popescu et al., 2013)
1594-1597	C=C stretching of aromatic skeletal in lignin (Popescu et al., 2013; Zheng et al., 2015)
1507-1514	C=C stretching of aromatic skeletal in lignin (Özgenç et al., 2017; Popescu et al., 2013)
1452-1459	C=C and C-H bond, extractives, O-H in plane deformation, and CH_3 asymmetric bending in lignin (Özgenç et al., 2017; Popescu et al., 2013)
1421-1427	Aromatic skeletal vibrations in lignin, C-H deformation in lignin, CH_2 bending deformation in cellulose, and carbohydrates (Özgenç et al., 2017; Popescu et al., 2013)
1368-1370	C-H bending, -CH_3 in lignin, -CH_2 in carbohydrates, lignin-carbohydrate complexes bonds (Özgenç et al., 2017; Popescu et al., 2013)
1319-1333	C-H vibration in cellulose, and C-O vibration in syringyl derivatives-condensed structures in lignin, phenol group, and OH in plane bending in cellulose (Özgenç et al., 2017; Popescu et al., 2013)
1263-1269	C-O stretching in lignin (Lin et al., 2018)
1240-1245	C-O stretching vibration of Ph-O-C coupled with aromatic ring vibration in lignin, C-O stretching vibration in xyloglucan (Özgenç et al., 2017; Popescu et al., 2013)
1203-1210	C-O-C stretching vibration in cellulose and hemicelluloses, and OH-bending in cellulose (Özgenç et al., 2017; Popescu et al., 2013)
1155-1163	C-O-C stretching vibration in cellulose and hemicelluloses (Emmanuel et al., 2015; Popescu et al., 2013)
1104–1113	Glucose ring stretching vibration, OH association in cellulose (Özgenç et al., 2017; Popescu et al., 2013)
1023-1051	Symmetric C-O-C stretching of dialkyl ethers, C-O ester stretching vibrations in methoxyl groups, C=O deformation in cellulose, aromatic C-H deformation in lignin,

	and β-O-4 linkages in lignin (Özgenç et al., 2017; Popescu et al., 2013)
895-897	Aromatic C-H out-of-plane deformation in cellulose and hemicelluloses (Özgenç et al., 2017; Popescu et al., 2013)
807-810	Mainly vibration of mannan and C-H out-of-plane bending vibration in lignin, and guaiacyl lignin (Emmanuel et al., 2015; Özgenç et al., 2017; Zheng et al., 2015)

For wood materials, only a part of cellulose is crystalline, whereas hemicellulose and lignin are non-crystalline. The simplified cellulose microfibrils structure is illustrated in **Fig. 4-11** (Himmel et al., 2007; Poletto et al., 2012). The typically crystallographic planes from native cellulose structure have been identified by $(1\bar{1}0)$, (110), and (200), and their corresponding diffraction angles (2θ) from X-ray diffraction (XRD) are at 14.80-15.30°, 16.20-16.30°, and 21.90-22.20°, respectively. Alternatively, the 2θ of amorphous cellulose is at 18.30-18.40 ° (Poletto et al., 2012). The X-ray diffractograms of untreated and treated poplar and fir are sketched in **Fig. 4-12**. For 2θ between 10 and 25°, two notable peaks are observed. The smaller peaks at 2θ=14-17° stand for $(1\bar{1}0)$ and (110) crystallographic planes, while the peaks at 2θ=19-25° correspond to the (200) plane. It is noteworthy that a small peak at 2θ=32-37° can be found, which represents the (400) crystallographic plane in native cellulose (Hori & Wada, 2005).

The relative crystallinity (*CrI*) (Poletto et al., 2012; Yun et al., 2015) is defined as

$$CrI\ (\%) = \frac{I_{200} - I_{am}}{I_{200}} \times 100 \qquad \textbf{(4-3)}$$

where I_{200} is the maximum intensity of diffraction angle in the (200) plane, and I_{am} is the intensity of diffraction angle in amorphous cellulose. Meanwhile, the lattice spacing of the (200) plane is calculated using the Bragg equation (Poletto et al., 2012). The calculated values of the aforementioned quantities are summarized in **Table 4-3**. The diffraction peaks of (200) slightly shift toward lower 2θ angle when the treatment temperature increases. This arises from the lateral thermal expansion of the cellulose crystals after treatment, resulting in an increase in the lattice spacing, and further making diffraction angle (2θ) smaller (Hori & Wada, 2005).

An increase in the relative crystallinity from heat treatment can be found obviously. The value of *CrI* increases from 55.92 to 62.63 % for poplar, and from 55.59 to 61.41 % for fir. This characteristics is due to the degradation of amorphous cellulose during heat treatment, leading to the decreased accessibility of hydroxyl groups to water molecular (Esteves & Pereira,

2008). This is also one of the reasons why a significant reduction in hygroscopicity of wood after heat treatment is exhibited. However, it is noteworthy that the values of *CrI* of poplar and fir decline at 230 °C and 220 °C, respectively. The similar phenomenon has been found in other studies (Bhuiyan et al., 2000; Yun et al., 2015; Zheng et al., 2013), and could be attributed to thermal decomposition of crystalline cellulose (Bhuiyan et al., 2000). Bhuiyan et al. (2000) pointed out that a light thermal degradation might occur in crystalline cellulose when increasing the intensity of treatment.

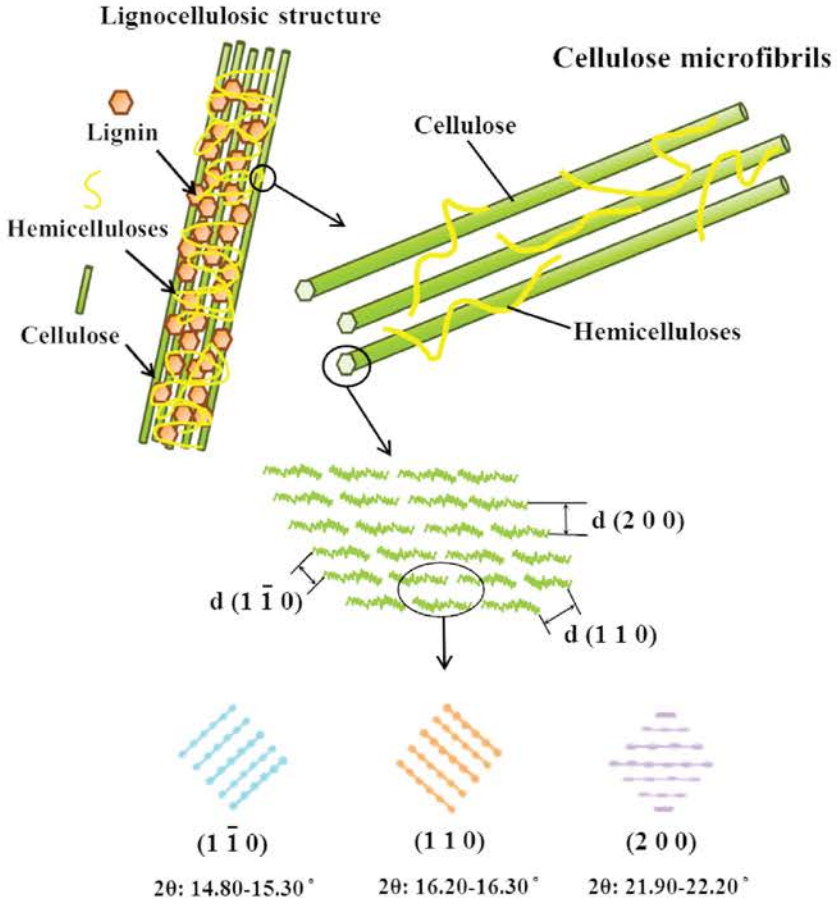

Fig. 4-11. Illustration of simplified cellulose microfibrils structure: cellulose chains with different d-spacings along the cellulose structure, and the lines indicate the crystallographic planes in native cellulose (2θ is the characteristic band position from X-ray diffraction).

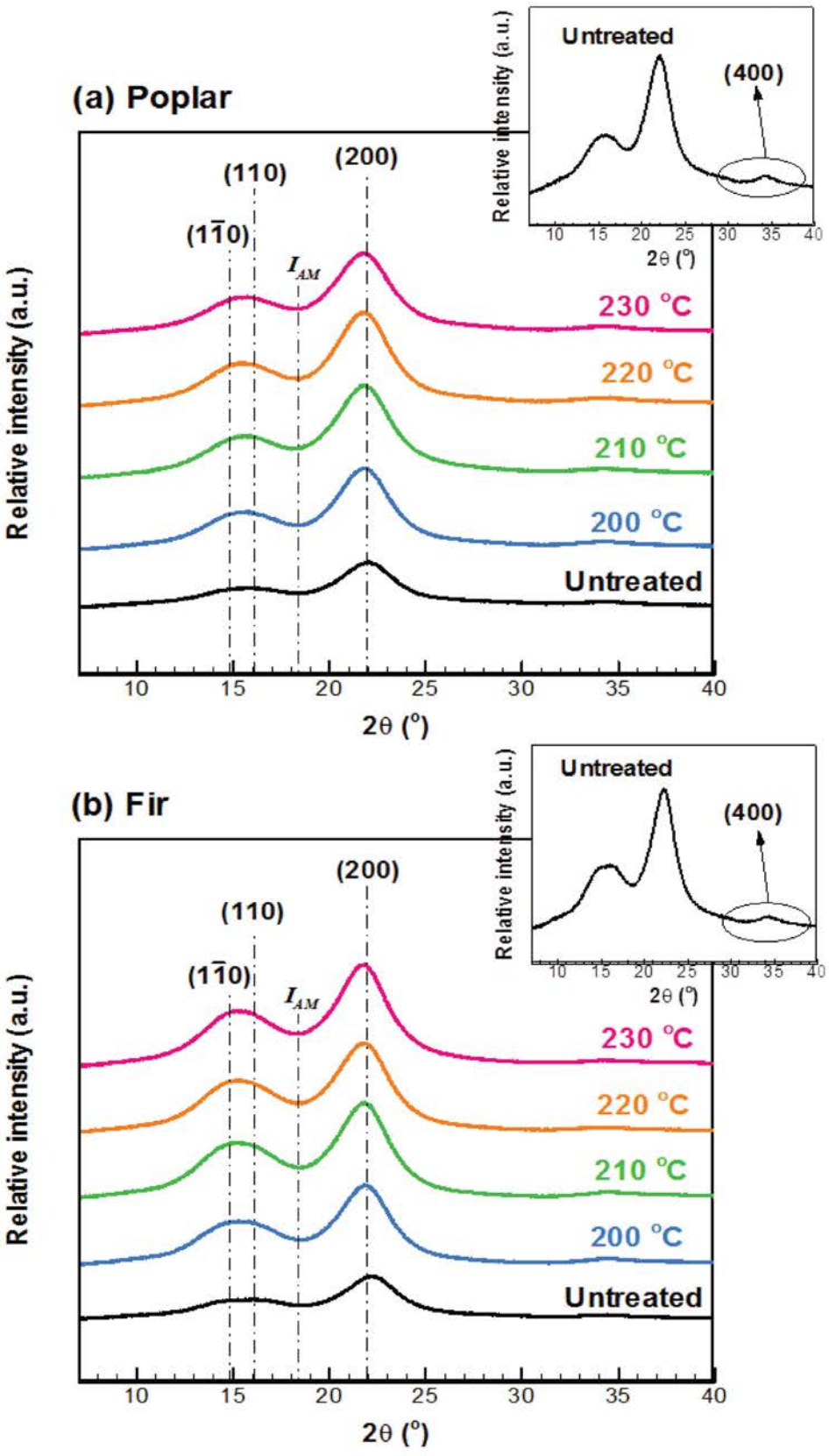

Fig. 4-12. X-ray diffractograms of untreated and treated wood: (a) poplar and (b) fir**.**

Table 4-3. Crystalline characteristics of untreated and treated poplar and fir.

Wood sample	2θ of (200) plane (^{o})	Lattice spacing of (200) plane (nm)	Relative crystallinity (*CrI*, %)
Poplar			
Untreated	22.06	0.403	55.92
200 °C	21.92	0.405	61.89
210 °C	21.82	0.407	61.36
220 °C	21.78	0.408	62.63
230 °C	21.76	0.408	59.84
Fir			
Untreated	22.14	0.402	55.59
200 °C	21.90	0.406	59.99
210 °C	21.86	0.407	60.70
220 °C	21.84	0.407	59.93
230 °C	21.84	0.407	61.41

4.2.2 Changes of color

Wood heat treatment accompanied by color change, stemming from devolatilization and carbonization mechanisms, is a remarkable feature where the color of biomass is modified from light brown to dark brown or black, depending on treatment severity. It has been reported that the color of treated wood changed from brown to black in the temperature range of 150-300 °C (Jaya et al., 2011). It has been underlined that mass loss (ML) is an effective measure to indicate treatment severity (Chen et al., 2017). The higher the ML, the higher the torrefaction severity. For this reason, the profiles of L^*, a^*, $b^*$and ΔE^* versus ML are plotted

in **Fig. 4-13** to examine the correlation between color change and treatment severity. For the raw poplar, its lightness (L^*) is 86.10, and after heat treatment the value decreases significantly, ranging from 31.09 to 35.68 (**Fig. 4-13a**). For the fir, its L^* decreases from 80.75 (raw) to 30.58 (at 230 °C of torrefaction). For the two woods, there is a clear linear relationship between L^* and treatment temperature, and decreasing L^* implies that the color of treated biomass becomes darker. Esteves et al. (2008) performed the thermal treatment of pine and eucalyptus, and showed that the lightness decreased significantly with increasing treatment time and temperature. The values of a^* in the poplar and fir increase at the lowest temperature of 200 °C, followed by a declination at higher temperatures (**Fig. 4-13b**). The maximum of a^* is 5.91 for the poplar, and 7.88 for the fir. For the vlaues of b^* in the poplar and fir, they both decrease with rising treatment severity (**Fig. 4-13c**), resembling the results of other studies (Esteves et al., 2008; González-Peña Marcos & Hale Michael, 2009). González-Peña et al. (2009) reported that the changes of a^* and b^* were more complex and depended on wood species, hence it was more difficult to identify the chemical reactions during treatment. The total color difference (ΔE^*) of the two woods is in the range of 41.49-51.66 and increases after torrefaction (**Fig. 4-13d**). Overall, L^* is the dominant factor in determining ΔE^* inasmuch as its variation before and after torrefaction is by far greater than the alterations of the others (i.e., a^* and b^*). The color variation in **Fig. 4-13d** is observably correlated to ML. This arises from the fact that the color changes of torrefied woods are mainly caused by the thermal degradation of biopolymers (Nguyen et al., 2012).

The color change of woody biomass from heat treatment is attributed to a number of reactions during torrefaction: (1) the colored byproducts are formed from the decomposition of hemicelluloses (Dubey et al., 2011; Esteves et al., 2008); (2) the cross-linking reactions, condensation reactions, and oxidation reactions from cleavage of lignin β-O-4 ether bonds and aromatic methyl groups in lignin lead to the formation of oxidative products like quinones, which facilitate color change during treatment (Dubey et al., 2011; Wikberg & Liisa Maunu,

2004); (3) the enzyme-mediated (Maillard) reactions between polysaccharides such as sugars, phenolic compounds, and amino acids are triggered during the thermal degradation (González-Peña Marcos & Hale Michael, 2009); and (4) the oxidative reactions between extractives (in woody biomass) and the atmosphere in the course of treatment (Dubey et al., 2011).

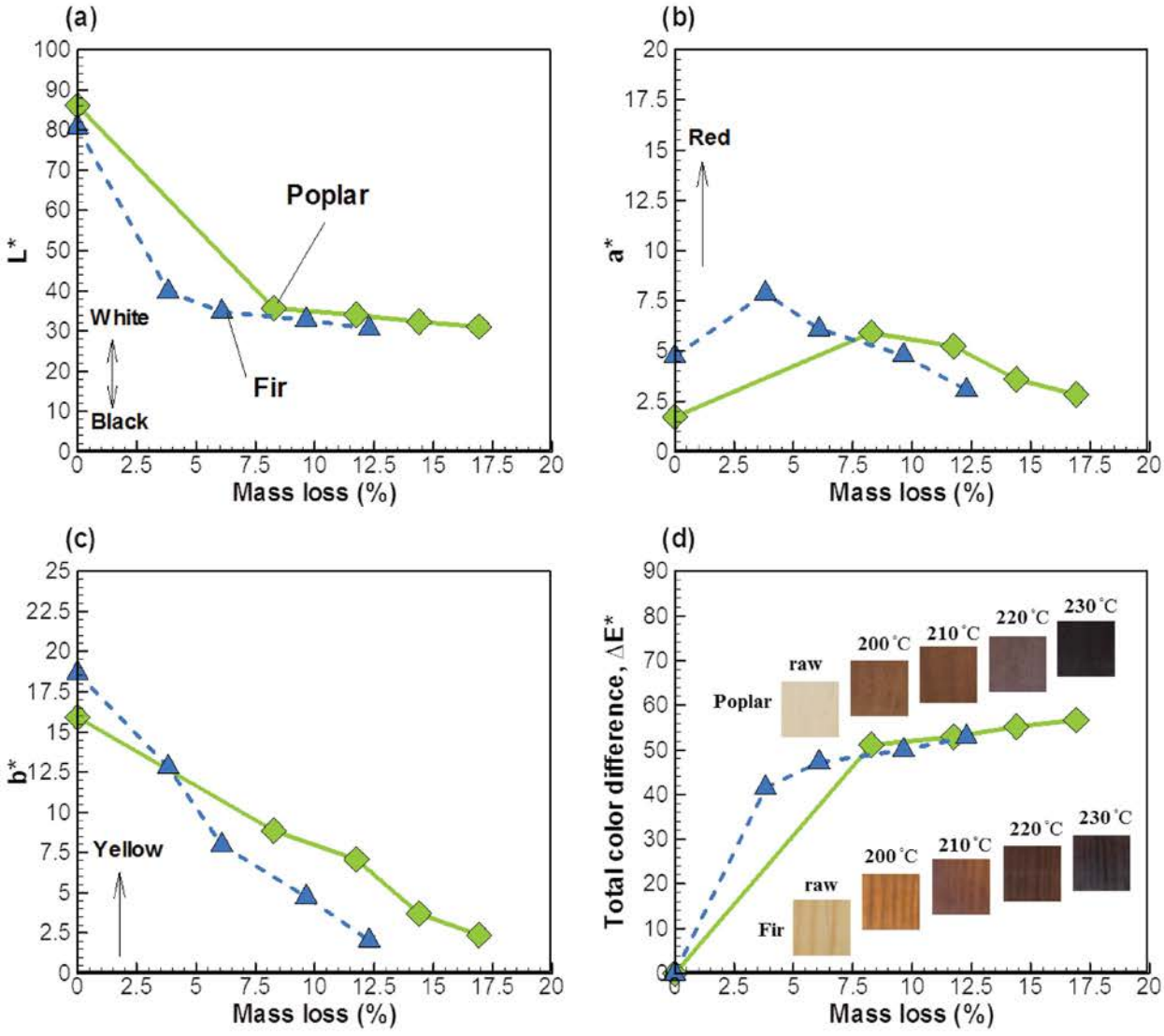

Fig. 4-13. Profiles of mass loss versus (a) lightness L*, (b) chrome value a*, (c) chrome value b*and (c) total color difference ($\Delta \boldsymbol{E}^*$).

4.2.3 Changes of hygroscopicity and wettability

Equilibrium moisture content (EMC) and contact angle are two important measures to show the hydrophobicity of biomass. In this study, the hygroscopicity reduction extent (HRE) is introduced to quantify the reduction of biomass hygroscopicity through heat treatment, and is defined as:

$$\mathrm{HRE}\ (\%) = (1 - \frac{\mathrm{EMC_{torrefied}}}{\mathrm{EMC_{raw}}}) \times 100 \qquad \textbf{(4-4)}$$

The larger the HRE value, the more hydrophobic the torrefied biomass. The profiles of EMC and HRE versus ML are shown in **Fig. 4-14**. A pronounced drop in the EMC occurs after torrefaction (**Fig. 4-14a**), and the EMC has a trend to decrease linearly with increasing torrefaction severity. The hydrophobicity of the fir is more sensitive to ML and its HRE can reach up to 57.39% at 230 °C (**Fig. 4-14b**). The obtained results are consonant with other studies (Järvinen & Agar, 2014; Mei et al., 2015). Strandberg et al. (2015) discovered that the EMC of torrefied biomass (spruce wood) decreased by at least 50% when biomass was torrefied at temperature higher than 260 °C.

The transient profiles of the contact angles of raw and torrefied woods are shown in **Fig. 4-15.** It has been pointed out that the contact angle close to 0° corresponded to a hydrophilic surface (with clearly hygroscopic property). If the angle is less than 90°, the sample is more hydrophilic than hydrophobic. Once the angle is above 90°, the surface is hydrophobic (Strandberg et al., 2015). **Fig. 4-15** shows the apparent absorption of water droplet into the raw poplar and fir, rendering their hygroscopic nature. For the raw poplar, the initial contact angle is 63.7° and the angle becomes 0° at around 3 s. As regard to the raw fir, the initial contact angle is 86.5°, and the angle is close to 0° after 19 s. Overall, it appears that poplar has higher wettability when compared to fir. Water absorbed by the woody materials is mainly due to the presence of hydroxyl groups (-OH) which attract and hold water molecules through hydrogen bonding. In wood materials, hemicelluloses are more hydrophilic than cellulose and lignin. Hemicelluloses and the non-crystalline region of cellulose chains can

attract water easier, owing to the availability of hydroxyl groups (Esteves et al., 2008). The carboxylic acid groups (-COOH) in hemicelluloses are also active to absorb water (Stokke & Gardner, 2003). The higher water absorption speed in the raw poplar is attributed to the specially large water-conducting pores (called vessels) and higher content of carboxylic acid groups in hardwood species (Paul et al., 2006).

Unlike the raw woods, the contact angles of heat treated samples can last for a longer time and are always greater than 90°. The higher the treatment severity, the larger the contact angle. The contact angles of the treated poplar and fir are in the ranges of 94.9-107.0° and 103.4-113.0°, respectively. The contact angles of the treated fir (**Fig. 4-15b**) are always greater than those of treated poplar (**Fig. 4-15a**), despite the lower ML of the former. This observation can be owing to the significant tar components present during heat treatment of fir where the tar condensates on the treated wood surface, thereby increasing hydrophobic properties (Strandberg et al., 2015). This is also the reason why the HRE of fir is higher than that of poplar (**Fig. 4-15b**). In summary, the reduction in the hygroscopic behavior of heat treated woods can be assigned to the following reasons: (1) the degradation of hemicelluloses and amorphous cellulose results in removing -OH and -COOH groups and further decreasing hydrogen bonding with water after torrefaction; (2) tar condenses inside the pores, thereby obstructing the passage of moist air through the solid and then avoiding water vapor adsorption; (3) the apolar character of condensed tar on the solid also prevents the condensation of water vapor inside the pores (Chen et al., 2015c; Pelaez-Samaniego et al., 2013; Stokke & Gardner, 2003), as illustrated in **Fig. 4-16**.

Most importantly, the observed hygroscopicity transformation of woods after heat treatment can markedly improve their dimensional stability and avoid the biodegradation from microorganism (Pelaez-Samaniego et al., 2013). Paul et al. (2006) examined the correlation between the EMC change and fungal resistance of thermally treated wood

materials, and discovered that the fungal decay of treated wood tended to disappear when the EMC of treated wood was decreased by around 37-40 % compared to untreated wood.

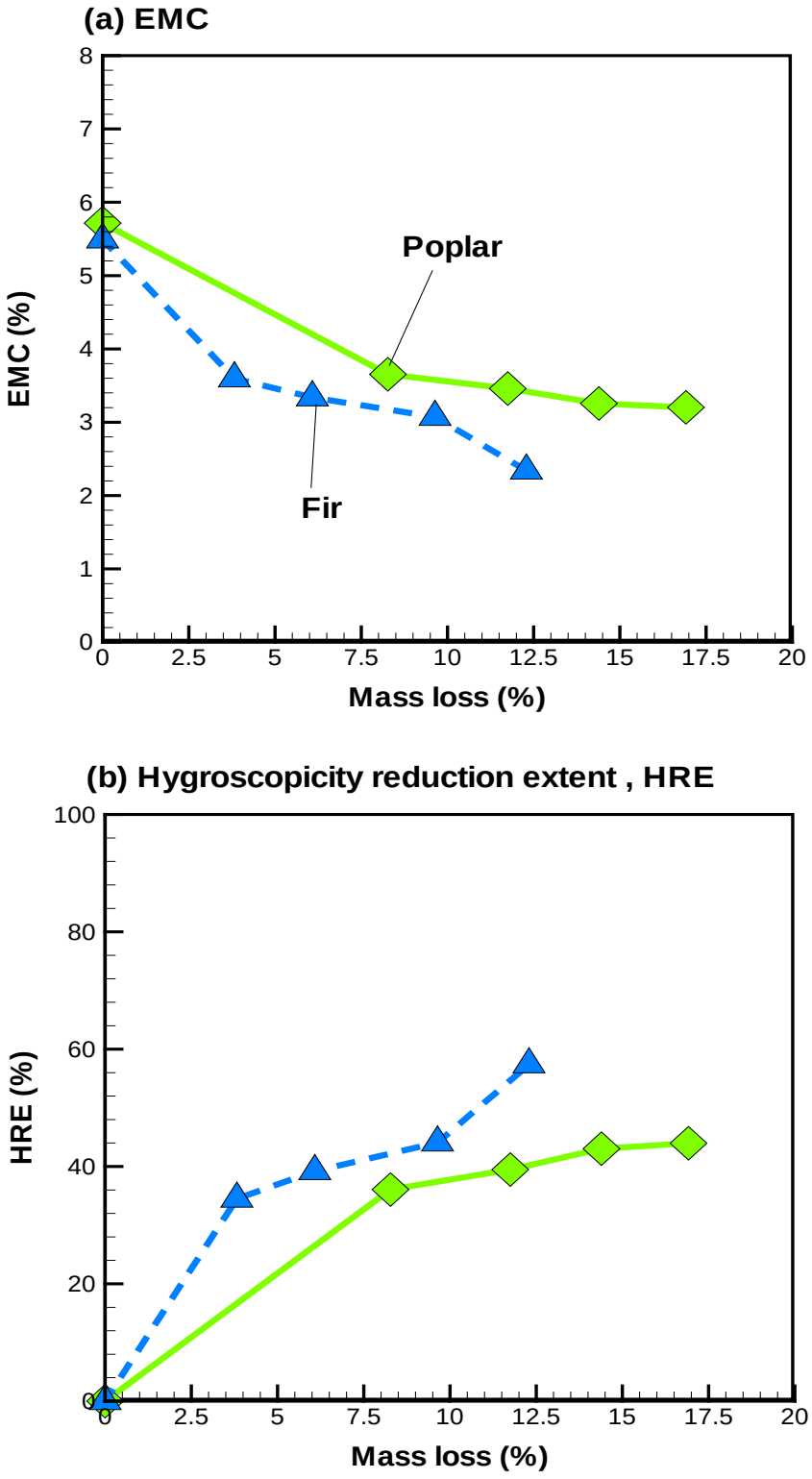

Fig. 4-14. Profiles of mass loss versus (a) EMC, and (b) hygroscopicity reduction extent (HRE).

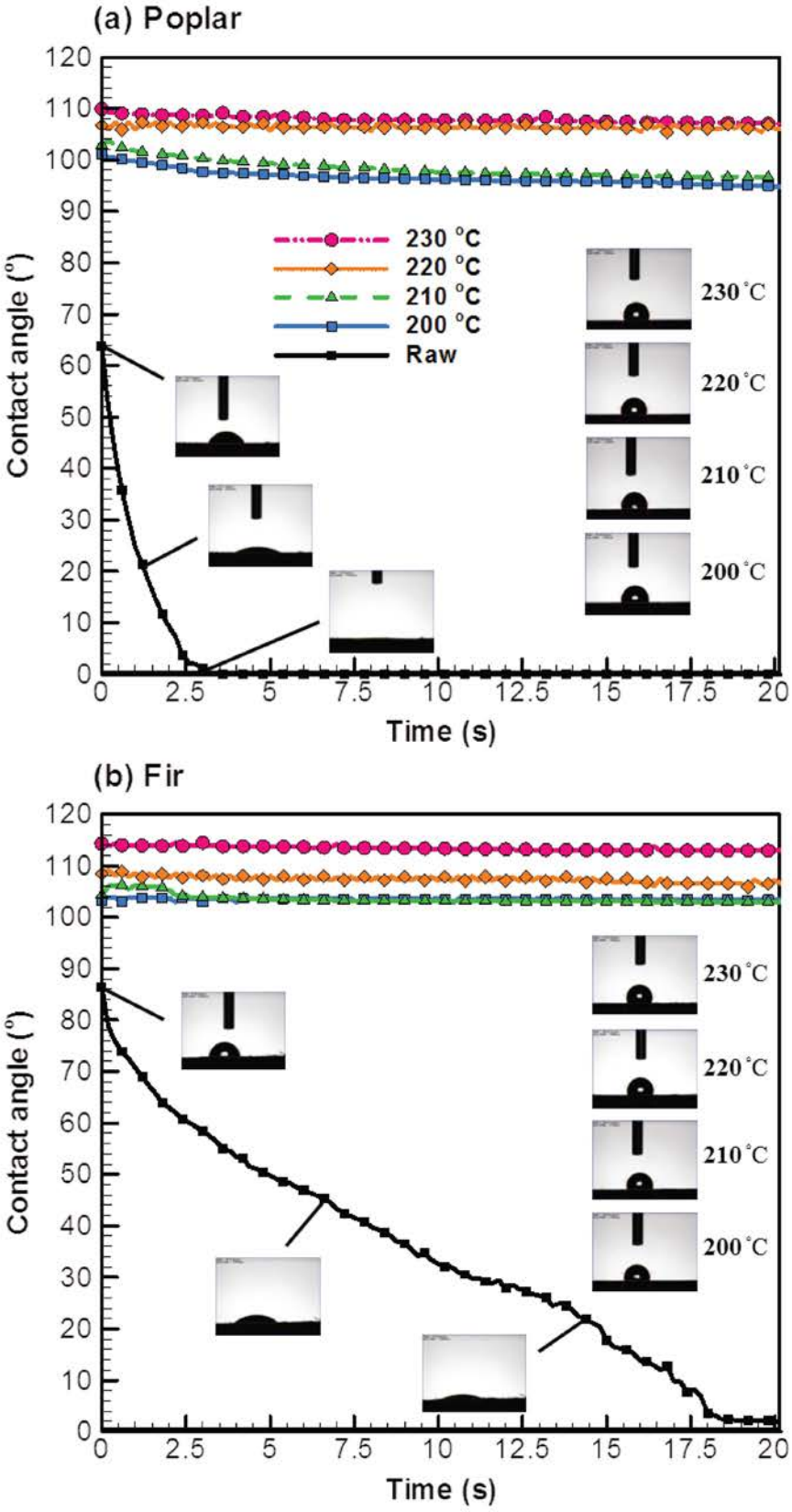

Fig. 4-15. Profiles of contact angle on the surface of raw and heat treated (a) poplar and (b) fir.

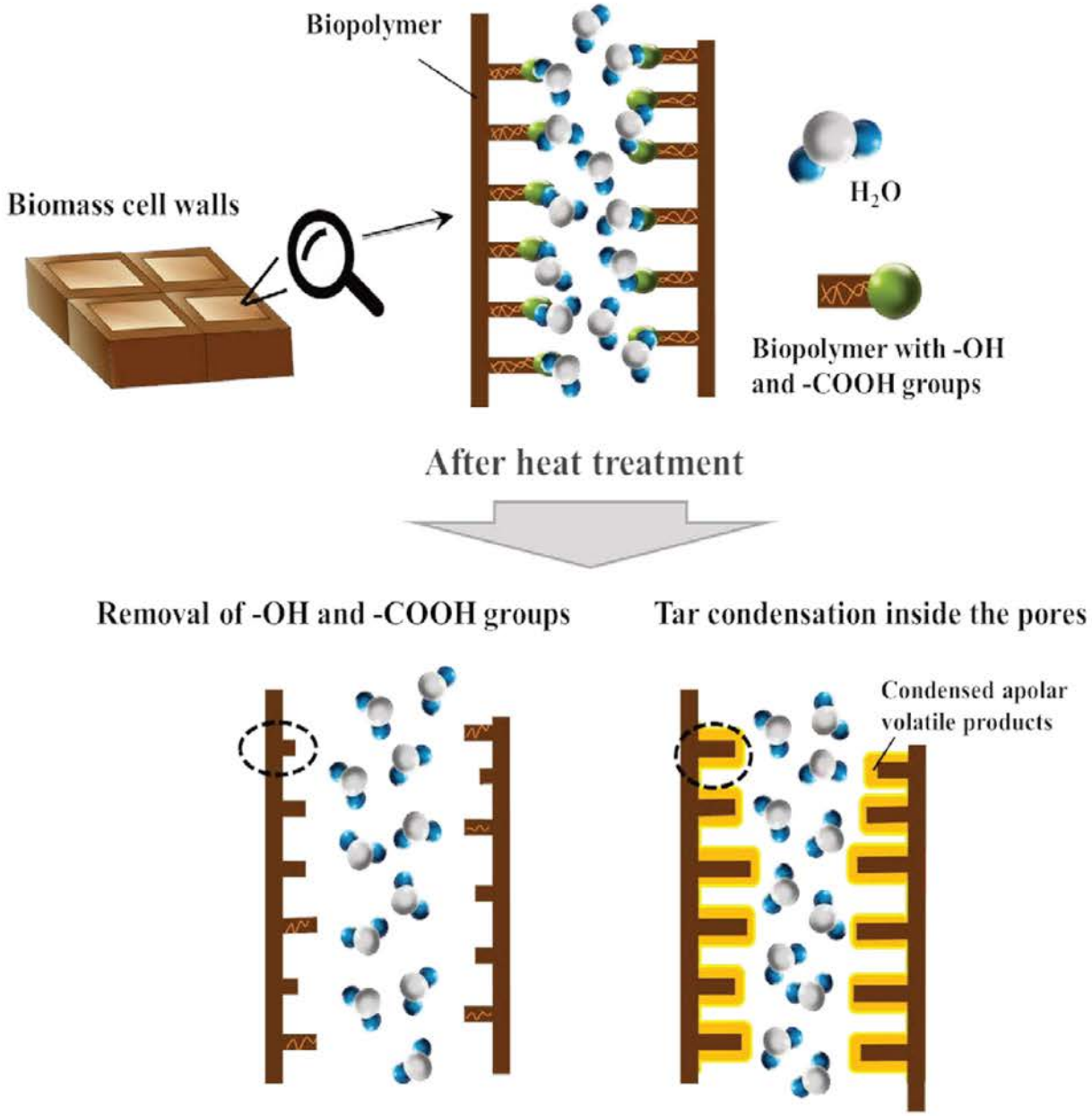

Fig. 4-16. Phenomenon of hygroscopic transformation after heat treatment.

4.2.4 Correlations between element removals and changes of color and hygroscopicity

In the earlier discussion, the changes of color and hygroscopicity of woody biomass are mainly attributed to the devolatilization during torrefaction. In order to evaluate the characteristics of devolatilization during torrefaction; decarbonization (DC), dehydrogenation (DH), deoxygenation (DO) are analyzed. According to the elemental analysis of the wood samples (**Table 4-1**), the original carbon amount (O_C) in a raw material is expressed as (Chen et al., 2016):

$$O_C(g) = W_0 \times Y_{C,0} \quad \textbf{(4-5)}$$

where W_0, and $Y_{C,0}$ denote the weight (g) of the sample (in dry-ash-free basis) and mass fraction of carbon, respectively, and the subscript 0 stands for raw material. The residual carbon amount (R_C) in heat treated wood is determined in accordance with the following formula:

$$R_C(g) = W_0 \times SY \times 10^{-2} \times Y_{C,t} \quad \textbf{(4-6)}$$

where SY designates solid yield, and the subscript t denotes treated wood. Consequently, decarbonization (DC), which represents the carbon loss percentage in the wood through heat treatment, is calculated by

$$DC\ (\%) = \left(1 - \frac{R_c}{O_C}\right) \times 100 \quad \textbf{(4-7)}$$

DH and DO are also determined using the same way.

The values of DC, DH, and DO are listed in **Table 4-4**, which shows that the general trend is ranked as DO > DH > DC, stemming from the removal of moisture and light volatiles during wood heat treatment (Wang et al., 2018a). This reflects the more significant impact of heat treatment upon oxygen and hydrogen than on carbon. However, the DH is larger than DO for the fir treated at 200 and 210 °C. This can be explained by stronger dehydration and more release of extractives which mainly consist of aliphatic, alicyclic, and phenolic compounds (Valette et al., 2017). It has been reported that the extractives in softwoods were

higher than hardwoods (Grønli et al., 2002), and the maximum thermal degradation rate of extractives occurred at approximately 205 °C (Wang et al., 2017). In this study, the extractives of poplar and fir are 2.63 and 3.80 wt%, respectively (**Table 3.1**). Moreover, the existence of extractives indeed influences the biomass pyrolysis behavior and its products, especially when pyrolyzing extractives-rich biomass (Wang et al., 2017).

The profiles of DC, DH, and DO versus ΔE^* and HRE are plotted in **Fig.4-17.** The profiles are characterized by strongly linear relationships ($R^2 > 0.87$), especially for the poplar (R^2 is in the range of 0.9412-0.9933). The slops of regression lines of the poplar are greater than those of the fir, elucidating more severe degradation of the former during heat treatment. Some studies have used EMC and color change to predict mass loss of heat treated wood (Chaouch et al., 2013; Nguyen et al., 2012). Nguyen et al. (Nguyen et al., 2012) performed the heat treatment of bamboo in the temperature range of 130-220 °C, and found that the mass loss of bamboo was well-correlated with the color change and the EMC in that the R^2 values were in the range of 0.87-0.93 and 0.74-0.86, respectively. As a consequence, this study suggests that, aside from mass loss, the total color difference and HRE can also be used to predict carbon, hydrogen, and oxygen removals in wood from heat treatment.

Table 4-4. Decarbonization, dehydrogenation, and deoxygenation in treated poplar and fir.

Untreated and treated wood		DC [a] (%)	DH [b] (%)	DO [c] (%)
Poplar				
	Untreated	0	0	0
	200 °C	2.71	8.93	13.73
	210 °C	4.48	14.63	19.08
	220 °C	6.52	19.57	22.15
	230 °C	7.13	22.87	26.67
Fir				
	Untreated	0	0	0
	200 °C	1.39	7.35	5.86
	210 °C	1.75	11.37	9.93
	220 °C	2.84	15.72	16.05
	230 °C	3.66	18.74	20.59

[a]: decarbonization; [b]: dehydrogenation; [c]: deoxygenation.

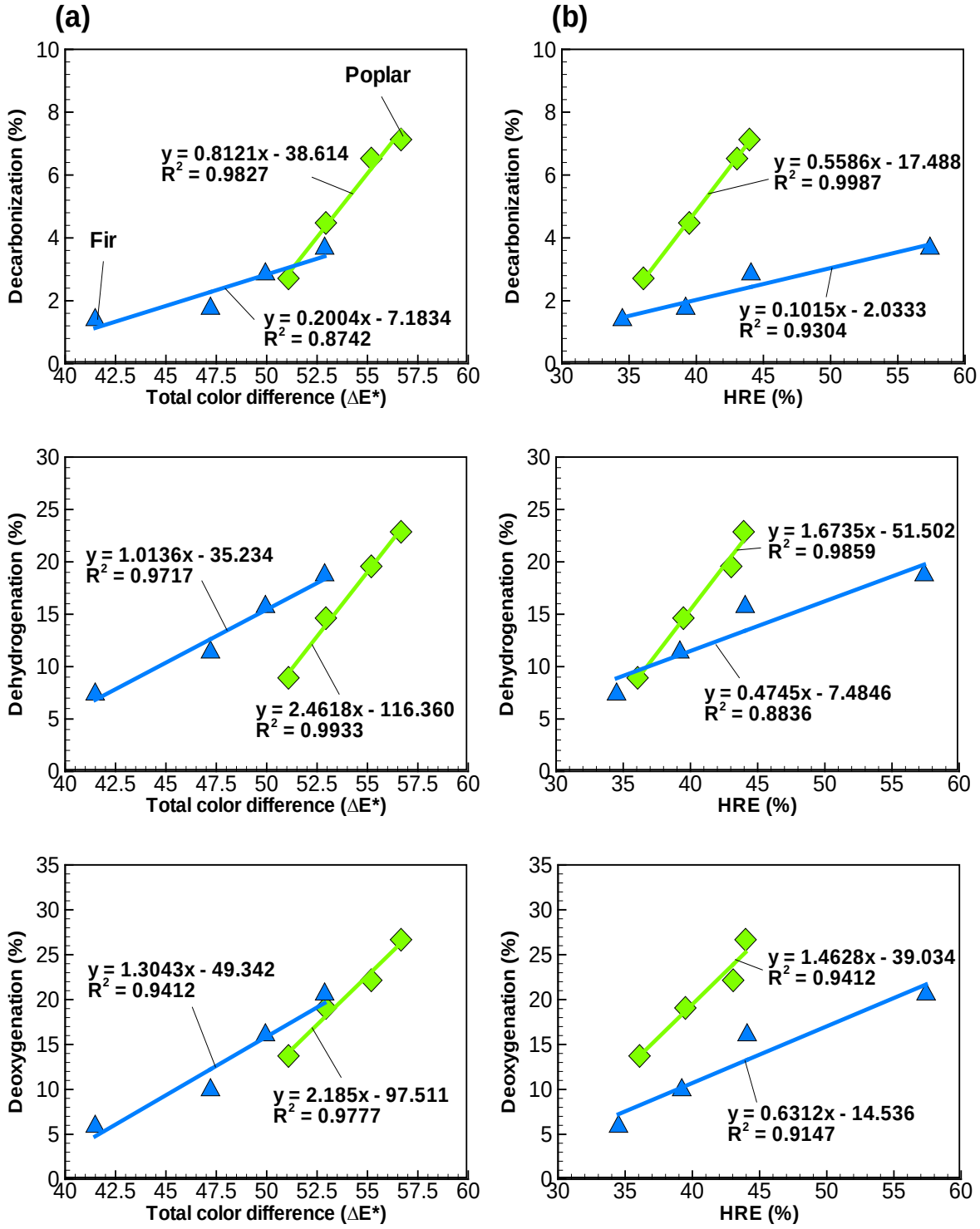

Fig. 4-17. Profiles and linear regressions of (a) total color difference (ΔE^*) and (b) hygroscopicity reduction extent (HRE) versus decarbonization, dehydrogenation, and deoxygenation.

4.3 Kinetic modeling of wood heat treatment

4.3.1 Solid yield prediction and kinetic parameters

In this study, a two-step kinetic model is established and used to predict the thermal degradation dynamics during wood treatment. According to the algorithm displayed in **Fig. 3-8**, the predicted solid yields of poplar and fir by curve-fittings to fit the experimental data are shown in **Fig. 4-18a**. As a whole, these established curves accurately fit the experimental data in that the value of coefficient of determination (R^2) is in the range of 0.9656-0.9997, yielding a well goodness-of-fit with experimental results. **Fig 4-18a** depicts a strong influence of treatment temperature on thermal degradation of the woods. The solid yield of poplar decreases with increasing temperature, and the yield at the end of the treatment under 200, 210, 220, and 230 °C are 91.69, 88.25, 85.74, and 83.08 %, respectively. The thermal degradation of fir is lighter than that of poplar with solid yields in the range of 96.17-87.71 %. The higher thermal sensitivity of hardwoods compared to softwoods is attributed to the higher content in acetyl groups from acetylated glucuronoxylan in hardwoods, which lead to acetic acid formation thus accelerating the degradation of woods (Candelier et al., 2016; Lin et al., 2018).

The profiles of the rate constants k_1, k_{V1}, k_2, and k_{V2} versus temperature are plotted in **Fig 4-18b,** and their expressions in terms of temperature are listed in **Table 4-5**. The obtained kinetic parameters are in a reasonable range compared with other studies on thermal degradation of wood materials and xylan (Di Blasi & Lanzetta, 1997; Shang et al., 2014). **Fig 4-18b** suggests that the rate constants follow the order of $k_1 > k_{V1} > k_2 > k_{V2}$.This reflects that the first step of degradation (A→B & V_1) is faster than the second step (B→C & V_2). Similar results have also been observed in other studies (Bach et al., 2016; Silveira et al., 2018). According to the Arrhenius equation, the reactivity of a material is typically represented by the rate constant which contains the pre-exponential factor and activation energy. **Table 4-5** indicates that poplar has the higher activation energy for intermediate (B) and solid residue (C) production, whereas it has lower activation energy for volatiles production. On the other hand, similar

results are also found on the pre-exponential factors. It is known that a higher activation energy lowers the rate constant, whereas a higher pre-exponential factor intensifies the constant. Seeing that poplar has a higher pre-exponential factor and a more pronounced mass loss during treatment when compare to fir (**Fig. 4-18a** & **Table 4-5**), it is thus recognized that the role played by the pre-exponential factor on the thermal degradation precedes that by the activation energy.

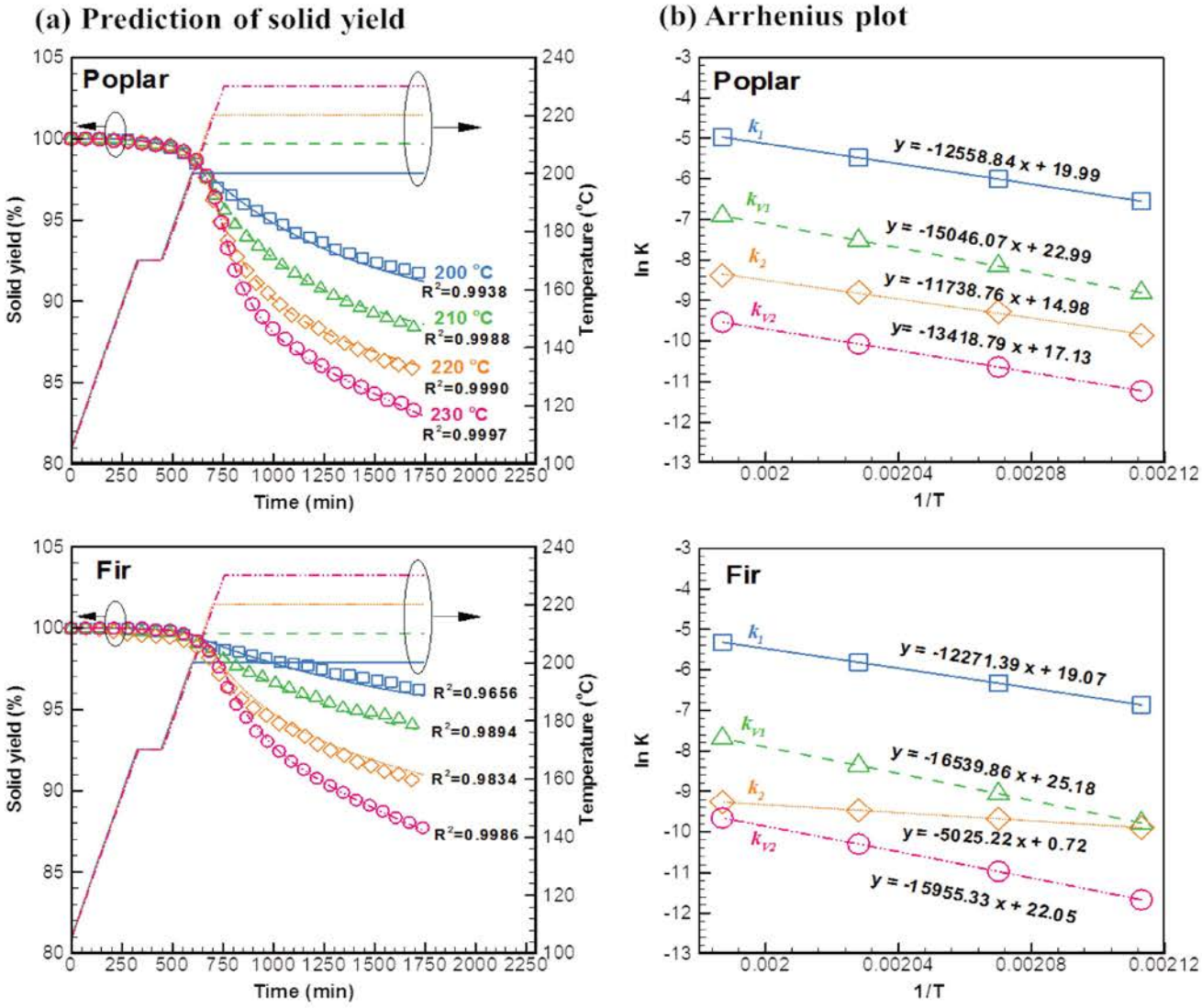

Fig. 4-18. (a) Predicted (lines) and experimental (symbols) curves of solid yield during heat treatment, and the (b) Arrhenius plot of k_1, k_{v1}, k_2, and k_{v2}.

Table 4-5. Kinetic parameters of poplar and fir.

Rate constant (s^{-1}) [a]	**Reaction equation**	**Poplar (*Populus nigra*)**	**Fir (*Abies pectinata*)**
k_1	A→B (1st step)	$4.80 \times 10^{8}\exp\left(\frac{-104420}{RT}\right)$	$1.91 \times 10^{8}\exp\left(\frac{-102030}{RT}\right)$
k_{v1}	A→V_1 (1st step)	$9.65 \times 10^{9}\exp\left(\frac{-125100}{RT}\right)$	$8.62 \times 10^{10}\exp\left(\frac{-137520}{RT}\right)$
k_2	B→C (2nd step)	$3.20 \times 10^{6}\exp\left(\frac{-97601}{RT}\right)$	$2.05\exp\left(\frac{-41782}{RT}\right)$
k_{v2}	B→V_2 (2nd step)	$2.75 \times 10^{7}\exp\left(\frac{-111570}{RT}\right)$	$3.77 \times 10^{9}\exp\left(\frac{-132660}{RT}\right)$

[a]: where the unit of pre-exponential factor is s^{-1}; the unit of activation energy is J mol^{-1}; R is the ideal gas constant (8.314 J K^{-1} mol^{-1}); and T is the absolute temperature (K).

4.3.2 Characteristics of solid and volatile products

The three-dimensional profiles of solid yield, solid proportions (A, B, and C), and volatile products (V_1, and V_2) during the treatment of poplar and fir are displayed in **Fig. 4-19** and **Fig. 4-20**, respectively. The sensitivity of the two biomass species to temperature can be identified from the solid yield profiles (**Fig. 4-19a** and **Fig. 4-20a**). The thermal degradation depends strongly on the contents of hemicelluloses in hardwoods and softwoods (Chaouch et al., 2013). In Europe industry, the mass loss of wood material after treatment is normally controlled in the range of 8-10 % (i.e. 90-92 % of solid yield) for building and construction. From the profiles in **Fig. 4-19a** and **Fig. 4-20a**, with the target of wood modification of 90 % of solid yield, the duration of treatment at 230 °C for poplar and fir should be 883 and 1326 min, respectively. These observations can be used to select wood species for reducing treatment energy consumption and carbon footprint as well as optimizing the economical balance. Moreover, it appears that poplar is more proper for producing treated wood from the energy consumption point of view, as a consequence of faster thermal degradation.

Concerning the solids of A, B and C, the thermal degradation of feedstock (A) is more sensitive to temperature (**Fig. 4-19b** and **Fig. 4-20b**) when compared to B (**Fig. 4-19c** and **Fig. 4-20c**) and C (**Fig. 4-19d** and **Fig. 4-20d**). At lower temperatures such as 200 and 210 °C, only little amount of A is retained in the final solid product. The final A contents in poplar and fir are 3.70-13.77 and 9.85-24.33 wt %, respectively. For the treatment temperature of 230 °C, the final A contents in both poplar and fir are close to 0 wt%, implying that the raw materials are almost completely converted. The predictions reveal that the main solid product at the end of treatment is intermediate B, ranging from 68.7 to 82.8 wt% (**Fig. 4-19c** and **Fig. 4-20c**). In contrast, the maximum values of residue C from poplar and fir treatment are 7.85 and 7.50 wt%, respectively, accounting for less than 10 wt% in the final product. It is noteworthy that the final proportion of C is sensitive to the treatment temperature to a great extent (**Fig. 4-19d** and **Fig. 4-20d**). The proportion of B in the solid product is similar to

treated wood after light torrefaction (Bach et al., 2016). Some studies have been investigated the torrefaction kinetics using the two-step model (Bach et al., 2016; Rashid et al., 2017). The results reported that the main content of torrefied wood was intermediate B (around 50-80 wt%) when the temperature was lower than 260 °C (light and mild torrefaction). On the other hand, the main content of torrefied wood changed into residue C (around 20-40 wt%) once the temperature was higher than 260 °C (severe torrefaction).

The profiles of volatile products (V_1 and V_2) are demonstrated in **Fig. 4-19e** and **Fig. 4-20e**. It is not surprising that their amounts increase with increasing treatment temperature, and the amount of V_1 is always higher than that of V_2. At the end of wood treatment, the value of V_1 from the thermal degradation of poplar is in the range of 7.95-11.34 wt%, while it is between 3.70 and 7.41 wt% from the thermal degradation of fir. The summation of V_1 and V_2 after poplar treatment at the temperature of 230°C is 17.05 wt%, while it is 12.44 wt% after fir treatment. The release of V_1 and V_2 is responsible for the weight loss of the biomass. That is, the higher the V_1 and V_2 values, the lower the solid yield. This is the reason why the solid yield at the end of the treatment is also sensitive to the temperature (**Fig. 4-19a** and **Fig. 4-20a**).

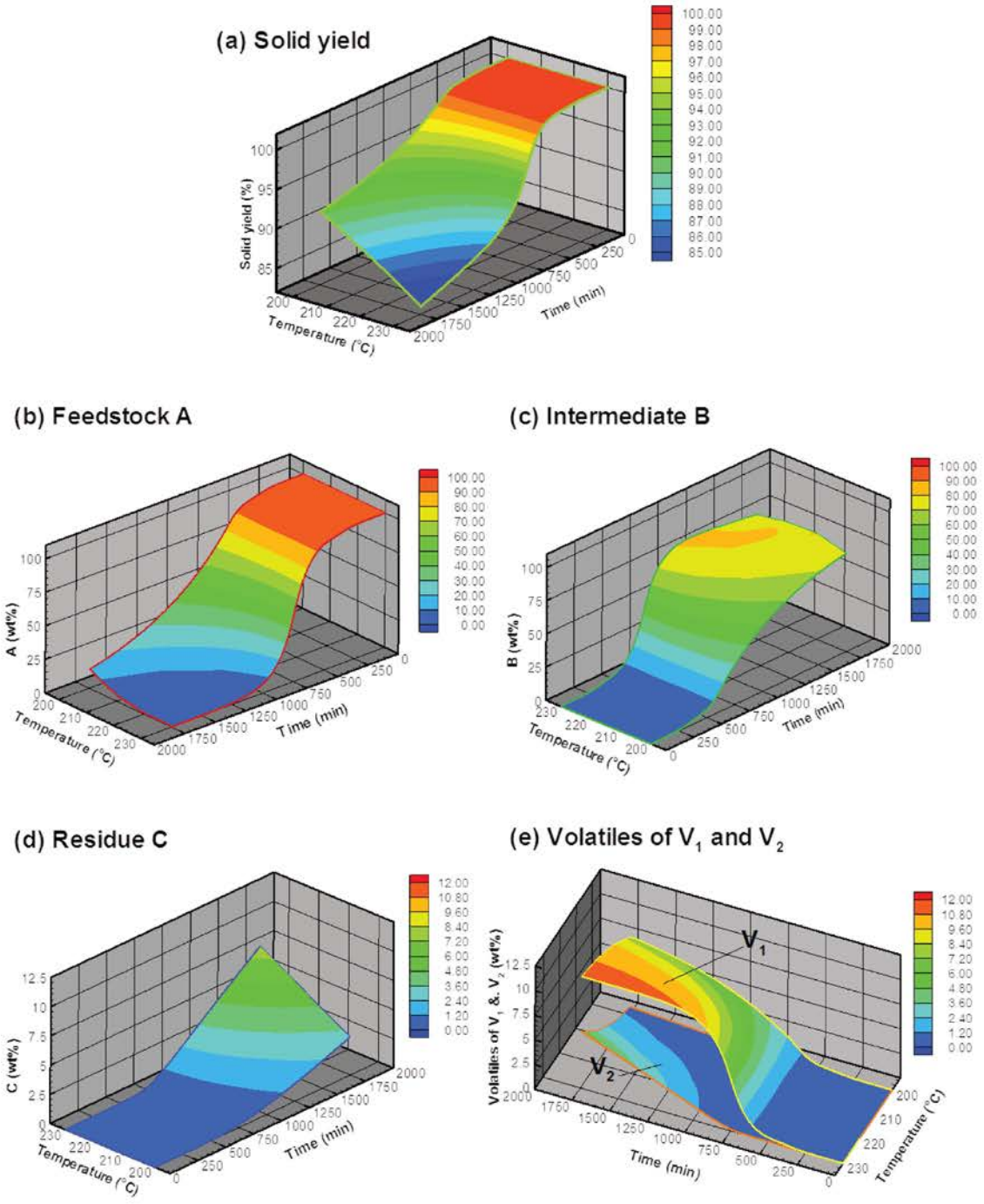

Fig. 4-19. (a) Solid yield, (b) feedstock A, (c) intermediate B, (d) residue C, and (e) volatile products (V_1 and V_2) during heat treatment of poplar.

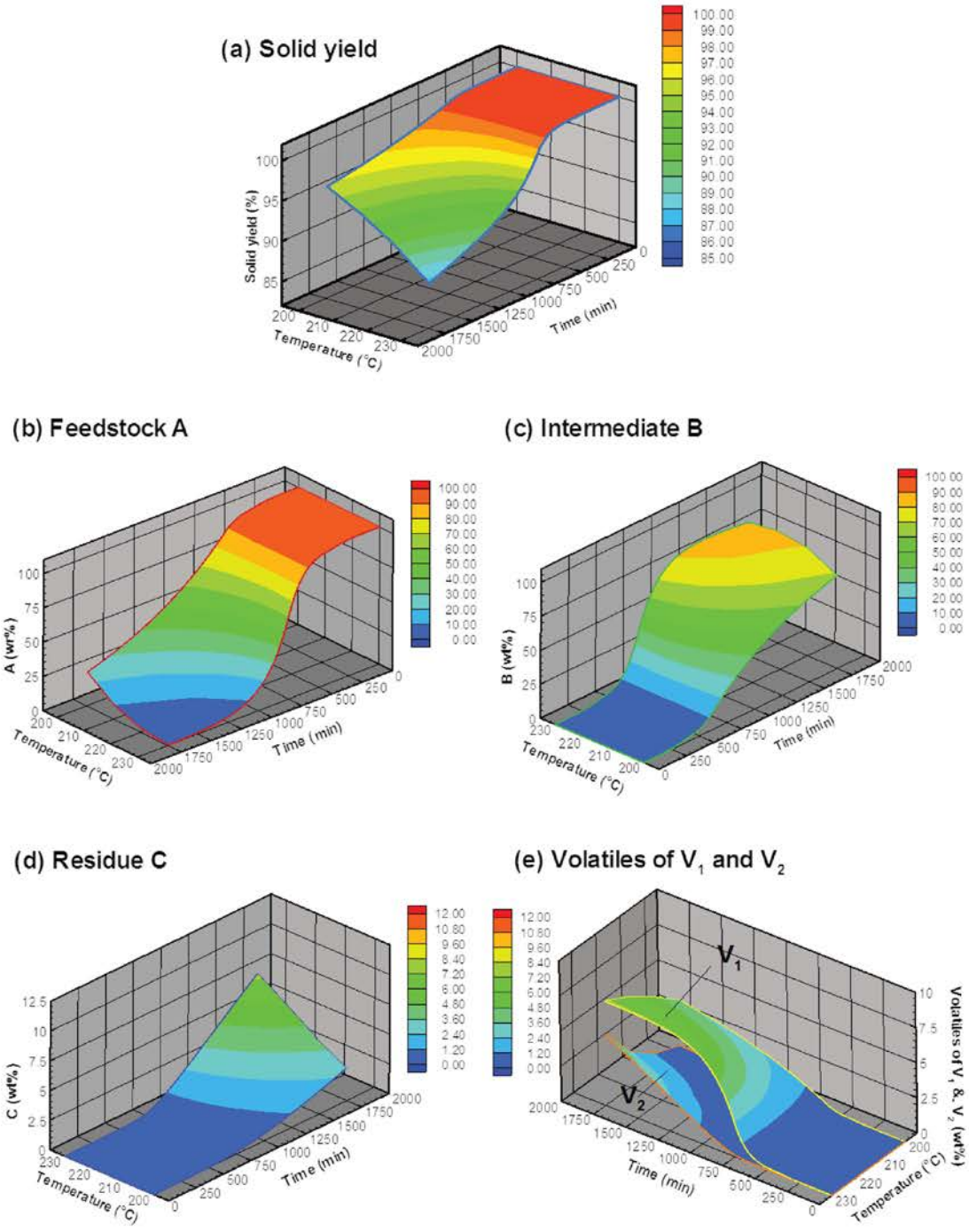

Fig. 4-20. (a) Solid yield, (b) feedstock A, (c) intermediate B, (d) residue C, and (e) volatile products (V_1 and V_2) during heat treatment of fir.

4.3.3 Prediction of elemental composition

The information of elemental composition is conductive to evaluating the heat treatment intensity of wood materials and the treatment performance (Chaouch et al., 2013; Šušteršic et al., 2010). According to the established kinetics, the predicted profiles of elemental composition during wood treatment are sketched in **Fig. 4-21**. When increasing the treatment temperature, the elemental compositions in treated woods tend to change more aggressively. At the temperature of 230 °C, the C contents in the treated poplar and fir significantly increase, whereas the O contents dramatically decrease. This can be explained by the thermal cross-linking reactions that obviously occur at higher temperatures (Hill, 2007). Furthermore, the predicted distributions of atomic H/C and O/C ratios are demonstrated in **Fig. 4-22**. The two ratios start to obviously decrease after the thermal homogenization stage (> 170 °C). This is assigned to the devolatilization reactions of the woods during thermal degradation (Chaouch et al., 2013; Lin et al., 2018).

In this study, the higher heating values (HHVs) of treated woods are also calculated from the predicted elemental composition. The predicted HHVs can be applied to evaluate the potential of treated wood as a solid fuel. The HHVs of the woods during treatment are calculated based on the correlation of Sheng and Azevedo (2005) which is expressed as

$$HHV\ (\mathrm{MJ\ kg^{-1}}) = -1.3675 + 0.3137 \times C + 0.7009 \times H + 0.0318 \times O \qquad \textbf{(4-8)}$$

where C, H, and O stand for the mass percentages of carbon, hydrogen, and oxygen on a dry-ash-free basis. The enhancement factor of HHV, which is a HHV ratio of treated wood to untreated wood, is also determined and expressed as:

$$\text{Enhancement factor} = \frac{\mathrm{HHV}_{treated}}{\mathrm{HHV}_{untreated}} \qquad \textbf{(4-9)}$$

The HHV profiles shown in **Fig. 4-23** start to increase at the thermal homogenization stage, stemming from the removal of extractives and light volatiles (Lin et al., 2018). As a whole, the final HHVs of poplar and fir are in the range of 19.62-20.55 MJ kg^{-1}. The increased HHV is

mainly due to the change of elemental composition in treated wood. Chen et al. (2015c) have pointed out that C and H in a fuel are the major sources of heat released from combustion. More oxygen contained in biomass facilitates the burning of the fuel, but it reduces the calorific value of the biomass.

The enhancement factor of HHV can be regarded as an index of improved energy density, and has been widely used to examine the performance of torrefaction (Chen et al., 2017). A high correlation between the enhancement factor and the mass loss, as a consequence of V_1 and V_2 liberation (**Figs. 4-19e** and **4-20e**), can be observed in **Fig. 4-23**, and this observation is in line with past studies (Chen et al., 2017; Chen et al., 2015c). The enhancement factor at the end of treatment is in the range of 1.01-1.07, which is close to torrefied wood after light torrefaction (Colin et al., 2017; Gul et al., 2017). For instance, Gul et al. (2017) performed the torrefaction of different biomass substances (beech, pine, wheat straw, and willow). The results revealed that the enhancement factors of torrefied samples at 200 and 240 °C were in the range of 1.01-1.13. Overall, the HHVs of heat treated wood are lower than mildly and severely torrefied woods (Chen et al., 2015c). However, the treated woods still have the potential to mix with biochar or coal for the applications of co-gasification and co-combustion to produce energy.

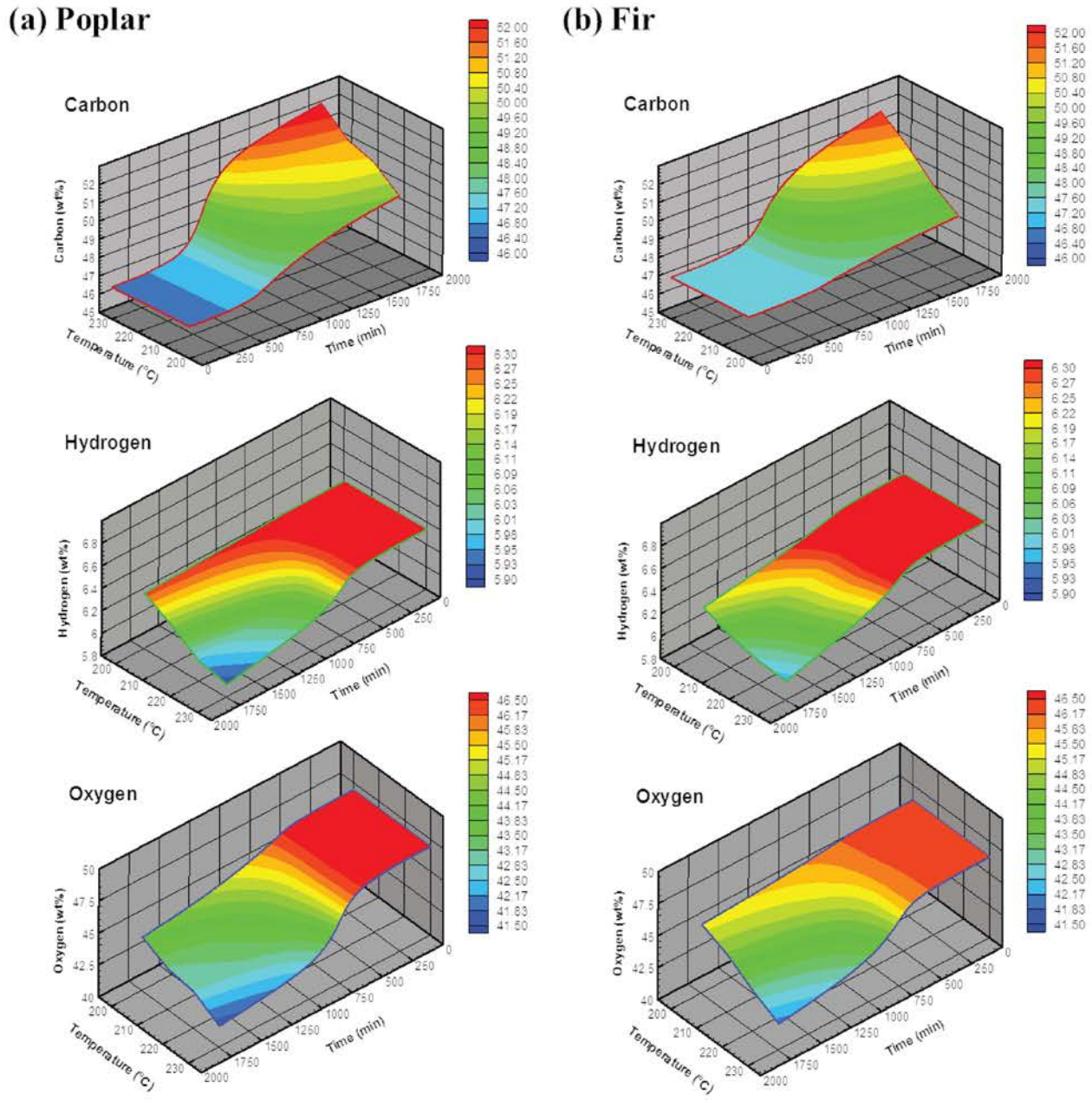

Fig. 4-21. Prediction of C, H, and O during heat treatment of (a) poplar(b) fir.

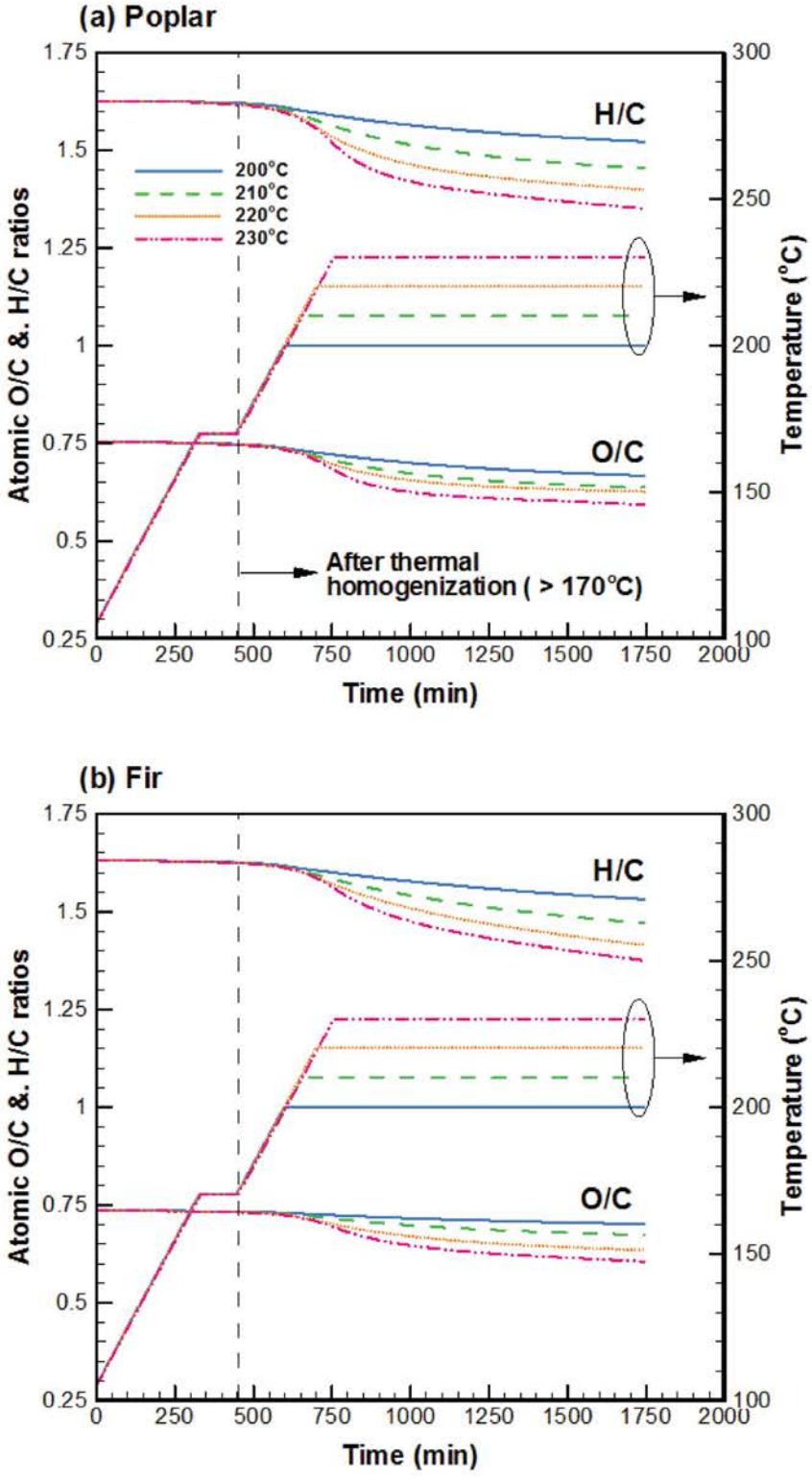

Fig. 4-22. Profile of atomic H/C and O/C during heat treatment of (a) poplar(b) fir.

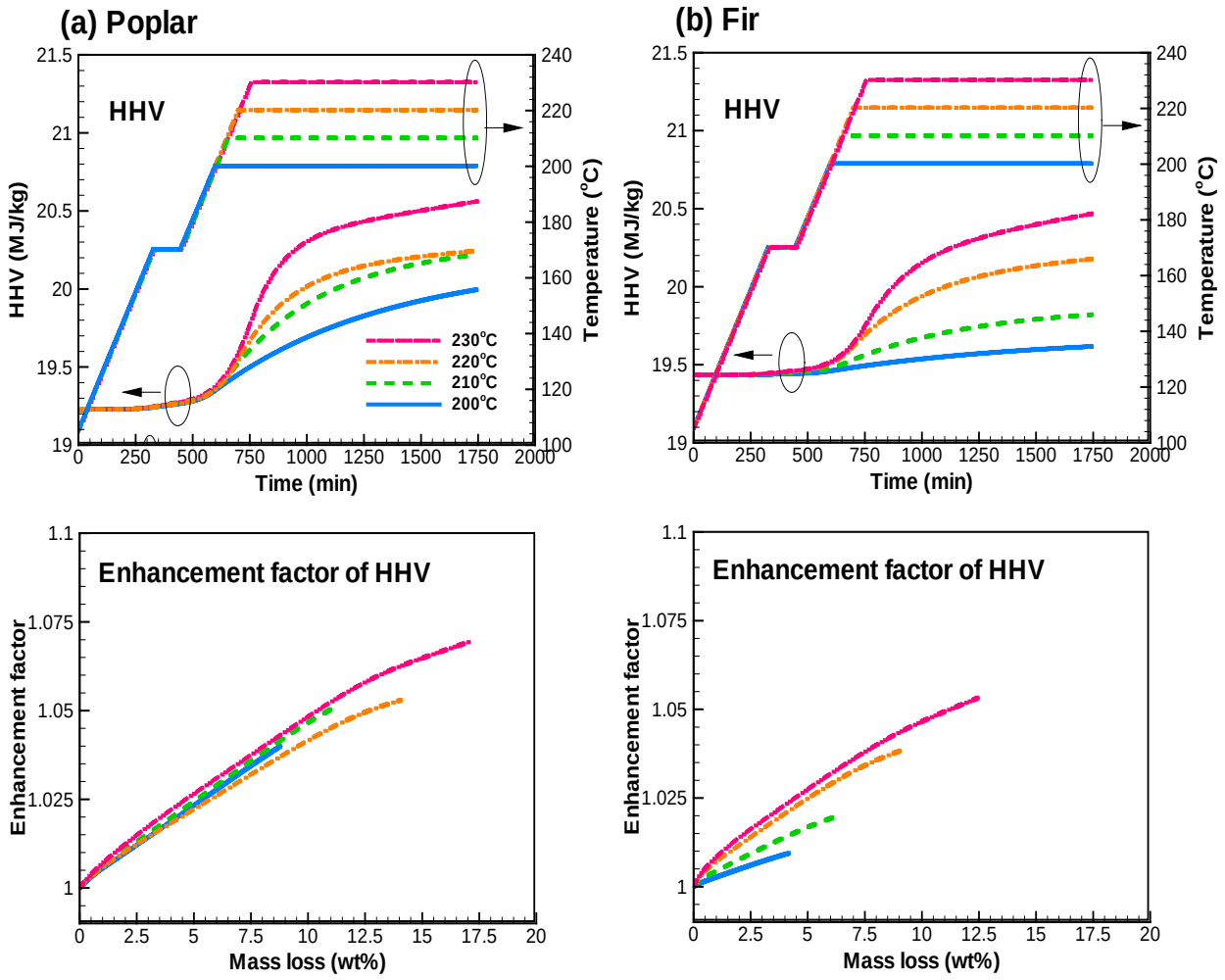

Fig. 4-23. Profiles of HHV and enhancement factor during heat treatment of (a) poplar(b) fir.

4.3.4 Characteristics of devolatilization

In the previous discussion (**Section 4.3.3**), the results of solid yield and elemental composition of treated wood have been obtained. These results are able to calculate the decarbonization (DC), dehydrogenation (DH), deoxygenation (DO), the formulas have been defined in **Section 4.2.4**. The behavior of devolatilization during thermal degradation can be evaluated by these three indicators (Chen et al., 2016).

The profiles of DC, DH, and DO in poplar and fir during treatment are presented in **Fig. 4-24**. Depending on the treatment temperature, the DC, DH, and DO extents in treated wood

at the end of treatment are in the ranges 1.71-6.84 %, 7.66-22.63 % and 6.16-26.44 %, respectively. The smaller extent of DC and larger extents of DH and DO are responsible for the decrease in the atomic H/C and O/C ratios in treated wood (Chen et al., 2016). Overall, the extents of DC, DH, and DO in fir are all smaller than in poplar, resulting from lower intensity of thermal degradation or devolatilization (i.e., V_1 and V_2 release) in fir (**Fig. 4-18a**).

The profiles of DC, DH, and DO versus mass loss in the treated woods are plotted in **Fig. 4-25** to examine the characteristics of DC, DH, and DO during treatment. Both the DH and DO have the trend to linearly increase with increasing mass loss, but DC doesn't at higher treatment temperatures (220 and 230 °C). These results could be ascribed to the dehydration reactions at the initial period of wood thermal degradation (Esteves & Pereira, 2008). The dehydration reactions caused by the degradation of polysaccharides during heat treatment reduces the number of hydroxyl groups in woods, resulting in the decrease of hygroscopicity in treated woods (Candelier et al., 2016; Yang et al., 2016). It is worthy of note that the DC extent is still close to zero in fir when the mass loss reaches 4%. These results could be owing to the larger extent of dehydration reactions in fir (Chen et al., 2018b). In summary, the characteristics of devolatilization in hardwood (poplar) and softwood (fir) are well evaluated by DC, DH, and DO. More importantly, these results are obtained from the kinetics of heat treated wood, and the predictions have a good agreement with the experimental results from the literature.

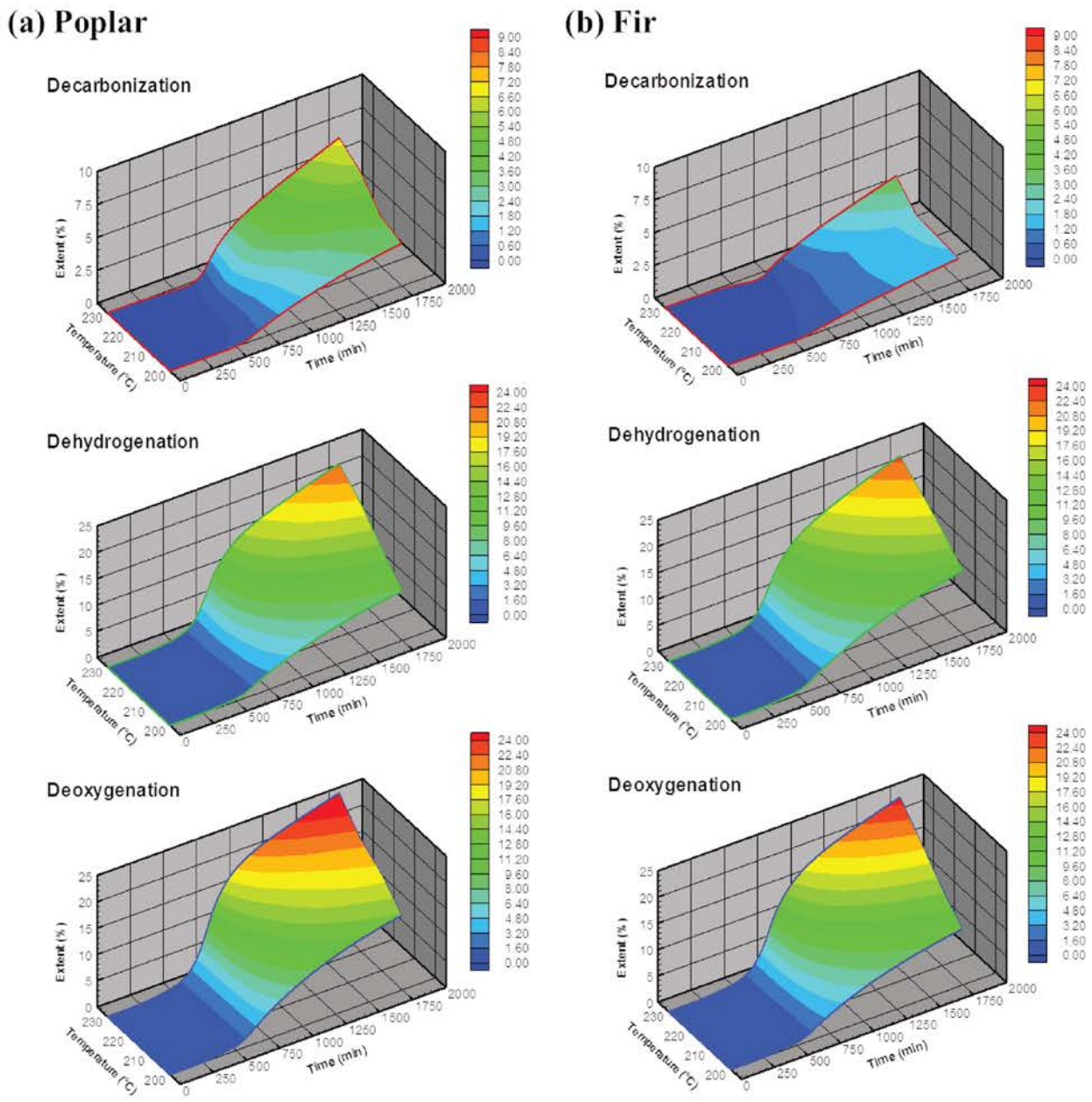

Fig. 4-24. Profiles of decarbonization, dehydrogenation, and deoxygenation of (a) poplar and (b) fir during treatment.

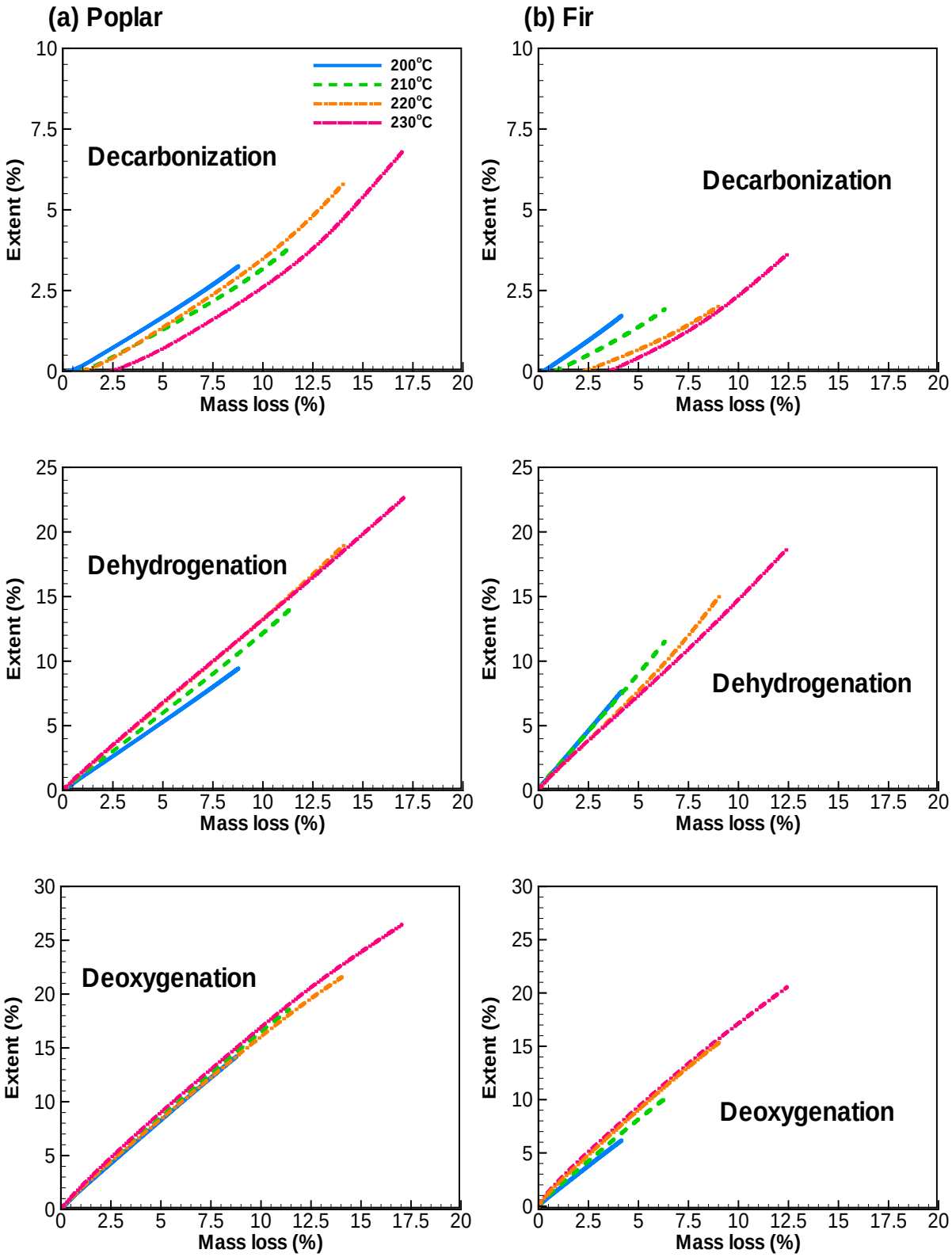

Fig. 4-25. Profiles of decarbonization, dehydrogenation, and deoxygenation versus mass loss of heat treated (a) poplar and (b) fir.

Chapter 5 Conclusions and Perspectives

The study focuses on mild pyrolysis of wood under industrial conditions for sustainable material production, and is divided into three parts: (1) thermal behavior of wood in a semi-industrial scale reactor; (2) property changes of treated wood; and (3) the kinetics and prediction of elemental compositions during treatment. The conclusions are descripted in **section 5.1.**

5.1 Conclusions

In the first part of study, the thermal degradation characteristics of woods during heat treatment in a semi-industrial scale reactor under vacuum have been investigated experimentally. Two wood species (poplar and fir) and four different treatment temperatures (200, 210, 220 and 230 °C) have been employed. From the differential mass loss (DML) curves, the thermal degradation of the wood materials during treatment can be divided into four different stages, and the thermal sensitivity of hardwood (poplar) is higher than that of softwood (fir), leading to higher mass loss. The TGA, DTG, and 2nd DTG curves can clearly identify the degradation of hemicelluloses, cellulose, and lignin in untreated and treated woods. The proximate and elemental analyses indicate that dehydrogenation and deoxygenation reactions of fir are stronger than those of poplar, resulting from stronger dehydration and removal of methoxyl from lignin condensation and stronger deoxygenation of hemicelluloses during degradation of the softwood. The correlations of atomic H/C and O/C ratios and devolatilization index versus mass loss are characterized by a strongly linear relationship. This last correlation provides a feasible and simple tool in predicting the mass loss of different woods undergoing heat treatment when a variety of operating parameters such as temperature, duration, and atmosphere have been inherently considered.

In the second part of the study, the results indicate that the changes in chemical structures before and after treatment can be examined from FTIR spectra. The detailed mechanisms such as deacetylation of hemicelluloses, depolymerization and dehydration of

hemicelluloses and cellulose, and condensation and split of lignin during treatment can be figured out. The XRD analysis further reveal the degradation of amorphous cellulose during heat treatment, leading to an increase in relative crystallinity after treatment. The measured color changes based on CIELAB color space indicate that lightness (L*) is the dominant factor in determining the total color difference (ΔE^*). The values of ΔE^* of the two woods are in range of 41.49-51.66 and increase with mass loss or torrefaction severity. A measurement of the hygroscopicity reduction extent is introduced to quantify the hygroscopic transformation of biomass. Overall, the hygroscopicity reduction extents of torrefied poplar and fir are in the range of 34.50-57.39 %, suggesting the strong transformation of the biomass from hygroscopic nature to hydrophobic behavior. The contact angles of the raw poplar and fir decay rapidly when water is dropped on the boards. The contact angles of all the torrefied samples are higher than 90 ° (in the range of 94-113 °), showing the hydrophobic nature of the surfaces. In addition, the contact angles of the torrefied fir are greater than those of torrefied poplar, ascribing to more tars present and condensed during the torrefaction of the fir. The extents of decarbonization (DC), dehydrogenation (DH), and deoxygenation (DO) from heat treatment are also evaluated, and strong linear relationships ($R2 > 0.87$) between these three indexes versus ΔE^*and hygroscopicity reduction extent are exhibited.

In the third part of study, a two-step model was adopted to evaluate the heat treated wood kinetics. The predictions of solid yields are in a well goodness-of-fit, and the values of R2 are in the range of 0.9656-0.9997. The evolutions of the three types of solids A (feedstock), B (intermediate), and C (residue) from the analysis suggest that the intermediate (B), ranging from 74.2 to 82.8 wt%, is the prime solid product in the heat treated woods. These results are similar to the woods undergoing light torrefaction. Meanwhile, the amounts of volatiles released from poplar and fir at 230°C are 17.05 and 12.44 wt%, respectively, and are responsible for the mass loss of wood. The predictions point out that the atomic H/C and O/C ratios start to obviously decrease after thermal homogenization stage (> 170 °C),

resulting from the devolatilization of woods. The HHVs of the treated woods computed from the predicted elemental compositions in association with an empirical formula reveal that they are in a range of 19.62-20.55 MJ kg-1, while the enhancement factors of HHV at the end of the treatments are in a range of 1.01-1.07. The intensities of decarbonization (DC), dehydrogenation (DH), and deoxygenation (DO) due to the devolatilization in fir are all smaller than those in poplar, resulting from lower intensity of thermal degradation or devolatilization in the former. Overall, the developed kinetics for wood heat treatment and the predictions on wood thermal degradation are able to provide valuable references for practical operation and reactor design.

5.2 Perspectives and suggestions

Wood heat treatment is an important and promising way to produce sustainable materials, which have been applied in bio-adsorbent, building and furniture materials. The development of pyrolysis kinetics has also been considered as an attractive approach to predict the products distributions, as well as evaluate the behavior and reactivity of thermal reactions. There are still several topics concerning the process improvement and development of wood heat treatment, the applications of treated woods, and the simulation and modeling that have to be explored. According to the experimental and numerical results presented in this study, the perspectives and suggestions are the followings:

1. Thermal behavior of wood boards heat treated under vacuum has been investigated in this study. However, in order to improve the knowledge about the thermal degradation of wood under different atmospheres, it is recommended to perform a comprehensive study comparing experiments from different processes (such as oil or steam treatment).
2. Recently, a number of studies have investigated the effects of potassium on biomass thermal degradation, and showed that they might act as catalysts in thermal reactions of biomass. However, very few studies have been performed on the influence of potassium

on biomass mild pyrolysis (heat treatment or torrefaction). For that, the catalytic effects of potassium on mild pyrolysis of wood are also suggested to be studied.

3. The kinetics obtained in the present study are based on a simplified global approach. However, the two-step kinetic model directly applied to the solid yield prediction of the heat treated wood boards in a semi-industrial scale reactor has shown promising results. Future development will aim to employ the model for practical applications in industry. For instance, a revised model coupling with the reaction heat, which is inserted as the heat source, could provide a more accurate characterization of thermal degradation during treatment.

References

Acharya, B., Dutta, A., Minaret, J. 2015. Review on comparative study of dry and wet torrefaction. *Sustainable Energy Technologies and Assessments*, **12**, 26-37.

Agudo, J.E., Pardo, P.J., Sánchez, H., Pérez, Á.L., Suero, M.I. 2014. A low-cost real color picker based on arduino. *Sensors*, **14**(7), 11943-11956.

Allegretti, O., Brunetti, M., Cuccui, I., Ferrari, S., Nocetti, M., Terziev, N. 2012. Thermo-vacuum modification of spruce (Picea abies Karst.) and fir (Abies alba Mill.) wood. *BioResources*, **7**(3), 3656-3669.

Bach, Q.-V., Chen, W.-H. 2017a. A comprehensive study on pyrolysis kinetics of microalgal biomass. *Energy conversion and management*, **131**, 109-116.

Bach, Q.-V., Chen, W.-H. 2017b. Pyrolysis characteristics and kinetics of microalgae via thermogravimetric analysis (TGA): A state-of-the-art review. *Bioresource Technology*, **246**, 88-100.

Bach, Q.-V., Chen, W.-H. 2017c. Pyrolysis characteristics and kinetics of microalgae via thermogravimetric analysis (TGA): a state-of-the-art review. *Bioresource technology*.

Bach, Q.-V., Chen, W.-H., Chu, Y.-S., Skreiberg, Ø. 2016. Predictions of biochar yield and elemental composition during torrefaction of forest residues. *Bioresource technology*, **215**, 239-246.

Bach, Q.-V., Skreiberg, Ø. 2016. Upgrading biomass fuels via wet torrefaction: A review and comparison with dry torrefaction. *Renewable and Sustainable Energy Reviews*, **54**, 665-677.

Balat, M., Balat, H., Öz, C. 2008. Progress in bioethanol processing. *Progress in Energy and Combustion Science*, **34**(5), 551-573.

Bamdad, H., Hawboldt, K., MacQuarrie, S. 2018. A review on common adsorbents for acid gases removal: Focus on biochar. *Renewable and Sustainable Energy Reviews*, **81**, 1705-1720.

Bates, R.B., Ghoniem, A.F. 2012. Biomass torrefaction: modeling of volatile and solid product evolution kinetics. *Bioresource technology*, **124**, 460-469.

Bhuiyan, M.T.R., Hirai, N., Sobue, N. 2000. Changes of crystallinity in wood cellulose by heat treatment under dried and moist conditions. *Journal of Wood Science*, **46**(6), 431-436.

Branca, C., Di Blasi, C. 2003. Kinetics of the isothermal degradation of wood in the temperature range 528–708 K. *Journal of Analytical and applied Pyrolysis*, **67**(2), 207-219.

Brosse, N., El Hage, R., Chaouch, M., Pétrissans, M., Dumarçay, S., Gérardin, P. 2010. Investigation of the chemical modifications of beech wood lignin during heat treatment. *Polymer Degradation and Stability*, **95**(9), 1721-1726.

Broström, M., Nordin, A., Pommer, L., Branca, C., Di Blasi, C. 2012. Influence of torrefaction on the devolatilization and oxidation kinetics of wood. *Journal of Analytical and Applied Pyrolysis*, **96**, 100-109.

Burra, K.R.G., Gupta, A.K. 2019. Modeling of biomass pyrolysis kinetics using sequential multi-step reaction model. *Fuel*, **237**, 1057-1067.

Candelier, K., Chaouch, M., Dumarçay, S., Pétrissans, A., Pétrissans, M., Gérardin, P. 2011. Utilization of thermodesorption coupled to GC–MS to study stability of different wood species to thermodegradation. *Journal of Analytical and Applied Pyrolysis*, **92**(2), 376-383.

Candelier, K., Dumarçay, S., Pétrissans, A., Desharnais, L., Gérardin, P., Pétrissans, M. 2013a. Comparison of chemical composition and decay durability of heat treated wood cured under different inert atmospheres: Nitrogen or vacuum. *Polymer Degradation and Stability*, **98**(2), 677-681.

Candelier, K., Dumarçay, S., Pétrissans, A., Gérardin, P., Pétrissans, M. 2013b. Comparison of mechanical properties of heat treated beech wood cured under nitrogen or vacuum. *Polymer Degradation and Stability*, **98**(9), 1762-1765.

Candelier, K., Dumarçay, S., Pétrissans, A., Pétrissans, M., Kamdem, P., Gérardin, P. 2013c. Thermodesorption coupled to GC–MS to characterize volatiles formation kinetic during wood thermodegradation. *Journal of analytical and applied pyrolysis*, **101**, 96-102.

Candelier, K., Thevenon, M.-F., Petrissans, A., Dumarcay, S., Gerardin, P., Petrissans, M. 2016. Control of wood thermal treatment and its effects on decay resistance: a review. *Annals of Forest Science*, **73**(3), 571-583.

Cao, Y., Lu, J., Huang, R., Jiang, J. 2012. Increased dimensional stability of Chinese fir through steam-heat treatment. *European Journal of Wood and Wood Products*, **70**(4), 441-444.

Carrier, M., Hardie, A.G., Uras, Ü., Görgens, J., Knoetze, J. 2012. Production of char from vacuum pyrolysis of South-African sugar cane bagasse and its characterization as activated carbon and biochar. *Journal of Analytical and Applied Pyrolysis*, **96**, 24-32.

Cavagnol, S., Sanz, E., Nastoll, W., Roesler, J.F., Zymla, V., Perré, P. 2013. Inverse analysis of wood pyrolysis with long residence times in the temperature range 210–290 C: Selection of multi-step kinetic models based on mass loss residues. *Thermochimica acta*, **574**, 1-9.

Chaouch, M., Dumarçay, S., Pétrissans, A., Pétrissans, M., Gérardin, P. 2013. Effect of heat treatment intensity on some conferred properties of different European softwood and hardwood species. *Wood Science and Technology*, **47**(4), 663-673.

Chaouch, M., Pétrissans, M., Pétrissans, A., Gérardin, P. 2010. Use of wood elemental composition to predict heat treatment intensity and decay resistance of different softwood and hardwood species. *Polymer Degradation and Stability*, **95**(12), 2255-2259.

Chen, D., Zheng, Z., Fu, K., Zeng, Z., Wang, J., Lu, M. 2015a. Torrefaction of biomass stalk and its effect on the yield and quality of pyrolysis products. *Fuel*, **159**, 27-32.

Chen, D., Zhou, J., Zhang, Q. 2014a. Effects of heating rate on slow pyrolysis behavior, kinetic parameters and products properties of moso bamboo. *Bioresource Technology*, **169**, 313-319.

Chen, W.-H., Cheng, W.-Y., Lu, K.-M., Huang, Y.-P. 2011. An evaluation on improvement of pulverized biomass property for solid fuel through torrefaction. *Applied Energy*, **88**(11), 3636-3644.

Chen, W.-H., Chu, Y.-S., Liu, J.-L., Chang, J.-S. 2018a. Thermal degradation of carbohydrates, proteins and lipids in microalgae analyzed by evolutionary computation. *Energy Conversion and Management*, **160**, 209-219.

Chen, W.-H., Hsu, H.-J., Kumar, G., Budzianowski, W.M., Ong, H.C. 2017. Predictions of biochar production and torrefaction performance from sugarcane bagasse using interpolation and regression analysis. *Bioresource technology*, **246**, 12-19.

Chen, W.-H., Kuo, P.-C. 2011a. Isothermal torrefaction kinetics of hemicellulose, cellulose, lignin and xylan using thermogravimetric analysis. *Energy*, **36**(11), 6451-6460.

Chen, W.-H., Kuo, P.-C. 2010. A study on torrefaction of various biomass materials and its impact on lignocellulosic structure simulated by a thermogravimetry. *Energy*, **35**(6), 2580-2586.

Chen, W.-H., Kuo, P.-C. 2011b. Torrefaction and co-torrefaction characterization of hemicellulose, cellulose and lignin as well as torrefaction of some basic constituents in biomass. *Energy*, **36**(2), 803-811.

Chen, W.-H., Lin, B.-J., Colin, B., Chang, J.-S., Pétrissans, A., Bi, X., Pétrissans, M. 2018b. Hygroscopic transformation of woody biomass torrefaction for carbon storage. *Applied Energy*, **231**, 768-776.

Chen, W.-H., Lin, B.-J., Huang, M.-Y., Chang, J.-S. 2015b. Thermochemical conversion of microalgal biomass into biofuels: A review. *Bioresource Technology*, **184**, 314-327.

Chen, W.-H., Peng, J., Bi, X.T. 2015c. A state-of-the-art review of biomass torrefaction, densification and applications. *Renewable and Sustainable Energy Reviews*, **44**, 847-866.

Chen, W.-H., Tu, Y.-J., Sheen, H.-K. 2010. Impact of dilute acid pretreatment on the structure of bagasse for bioethanol production. *International Journal of Energy Research*, **34**(3), 265-274.

Chen, W.-H., Wu, Z.-Y., Chang, J.-S. 2014b. Isothermal and non-isothermal torrefaction characteristics and kinetics of microalga Scenedesmus obliquus CNW-N. *Bioresource technology*, **155**, 245-251.

Chen, Y.-C., Chen, W.-H., Lin, B.-J., Chang, J.-S., Ong, H.C. 2016. Impact of torrefaction on the composition, structure and reactivity of a microalga residue. *Applied Energy*, **181**, 110-119.

Cheng, G., Zhang, X., Simmons, B., Singh, S. 2015. Theory, practice and prospects of X-ray and neutron scattering for lignocellulosic biomass characterization: towards understanding biomass pretreatment. *Energy & Environmental Science*, **8**(2), 436-455.

Ciolkosz, D., Wallace, R. 2011. A review of torrefaction for bioenergy feedstock production. *Biofuels, Bioproducts and Biorefining*, **5**(3), 317-329.

Clarivate Analytics: https://login.webofknowledge.com

Cogulet, A., Blanchet, P., Landry, V., Morris, P. 2018. Weathering of wood coated with semi-clear coating: Study of interactions between photo and biodegradation. *International Biodeterioration & Biodegradation*, **129**, 33-41.

Colin, B., Dirion, J.-L., Arlabosse, P., Salvador, S. 2017. Quantification of the torrefaction effects on the grindability and the hygroscopicity of wood chips. *Fuel*, **197**, 232-239.

Collard, F.-X., Blin, J. 2014. A review on pyrolysis of biomass constituents: Mechanisms and composition of the products obtained from the conversion of cellulose, hemicelluloses and lignin. *Renewable and Sustainable Energy Reviews*, **38**, 594-608.

Davison, B.H., Parks, J., Davis, M.F., Donohoe, B.S. 2013. Plant cell walls: basics of structure, chemistry, accessibility and the influence on conversion. *Aqueous Pretreatment of Plant Biomass for Biological and Chemical Conversion to Fuels and Chemicals*, 23-38.

de Oliveira Araújo, S., Rocha Vital, B., Oliveira, B., Oliveira Carneiro, A.d.C., Lourenço, A., Pereira, H. 2016. Physical and mechanical properties of heat treated wood from Aspidosperma populifolium, Dipteryx odorata and Mimosa scabrella. *Maderas. Ciencia y tecnología*, **18**(1), 143-156.

Dewayanto, N., Isha, R., Nordin, M.R. 2014. Use of palm oil decanter cake as a new substrate for the production of bio-oil by vacuum pyrolysis. *Energy Conversion and Management*, **86**, 226-232.

Di Blasi, C., Lanzetta, M. 1997. Intrinsic kinetics of isothermal xylan degradation in inert atmosphere. *Journal of Analytical and Applied Pyrolysis*, **40**, 287-303.

Ding, Y., Ezekoye, O.A., Zhang, J., Wang, C., Lu, S. 2018. The effect of chemical reaction kinetic parameters on the bench-scale pyrolysis of lignocellulosic biomass. *Fuel*, **232**, 147-153.

Ding, Y., Wang, C., Chaos, M., Chen, R., Lu, S. 2016. Estimation of beech pyrolysis kinetic parameters by Shuffled Complex Evolution. *Bioresource Technology*, **200**, 658-665.

Doddapaneni, T.R.K.C., Konttinen, J., Hukka, T.I., Moilanen, A. 2016. Influence of torrefaction pretreatment on the pyrolysis of Eucalyptus clone: A study on kinetics, reaction mechanism and heat flow. *Industrial Crops and Products*, **92**, 244-254.

Dubey, M.K., Pang, S., Walker, J. 2011. Effect of oil heating age on colour and dimensional stability of heat treated Pinus radiata. *European Journal of Wood and Wood Products*, **69**(2), 255-262.

Dwianto, W., Tanaka, F., Inoue, M., NORIMOTO, M. 1996. Crystallinity changes of wood by heat or steam treatment.

Emmanuel, V., Odile, B., Céline, R. 2015. FTIR spectroscopy of woods: A new approach to study the weathering of the carving face of a sculpture. *Spectrochimica Acta Part A: Molecular and Biomolecular Spectroscopy*, **136**, 1255-1259.

Esteves, B., Marques, A.V., Domingos, I., Pereira, H. 2006. Influence of steam heating on the properties of pine (Pinus pinaster) and eucalypt (Eucalyptus globulus) wood. *Wood Science and Technology*, **41**(3), 193.

Esteves, B., Pereira, H. 2008. Wood modification by heat treatment: A review. *BioResources*, **4**(1), 370-404.

Esteves, B., Velez Marques, A., Domingos, I., Pereira, H. 2013. Chemical changes of heat treated pine and eucalypt wood monitored by FTIR. *Maderas. Ciencia y tecnología*, **15**(2), 245-258.

Esteves, B., Velez Marques, A., Domingos, I., Pereira, H. 2008. Heat-induced colour changes of pine (Pinus pinaster) and eucalypt (Eucalyptus globulus) wood. *Wood Science and Technology*, **42**(5), 369-384.

Fan, Y., Cai, Y., Li, X., Yin, H., Yu, N., Zhang, R., Zhao, W. 2014. Rape straw as a source of bio-oil via vacuum pyrolysis: Optimization of bio-oil yield using orthogonal design

method and characterization of bio-oil. *Journal of Analytical and Applied Pyrolysis*, **106**, 63-70.

FAO : http://www.fao.org/fishery/publications/en#container

Ferrari, S., Allegretti, O., Cuccui, I., Moretti, N., Marra, M., Todaro, L. 2013a. A revaluation of Turkey oak wood (Quercus cerris L.) through combined steaming and thermo-vacuum treatments. *BioResources*, **8**(4), 5051-5066.

Ferrari, S., Cuccui, I., Allegretti, O. 2013b. Thermo-vacuum modification of some European softwood and hardwood species treated at different conditions. *BioResources*, **8**(1), 1100-1109.

Fuller, A., Stegmaier, M., Schulz, N., Menke, M., Schellhorn, H., Knödler, F., Maier, J., Scheffknecht, G. 2018. Use of wood dust fly ash from an industrial pulverized fuel facility for rendering. *Construction and Building Materials*, **189**, 825-848.

Geng, A., Yang, H., Chen, J., Hong, Y. 2017. Review of carbon storage function of harvested wood products and the potential of wood substitution in greenhouse gas mitigation. *Forest Policy and Economics*, **85**, 192-200.

Giurca, A., Späth, P. 2017. A forest-based bioeconomy for Germany? Strengths, weaknesses and policy options for lignocellulosic biorefineries. *Journal of Cleaner Production*, **153**, 51-62.

González-Peña Marcos, M., Hale Michael, D.C. 2009. Colour in thermally modified wood of beech, Norway spruce and Scots pine. Part 1: Colour evolution and colour changes. in: *Holzforschung*, Vol. 63, pp. 385.

Grønli, M.G., Várhegyi, G., Di Blasi, C. 2002. Thermogravimetric analysis and devolatilization kinetics of wood. *Industrial & Engineering Chemistry Research*, **41**(17), 4201-4208.

Granados, D.A., Ruiz, R.A., Vega, L.Y., Chejne, F. 2017. Study of reactivity reduction in sugarcane bagasse as consequence of a torrefaction process. *Energy*, **139**, 818-827.

Gul, S., Ramzan, N., Hanif, M.A., Bano, S. 2017. Kinetic, volatile release modeling and optimization of torrefaction. *Journal of Analytical and Applied Pyrolysis*, **128**, 44-53.

Gustavsson, L., Madlener, R., Hoen, H.-F., Jungmeier, G., Karjalainen, T., KlÖhn, S., Mahapatra, K., Pohjola, J., Solberg, B., Spelter, H. 2006. The Role of Wood Material for Greenhouse Gas Mitigation. *Mitigation and Adaptation Strategies for Global Change*, **11**(5), 1097-1127.

Hakkou, M., Pétrissans, M., Gérardin, P., Zoulalian, A. 2006. Investigations of the reasons for fungal durability of heat-treated beech wood. *Polymer degradation and stability*, **91**(2), 393-397.

Hernández, W.Y., Lauwaert, J., Van Der Voort, P., Verberckmoes, A. 2017. Recent advances on the utilization of layered double hydroxides (LDHs) and related heterogeneous catalysts in a lignocellulosic-feedstock biorefinery scheme. *Green Chemistry*, **19**(22), 5269-5302.

Hill, C.A. 2007. *Wood modification: chemical, thermal and other processes*. John Wiley & Sons.

Himmel, M.E., Ding, S.-Y., Johnson, D.K., Adney, W.S., Nimlos, M.R., Brady, J.W., Foust, T.D. 2007. Biomass Recalcitrance: Engineering Plants and Enzymes for Biofuels Production. *Science*, **315**(5813), 804-807.

Hori, R., Wada, M. 2005. The Thermal Expansion of Wood Cellulose Crystals. *Cellulose*, **12**(5), 479.

Iroba, K.L., Baik, O.-D., Tabil, L.G. 2017. Torrefaction of biomass from municipal solid waste fractions II: Grindability characteristics, higher heating value, pelletability and moisture adsorption. *Biomass and Bioenergy*, **106**, 8-20.

Ismadji, S., Sudaryanto, Y., Hartono, S.B., Setiawan, L.E.K., Ayucitra, A. 2005. Activated carbon from char obtained from vacuum pyrolysis of teak sawdust: pore structure development and characterization. *Bioresource Technology*, **96**(12), 1364-1369.

Jaya, S.T., Shahab, S., Richard, H.J., T., W.C., D., B.R. 2011. REVIEW: A review on biomass torrefaction process and product properties for energy applications. *Industrial Biotechnology*, **7**(5), 384-401.

Järvinen, T., Agar, D. 2014. Experimentally determined storage and handling properties of fuel pellets made from torrefied whole-tree pine chips, logging residues and beech stem wood. *Fuel*, **129**, 330-339.

Kambo, H.S., Dutta, A. 2015. A comparative review of biochar and hydrochar in terms of production, physico-chemical properties and applications. *Renewable and Sustainable Energy Reviews*, **45**, 359-378.

Karinkanta, P., Ämmälä, A., Illikainen, M., Niinimäki, J. 2018. Fine grinding of wood – Overview from wood breakage to applications. *Biomass and Bioenergy*, **113**, 31-44.

Klinger, J., Klemetsrud, B., Bar-Ziv, E., Shonnard, D. 2014. Temperature dependence of aspen torrefaction kinetics. *Journal of Analytical and Applied Pyrolysis*, **110**, 424-429.

Korkut, S., Hiziroglu, S. 2009. Effect of heat treatment on mechanical properties of hazelnut wood (Corylus colurna L.). *Materials & Design*, **30**(5), 1853-1858.

Kymäläinen, M., Havimo, M., Keriö, S., Kemell, M., Solio, J. 2014. Biological degradation of torrefied wood and charcoal. *Biomass and Bioenergy*, **71**, 170-177.

Lee, S.H., Ashaari, Z., Lum, W.C., Abdul Halip, J., Ang, A.F., Tan, L.P., Chin, K.L., Md Tahir, P. 2018. Thermal treatment of wood using vegetable oils: A review. *Construction and Building Materials*, **181**, 408-419.

Li, K.-Y., Huang, X., Fleischmann, C., Rein, G., Ji, J. 2014. Pyrolysis of Medium-Density Fiberboard: Optimized Search for Kinetics Scheme and Parameters via a Genetic Algorithm Driven by Kissinger's Method. *Energy & Fuels*, **28**(9), 6130-6139.

Li, M.-F., Chen, L.-X., Li, X., Chen, C.-Z., Lai, Y.-C., Xiao, X., Wu, Y.-Y. 2016. Evaluation of the structure and fuel properties of lignocelluloses through carbon dioxide torrefaction. *Energy Conversion and Management*, **119**, 463-472.

Li, M.-Y., Cheng, S.-C., Li, D., Wang, S.-N., Huang, A.-M., Sun, S.-Q. 2015a. Structural characterization of steam-heat treated Tectona grandis wood analyzed by FT-IR and 2D-IR correlation spectroscopy. *Chinese Chemical Letters*, **26**(2), 221-225.

Li, T., Cheng, D.-l., Wålinder, M.E.P., Zhou, D.-g. 2015b. Wettability of oil heat-treated bamboo and bonding strength of laminated bamboo board. *Industrial Crops and Products*, **69**, 15-20.

Lin, B.-J., Colin, B., Chen, W.-H., Pétrissans, A., Rousset, P., Pétrissans, M. 2018. Thermal degradation and compositional changes of wood treated in a semi-industrial scale reactor in vacuum. *Journal of Analytical and Applied Pyrolysis*, **130**, 8-18.

Lohri, C.R., Rajabu, H.M., Sweeney, D.J., Zurbrügg, C. 2016. Char fuel production in developing countries – A review of urban biowaste carbonization. *Renewable and Sustainable Energy Reviews*, **59**, 1514-1530.

Lu, K.-M., Lee, W.-J., Chen, W.-H., Liu, S.-H., Lin, T.-C. 2012. Torrefaction and low temperature carbonization of oil palm fiber and eucalyptus in nitrogen and air atmospheres. *Bioresource Technology*, **123**, 98-105.

Lyon, F., Thevenon, M.-F., Hwang, W.-J., Imamura, Y., Gril, J., Pizzi, A. 2007. Effect of an oil heat treatment on the teachability and biological resistance of boric acid impregnated wood. *Annals of Forest Science*, **64**(6), 673-678.

Mathews, S.L., Pawlak, J., Grunden, A.M. 2015. Bacterial biodegradation and bioconversion of industrial lignocellulosic streams. *Applied microbiology and biotechnology*, **99**(7), 2939-2954.

Mazeau, K., Heux, L. 2003. Molecular Dynamics Simulations of Bulk Native Crystalline and Amorphous Structures of Cellulose. *The Journal of Physical Chemistry B*, **107**(10), 2394-2403.

Mei, Y., Liu, R., Yang, Q., Yang, H., Shao, J., Draper, C., Zhang, S., Chen, H. 2015. Torrefaction of cedarwood in a pilot scale rotary kiln and the influence of industrial flue gas. *Bioresource Technology*, **177**, 355-360.

Mohanty, A.K., Misra, M., Drzal, L.T. 2002. Sustainable Bio-Composites from Renewable Resources: Opportunities and Challenges in the Green Materials World. *Journal of Polymers and the Environment*, **10**(1), 19-26.

Mosier, N., Wyman, C., Dale, B., Elander, R., Lee, Y., Holtzapple, M., Ladisch, M. 2005. Features of promising technologies for pretreatment of lignocellulosic biomass. *Bioresource technology*, **96**(6), 673-686.

Na, B.-I., Ahn, B.-J., Lee, J.-W. 2015. Changes in chemical and physical properties of yellow poplar (Liriodendron tulipifera) during torrefaction. *Wood Science and Technology*, **49**(2), 257-272.

Nguyen, C.T., Wagenführ, A., Dai, V.H., Bremer, M., Fischer, S. 2012. The effects of thermal modification on the properties of two Vietnamese bamboo species, Part I: effects on physical properties. *BioResources*, **7**(4), 5355-5366.

Okon, K.E., Lin, F., Chen, Y., Huang, B. 2017. Effect of silicone oil heat treatment on the chemical composition, cellulose crystalline structure and contact angle of Chinese parasol wood. *Carbohydrate Polymers*, **164**, 179-185.

Oluoti, K., Doddapaneni, T.R.K.C., Richards, T. 2018. Investigating the kinetics and biofuel properties of Alstonia congensis and Ceiba pentandra via torrefaction. *Energy*, **150**, 134-141.

Özgenç, Ö., Durmaz, S., Boyaci, I.H., Eksi-Kocak, H. 2017. Determination of chemical changes in heat-treated wood using ATR-FTIR and FT Raman spectrometry. *Spectrochimica Acta Part A: Molecular and Biomolecular Spectroscopy*, **171**, 395-400.

Pétrissans, A., Hamada, J., Chaouch, M., Pétrissans, M., Gérardin, P. 2015. Modeling and numerical simulation of wood torrefaction. *Innovation in woodworking industry and engineering design*, **5**, 26-32.

Pétrissans, A., Younsi, R., Chaouch, M., Gérardin, P., Pétrissans, M. 2014. Wood thermodegradation: experimental analysis and modeling of mass loss kinetics. *Maderas. Ciencia y tecnología*, **16**(2), 133-148.

Pétrissans, M., Gérardin, P., bakali, I.E., Serraj, M. 2003. Wettability of Heat-Treated Wood. in: *Holzforschung*, Vol. 57, pp. 301.

Park, S.-W., Jang, C.-H., Baek, K.-R., Yang, J.-K. 2012. Torrefaction and low-temperature carbonization of woody biomass: Evaluation of fuel characteristics of the products. *Energy*, **45**(1), 676-685.

Paul, W., Ohlmeyer, M., Leithoff, H. 2006. Thermal modification of OSB-strands by a one-step heat pre-treatment – Influence of temperatureon weight loss, hygroscopicity and improved fungal resistance. *Holz als Roh- und Werkstoff*, **65**(1), 57.

Pelaez-Samaniego, M.R., Yadama, V., Lowell, E., Espinoza-Herrera, R. 2013. A review of wood thermal pretreatments to improve wood composite properties. *Wood Science and Technology*, **47**(6), 1285-1319.

Pettersen, R.C. 1984. The Chemical Composition of Wood. in: *The Chemistry of Solid Wood*, Vol. 207, American Chemical Society, pp. 57-126.

Poletto, M., Zattera, A.J., Forte, M.M.C., Santana, R.M.C. 2012. Thermal decomposition of wood: Influence of wood components and cellulose crystallite size. *Bioresource Technology*, **109**, 148-153.

Popescu, M.-C., Froidevaux, J., Navi, P., Popescu, C.-M. 2013. Structural modifications of Tilia cordata wood during heat treatment investigated by FT-IR and 2D IR correlation spectroscopy. *Journal of Molecular Structure*, **1033**, 176-186.

Pätäri, S., Arminen, H., Albareda, L., Puumalainen, K., Toppinen, A. 2017. A - Student values and perceptions of corporate social responsibility in the forest industry on the road to a bioeconomy. *Forest Policy and Economics*, **85**, 201-215.

Prida, A., Puech, J.-L. 2006. Influence of Geographical Origin and Botanical Species on the Content of Extractives in American, French, and East European Oak Woods. *Journal of Agricultural and Food Chemistry*, **54**(21), 8115-8126.

Prins, M.J., Ptasinski, K.J., Janssen, F.J. 2006. Torrefaction of wood: Part 1. Weight loss kinetics. *Journal of analytical and applied pyrolysis*, **77**(1), 28-34.

Purkus, A., Hagemann, N., Bedtke, N., Gawel, E. 2018. Towards a sustainable innovation system for the German wood-based bioeconomy: Implications for policy design. *Journal of Cleaner Production*, **172**, 3955-3968.

Ramage, M.H., Burridge, H., Busse-Wicher, M., Fereday, G., Reynolds, T., Shah, D.U., Wu, G., Yu, L., Fleming, P., Densley-Tingley, D., Allwood, J., Dupree, P., Linden, P.F., Scherman, O. 2017. The wood from the trees: The use of timber in construction. *Renewable and Sustainable Energy Reviews*, **68**, 333-359.

Ramos-Carmona, S., Martínez, J.D., Pérez, J.F. 2018. Torrefaction of patula pine under air conditions: A chemical and structural characterization. *Industrial Crops and Products*, **118**, 302-310.

Rapp, A.O. 2001. Review on heat treatments of wood. *Proceedings of special seminar, Antibes, France*. pp. 1-66.

Rapp, A.O., Sailer, M. 2000. Heat treatment of wood in Germany-state of the art. *Proceedings of the seminar on production of heat treated wood in Europe*. pp. 2000.

Rashid, S.R.M., Harun, N.H.H.M., Saleh, S., Samad, N.A.F.A. 2017. Modelling Anhydrous Weight Loss of Torrefied Wood Sawdust. *Energy Procedia*, **138**, 319-324.

Reza, M.T., Lynam, J.G., Vasquez, V.R., Coronella, C.J. 2012. Pelletization of biochar from hydrothermally carbonized wood. *Environmental Progress & Sustainable Energy*, **31**(2), 225-234.

Ridout, A.J., Carrier, M., Collard, F.-X., Görgens, J. 2016. Energy conversion assessment of vacuum, slow and fast pyrolysis processes for low and high ash paper waste sludge. *Energy Conversion and Management*, **111**, 103-114.

Sandak, A., Sandak, J., Allegretti, O. 2015. Quality control of vacuum thermally modified wood with near infrared spectroscopy. *Vacuum*, **114**, 44-48.

Sandberg, D., Kutnar, A. 2016. Thermally modified timber: recent developments in Europe and North America. *Wood and Fiber Science*, **48**(1), 28-39.

Sandberg, D., Kutnar, A., Mantanis, G. 2017. Wood modification technologies-a review. *iForest-Biogeosciences and Forestry*, **10**(6), 895.

Shang, L., Ahrenfeldt, J., Holm, J.K., Bach, L.S., Stelte, W., Henriksen, U.B. 2014. Kinetic model for torrefaction of wood chips in a pilot-scale continuous reactor. *Journal of analytical and applied pyrolysis*, **108**, 109-116.

Sheng, C., Azevedo, J. 2005. Estimating the higher heating value of biomass fuels from basic analysis data. *Biomass and Bioenergy*, **28**(5), 499-507.

Sheth, P.N., Babu, B.V. 2008. Differential Evolution Approach for Obtaining Kinetic Parameters in Nonisothermal Pyrolysis of Biomass. *Materials and Manufacturing Processes*, **24**(1), 47-52.

Shoulaifar, T.K., DeMartini, N., Karlström, O., Hemming, J., Hupa, M. 2016. Impact of organically bonded potassium on torrefaction: Part 2. Modeling. *Fuel*, **168**, 107-115.

Silveira, E.A., Lin, B.-J., Colin, B., Chaouch, M., Pétrissans, A., Rousset, P., Chen, W.-H., Pétrissans, M. 2018. Heat treatment kinetics using three-stage approach for sustainable wood material production. *Industrial Crops and Products*, **124**, 563-571.

Simoneit, B.R.T. 2002. Biomass burning — a review of organic tracers for smoke from incomplete combustion. *Applied Geochemistry*, **17**(3), 129-162.

Stokke, D.D., Gardner, D.J. 2003. Fundamental aspects of wood as a component of thermoplastic composites. *Journal of Vinyl and Additive Technology*, **9**(2), 96-104.

Strandberg, M., Olofsson, I., Pommer, L., Wiklund-Lindström, S., Åberg, K., Nordin, A. 2015. Effects of temperature and residence time on continuous torrefaction of spruce wood. *Fuel Processing Technology*, **134**, 387-398.

Šušteršic, Ž., Mohareb, A., Chaouch, M., Pétrissans, M., Petrič, M., Gérardin, P. 2010. Prediction of the decay resistance of heat treated wood on the basis of its elemental composition. *Polymer Degradation and Stability*, **95**(1), 94-97.

Syrjänen, T., Oy, K., Jämsä, S., Viitaniemi, P. 2000. Heat treatment of wood in Finland-state of the art. *Proceedings of the Trä skydd-, vä rmebehandlat trä-, egenskaper och anvä ndningsomra den, Stockholm, Sweden*, **21**.

Tankut, N., Tankut, A.N., Zor, M. 2014. Mechanical properties of heat-treated wooden material utilized in the construction of outdoor sitting furniture. *Turkish Journal of Agriculture and Forestry*, **38**(1), 148-158.

Tooyserkani, Z., Sokhansanj, S., Bi, X., Lim, J., Lau, A., Saddler, J., Kumar, L., Lam, P.S., Melin, S. 2013. Steam treatment of four softwood species and bark to produce torrefied wood. *Applied Energy*, **103**, 514-521.

Turner, I., Rousset, P., Rémond, R., Perré, P. 2010. An experimental and theoretical investigation of the thermal treatment of wood (Fagus sylvatica L.) in the range 200–260 C. *International Journal of Heat and Mass Transfer*, **53**(4), 715-725.

Valette, N., Perrot, T., Sormani, R., Gelhaye, E., Morel-Rouhier, M. 2017. Antifungal activities of wood extractives. *Fungal Biology Reviews*, **31**(3), 113-123.

Vo, T.K., Cho, J.-S., Kim, S.-S., Ko, J.-H., Kim, J. 2017. Genetically engineered hybrid poplars for the pyrolytic production of bio-oil: Pyrolysis characteristics and kinetics. *Energy Conversion and Management*, **153**, 48-59.

Wang, L., Barta-Rajnai, E., Skreiberg, Ø., Khalil, R., Czégény, Z., Jakab, E., Barta, Z., Grønli, M. 2018a. Effect of torrefaction on physiochemical characteristics and grindability of stem wood, stump and bark. *Applied Energy*, **227**, 137-148.

Wang, S., Dai, G., Ru, B., Zhao, Y., Wang, X., Zhou, J., Luo, Z., Cen, K. 2016. Effects of torrefaction on hemicellulose structural characteristics and pyrolysis behaviors. *Bioresource technology*, **218**, 1106-1114.

Wang, S., Dai, G., Yang, H., Luo, Z. 2017. Lignocellulosic biomass pyrolysis mechanism: a state-of-the-art review. *Progress in Energy and Combustion Science*, **62**, 33-86.

Wang, Y., Zhang, Z., Fan, H., Wang, J. 2018b. Wood carbonization as a protective treatment on resistance to wood destroying fungi. *International Biodeterioration & Biodegradation*, **129**, 42-49.

Weerachanchai, P., Tangsathitkulchai, C., Tangsathitkulchai, M. 2010. Comparison of pyrolysis kinetic models for thermogravimetric analysis of biomass. *Suranaree Journal of Science and Technology*, **17**(4), 387-400.

Wikberg, H., Liisa Maunu, S. 2004. Characterisation of thermally modified hard- and softwoods by 13C CPMAS NMR. *Carbohydrate Polymers*, **58**(4), 461-466.

Wu, W., Qiu, K. 2014. Vacuum co-pyrolysis of Chinese fir sawdust and waste printed circuit boards. Part I: Influence of mass ratio of reactants. *Journal of Analytical and Applied Pyrolysis*, **105**, 252-261.

Yang, H., Yan, R., Chen, H., Lee, D.H., Zheng, C. 2007. Characteristics of hemicellulose, cellulose and lignin pyrolysis. *Fuel*, **86**(12–13), 1781-1788.

Yang, T.-H., Chang, F.-R., Lin, C.-J., Chang, F.-C. 2016. Effects of temperature and duration of heat treatment on the physical, surface, and mechanical properties of Japanese cedar wood. *BioResources*, **11**(2), 3947-3963.

Yildiz, S., Gezer, E.D., Yildiz, U.C. 2006. Mechanical and chemical behavior of spruce wood modified by heat. *Building and environment*, **41**(12), 1762-1766.

Yin, J., Yuan, T., Lu, Y., Song, K., Li, H., Zhao, G., Yin, Y. 2017. Effect of compression combined with steam treatment on the porosity, chemical compositon and cellulose crystalline structure of wood cell walls. *Carbohydrate Polymers*, **155**, 163-172.

Yun, H., Tu, D., Li, K., Huang, J., Ou, L. 2015. Variation and Correlation of Heat-Treated Wood's Crystalline Structure and Impact Toughness. *BioResources*, **10**(1), 1487-1494.

Zhang, C., Ho, S.-H., Chen, W.-H., Xie, Y., Liu, Z., Chang, J.-S. 2018. Torrefaction performance and energy usage of biomass wastes and their correlations with torrefaction severity index. *Applied Energy*, **220**, 598-604.

Zhang, W., Yuan, C., Xu, J., Yang, X. 2015. Beneficial synergetic effect on gas production during co-pyrolysis of sewage sludge and biomass in a vacuum reactor. *Bioresource Technology*, **183**, 255-258.

Zheng, A., Jiang, L., Zhao, Z., Huang, Z., Zhao, K., Wei, G., Wang, X., He, F., Li, H. 2015. Impact of Torrefaction on the Chemical Structure and Catalytic Fast Pyrolysis Behavior of Hemicellulose, Lignin, and Cellulose. *Energy & Fuels*, **29**(12), 8027-8034.

Zheng, A., Zhao, Z., Chang, S., Huang, Z., Wang, X., He, F., Li, H. 2013. Effect of torrefaction on structure and fast pyrolysis behavior of corncobs. *Bioresource Technology*, **128**, 370-377.

Zhou, X., Li, W., Mabon, R., Broadbelt, L.J. 2017. A Critical Review on Hemicellulose Pyrolysis. *Energy Technology*, **5**(1), 52-79.

List of Publications

Book

1. **Bo-Jhih Lin.** "Reaction Characteristics of Syngas Production from Carbon Dioxide and Direct Dimethyl Ether Synthesis," Master thesis, National University of Tainan, 2012.
2. **Bo-Jhih Lin.** "Investigations of wood treated by mild pyrolysis in a semi-industrial reactor for sustainable material production: thermal behavior, property changes and kinetic modeling," PhD thesis, University of Lorraine, 2019.

International Journal

1. **Bo-Jhih Lin**, Baptiste Colin, Wei-Hsin Chen, Anélie Pétrissans, Patrick Rousset, Mathieu Pétrissans. Thermal degradation and compositional changes of wood treated in a semi-industrial scale reactor in vacuum. Journal of Analytical and Applied Pyrolysis 2018;130:8-18. **(SCI : IF=3.468)**
2. Edgar A. Silveira, **Bo-Jhih Lin**, Baptiste Colin, Mounir Chaouch, Anélie Pétrissans, Patrick Rousset, Wei-Hsin Chen, Mathieu Pétrissans. Heat treatment kinetics using three-stage approach for sustainable wood material production. Industrial Crops and Products 2018;124:563-571. **(SCI : IF=3.849)**
3. Wei-Hsin Chen, **Bo-Jhih Lin**, Baptiste Colin, Jo-Shu Chang, Anélie Pétrissans, Xiaotao Bi, Mathieu Pétrissans. Hygroscopic transformation of woody biomass torrefaction for carbon storage. Applied Energy 2018;231:768-776. **(SCI : IF=7.900)**
4. Michal Safar, **Bo-Jhih Lin**, Wei-Hsin Chen, David Langauer, Jo-Shu Chang, H. Raclavska, Anélie Pétrissans, Patrick Rousset, Mathieu Pétrissans. Catalytic effects of potassium on biomass pyrolysis, combustion and torrefaction. Applied Energy 2019;235:346-355. **(SCI : IF=7.900)**
5. **Bo-Jhih Lin,** Edgar A. Silveira, Baptiste Colin, Wei-Hsin Chen, Yu-Ying Lin , François Leconte, Anélie Pétrissans, Patrick Rousset, Mathieu Pétrissans. Modeling of elemental composition and characteristics of devolatilization in wood materials during mild pyrolysis in a pilot-scale reactor. Industrial Crops and Products 2019;131:357-370. **(SCI : IF=3.849)**
6. Wie-Hsin Chen, **Bo-Jhih Lin**, Baptiste Colin, Anélie Pétrissans, Mathieu Pétrissans. A study of hygroscopic property of biomass pretreated by torrefaction. Energy Procedia 2019;158:32-36. **(EI)**
7. Michal Safar, **Bo-Jhih Lin**, Wei-Hsin Chen, David Langauer, H. Raclavska, Anélie Pétrissans, Mathieu Pétrissans. Effects of impregnated potassium on biomass

torrefaction. Energy Procedia 2019;158:55-60. **(EI)**

8. **Bo-Jhih Lin**, Edgar A. Silveira, Baptiste Colin, Wei-Hsin Chen, Anélie Pétrissans, Patrick Rousset, Mathieu Pétrissans. Prediction of higher heating values (HHVs) and energy yield during torrefaction via kinetics. Energy Procedia 2019;158:111-116. **(EI)**

International Conference

1. Joël Hamada, **Bo-Jhih Lin**, Anélie Pétrissans, Wei-Hsin Chen, Philippe Gérardin, Mathieu Pétrissans. Effect of silver pin's forest management on radial density distribution, thermal behavior and final quality of the heat treated wood. COST Action FP1407 and Conference- Innovative production technologies and increased wood products recycling and reuse, September 29-30, Brno, Czech Republic, 2016.
2. **Bo-Jhih Lin**, Anelie Pétrissans, Patrick Rousset, Mathieu Pétrissans. Kinetic parameters from wood thermal degradation under vacuum to implement a mathematic model. 5émes Journées du GDR Sciences du Bois - Bordeaux, 8-10 November. 8-10, Bordeaux, France, 2016.
3. **Bo-Jhih Lin**, Edgar Silveira, Baptiste Colin, Mounir Chaouch, Anelie Pétrissans, Patrick Rousset, Mathieu Pétrissans. Experimental and numerical analysis of poplar thermodegradation. The 6th International Scientific Conference on Hardwood Processing (ISCHP-2017), Lahti, Finland, September 25-27, 2017.
4. Edgar Silveira, **Bo-Jhih Lin**, Baptiste Colin, Mounir Chaouch, Anelie Pétrissans, Patrick Rousset, Mathieu Pétrissans. Mathematical approach to build a numerical tool for mass loss prediction during wood torrefaction. The 6th International Scientific Conference on Hardwood Processing (ISCHP-2017), September 25-27, Lahti, Finland, 2017.
5. **Bo-Jhih Lin**, Edgar Silveira, Baptiste Colin, Anélie Pétrissans, Wei-Hsin Chen, Patrick Rousset, Mathieu Pétrissans. Prediction of mass loss dynamics during wood thermal modification under industrial conditions. COST Action FP1407 and 3rd Conference-Wood modification research and applications", September 14-15, Kuchl, Austria, 2017. (***First place award of student poster competition***)
6. M. Safar, **Bo-Jhih Lin**, D. Langauer,Wei-Hsin Chen, H. Raclavska, Mathieu Pétrissans, Anélie Pétrissans. Effect of potassium on the thermal degradation of biomass evaluated using thermogravimetric analysis. 7th International Conference on Engineering for Waste and Biomass Valorisation, July 2-5, Prague, Czech Republic, 2018.
7. Wie-Hsin Chen, **Bo-Jhih Lin**, Baptiste Colin, Anélie Pétrissans, Mathieu Pétrissans. A study of hygroscopic property of biomass pretreated by torrefaction. 10th International Conference on Applied Energy (ICAE2018), August 22-25, Hong Kong, China, 2018.

8. **Bo-Jhih Lin**, Edgar A. Silveira, Baptiste Colin, Wei-Hsin Chen, Anélie Pétrissans, Patrick Rousset, Mathieu Pétrissans. Prediction of higher heating values (HHVs) and energy yield during torrefaction via kinetics. 10th International Conference on Applied Energy (ICAE2018), August 22-25, Hong Kong, China, 2018.
9. M. Safar, **Bo-Jhih Lin**, Wei-Hsin Chen, D. Langauer, H. Raclavska, Anélie Pétrissans, Mathieu Pétrissans. Effects of impregnated potassium on biomass torrefaction. 10th International Conference on Applied Energy (ICAE2018), August 22-25, Hong Kong, China, 2018.
10. **Bo-Jhih Lin**, Baptiste Colin, Wei-Hsin Chen, Anélie Pétrissans, Patrick Rousset, Mathieu Pétrissans. Thermal degradation behavior of wood materials during heat treatment under vacuum. The 61st SWST International Convention - Era of a Sustainable World – Tradition and Innovation for Wood Science and Technology, November 5-9, Nagoya, Japan, 2018.

Appendix

A1. Validation of mass loss dynamics

As mentioned in above, one of the objectives is to predict the solid yield (or mass loss) during the treatment. It is important to have a good results of mass loss dynamics from the experiments. In this study, all the experiments of wood heat treatment were carried out in the semi-industrial scale reactor. This reactor can specially record the mass loss dynamics during treatment with a mass sensor and the software under vacuum condition. For that, before the experiments, it is necessary to validate the curves of mass loss dynamics.

In the beginning of thesis, the mass loss dynamic curves obtained from the software was with oscillation signal, as shown in the **Fig. a1.**

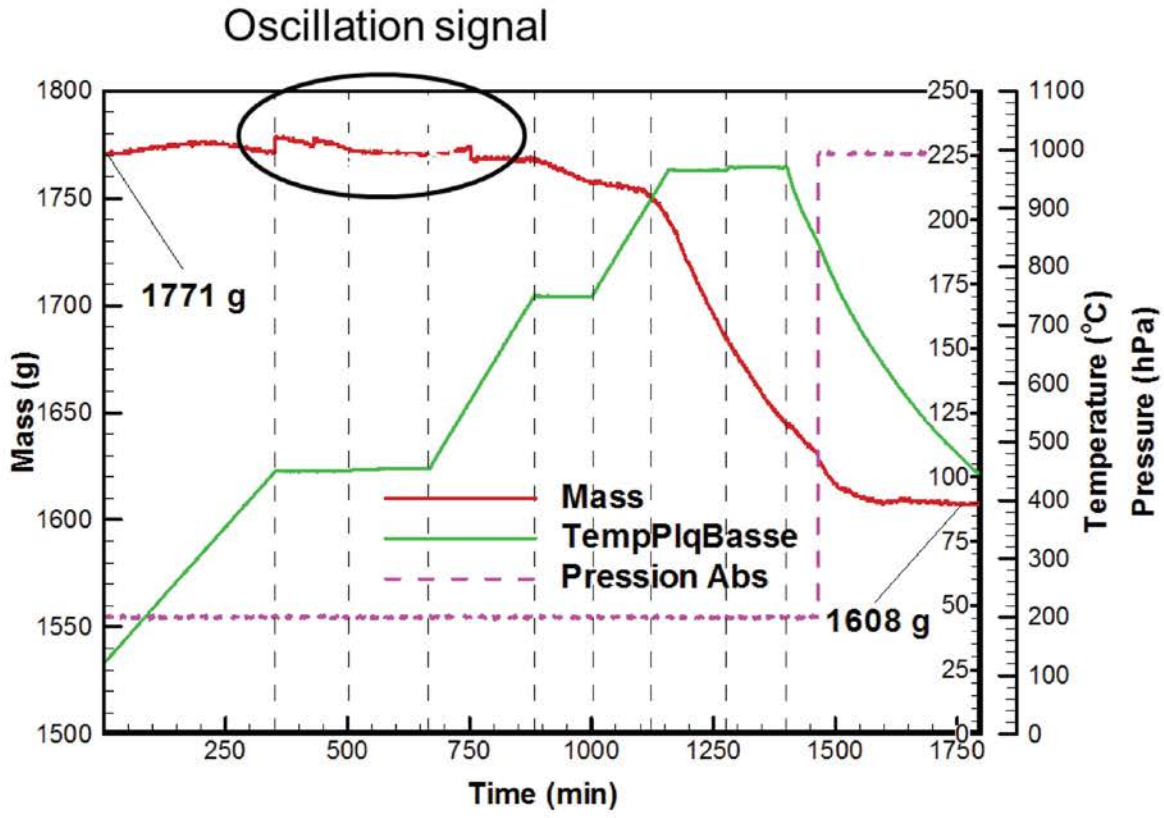

Fig. a1. Experimental result of poplar treated at 220 °C with oscillation signal.

In order to solve the problem, we tried to make the blank conditions without wood boards to evaluate whether the oscillation signals occurred or not. However, the results still presented the same oscillation signals, as shown in **Fig. a2**.

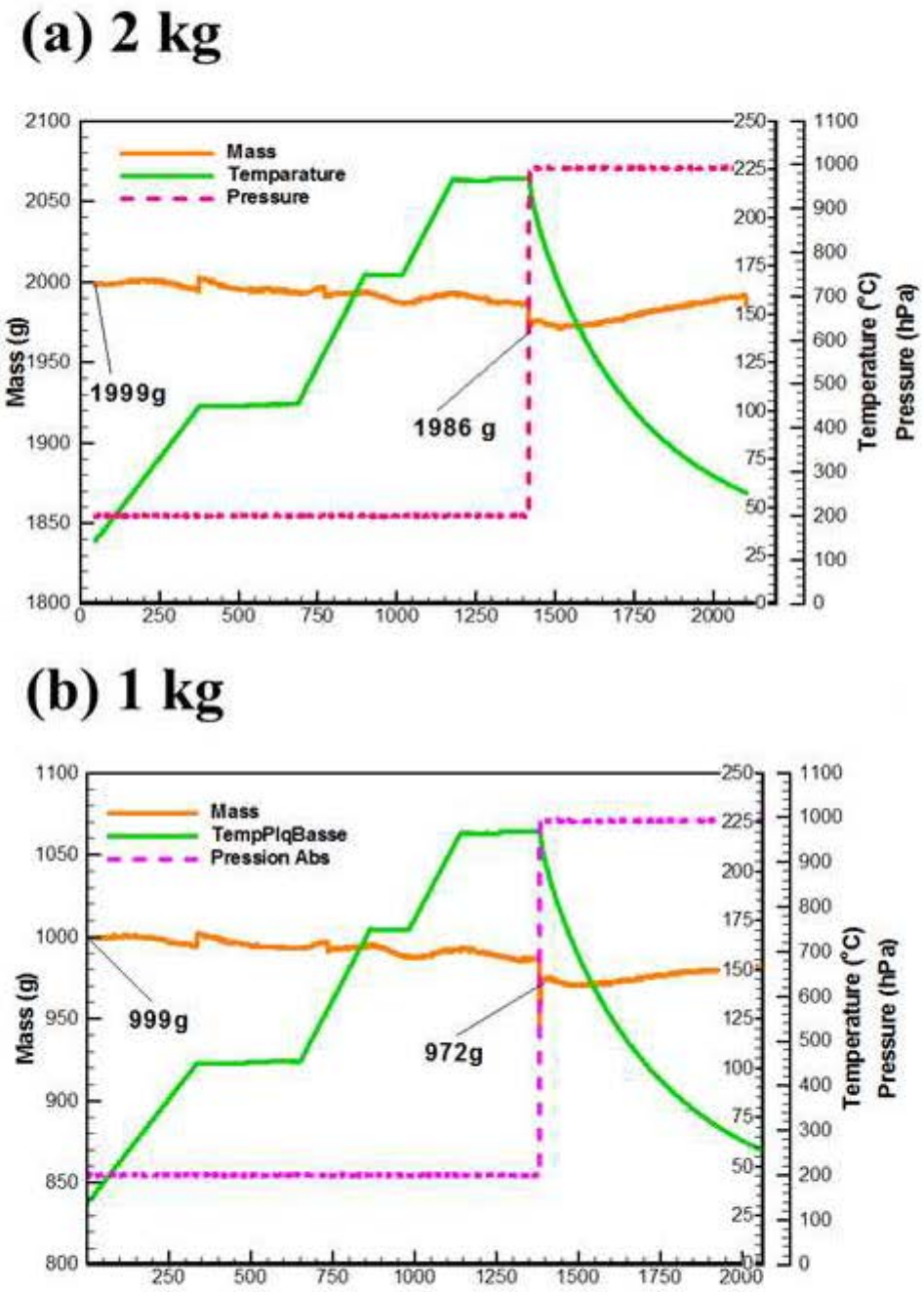

Fig. a2. Experimental result of blank condition with (a) 2 kg of mass and (b) 1 kg of mass at 220 °C.

After discussing with the technician in charge of the reactor, we found that the oscillation signals occurred mainly due to the calculation of mass signal from the software program. To overcome this problem, we decide to treat the data with the original signal from the blank and the experimental results.

The results of blank from original signal at different temperatures are illustrated in the **Fig a3**, and the results are very close.

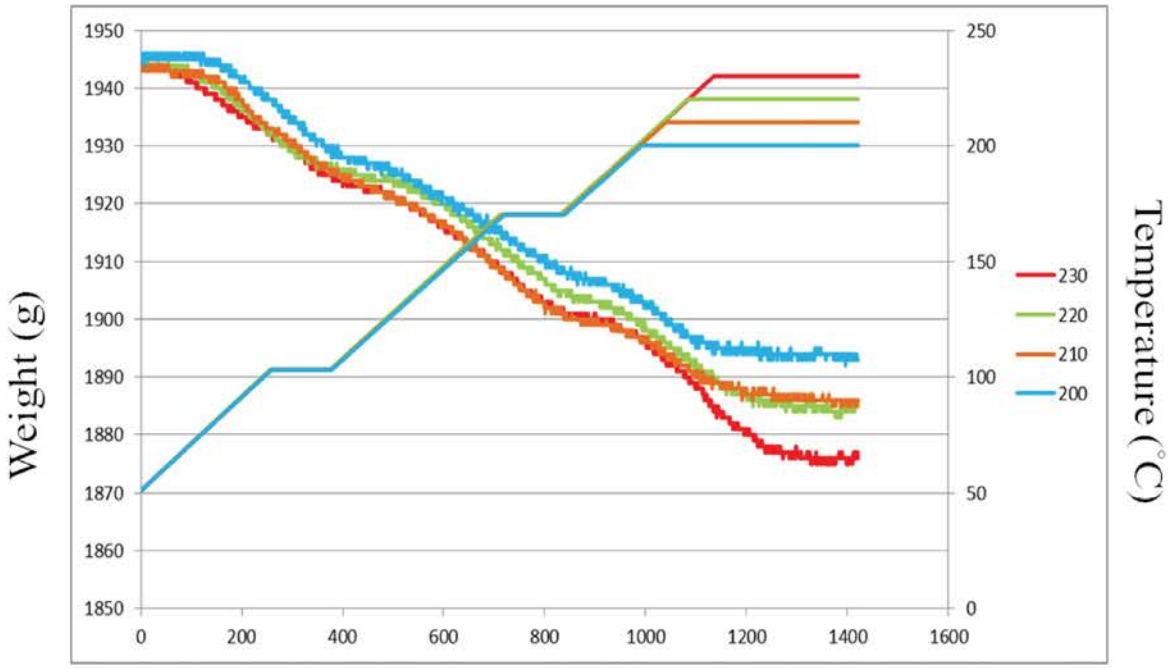

Fig. a3. Result of blank condition with 2 kg of mass at various temperatures.

The results of experimental results at different temperatures of treatment from original signal are illustrated in the **Fig a4.**

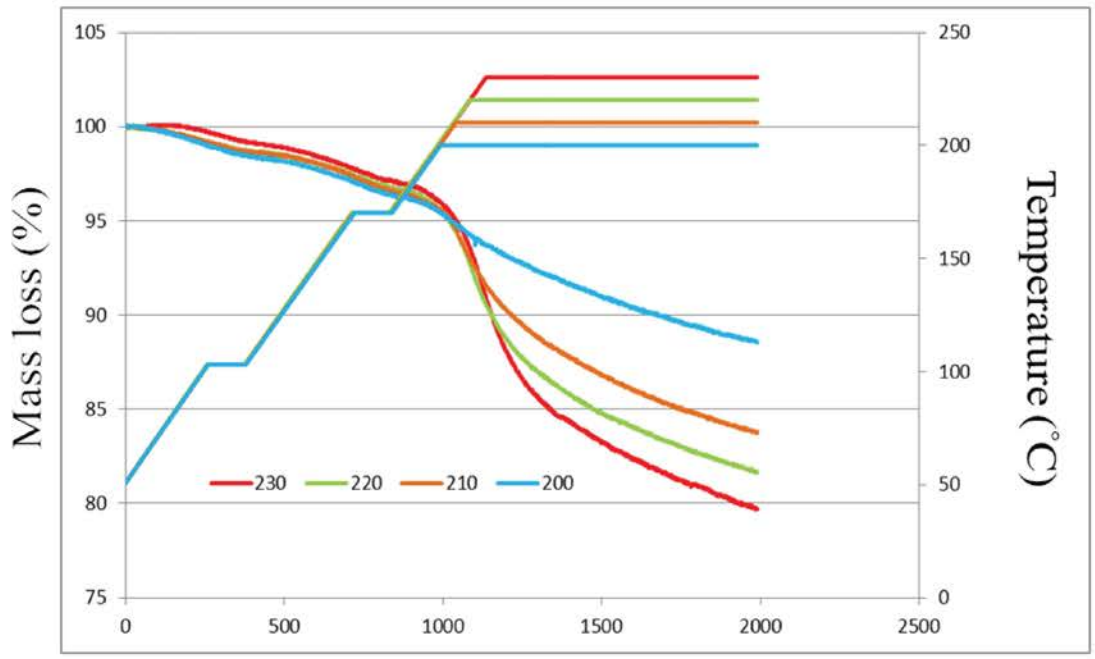

Fig. a4. Result of mass loss dynamics mass treated from poplar at various temperatures before calibration.

After, the calibration is made from the results of blank and experiments with the original signal. The profiles of mass loss dynamics are illustrated in **Fig. a5**. The obtained results are well and consist with the value of balance.

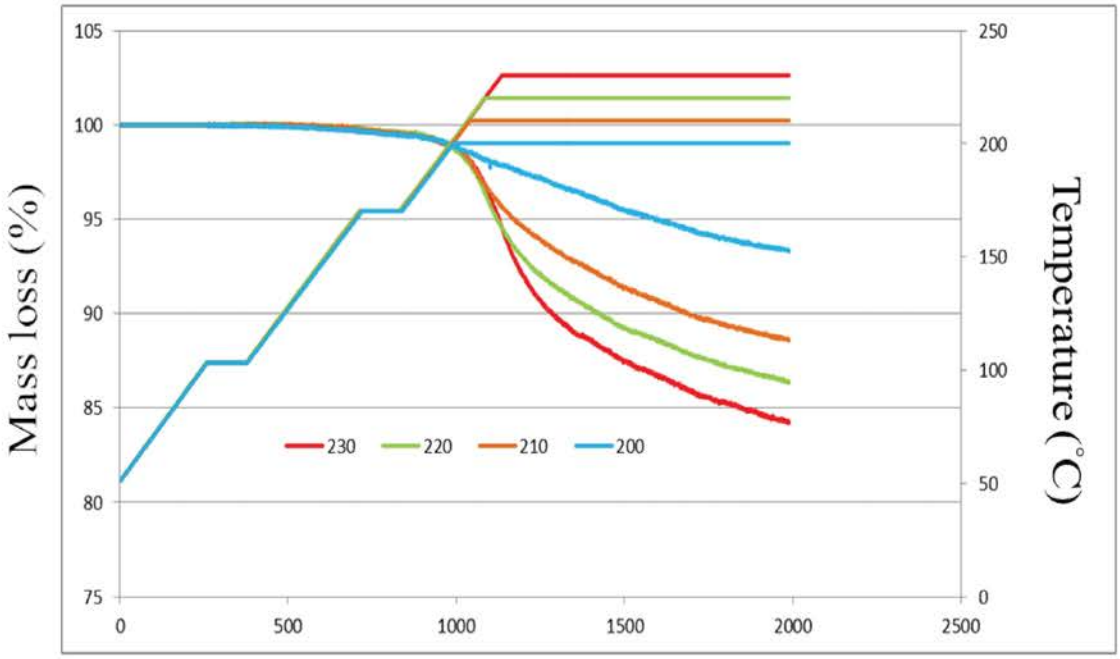

Fig. a5. Result of mass loss dynamics mass treated from poplar at various temperatures after calibration.

As a consequence, the validation of mass loss dynamics has been done with the calibration from the blank condition. In order to have a good results of mass loss dynamics, the blank condition has to be performed before each experiment. Meanwhile, the clean condition also has to be carried out after heat treatment to maintain the quantity of experiments. Overall, each line of mass loss dynamics obtained from the experiments takes 7 days (1 days of clean, 3 days of blank, and 3 days of heat treatment). More detail description about clean, blank, and heat treatment conditions are illustrated in **Appendix A2**.

A2. Operating procedures of wood heat treatment

The detail operating procedures are illustrated in this part: **(1) before the experiment**; **(2) recording software**; **(3) clean condition**; **(4) blank condition**; and **(5) wood heat treatment**. As in the following.

1. Before experiment

1.1 Preparation work

(1).Open the compressor

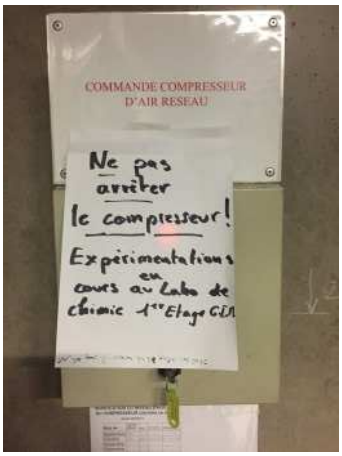

(2) Check the faucet (robinet), for protecting the compressor of vacuum reactor system,

(3) Open the exhaust fans (ventilateurs d'extraction).

For clean/blank condition: turn to “I”; For wood treatment: turn to “II”.

1.2 Sampling and drying

(1) Sample size: 600× 170× 22 mm.

Drilling the hole by drill (for 45 mm), this is for putting thermal couples inside the wood, two boards for one experiment. (the position of hole as showing in the picture, the hole of wood sample $_{\text{top side}}$ is in the right side, the hole of wood sample $_{\text{bottom}}$ is in in the center)

(2) Before experiment, put the wood boards into the drier at 103 ˚C for 3 days (at least 3 days or more).

1.3 Open the power (vacuum system and computer)

2. Recording software

(1). Turn on the computer

(2). Turn on the application for controlling and recording the vacuum reactor system

(3). Interface for operating

(a).ACCUEIL: to know the situation of vacuum reactor, such a temperature, mass, and pressure.

(b). DCY Utillsation: to make the zero (before Clean, Blank, or Wood heat treatment), click the green bottom for 1 or 2 second, then finish the zero.

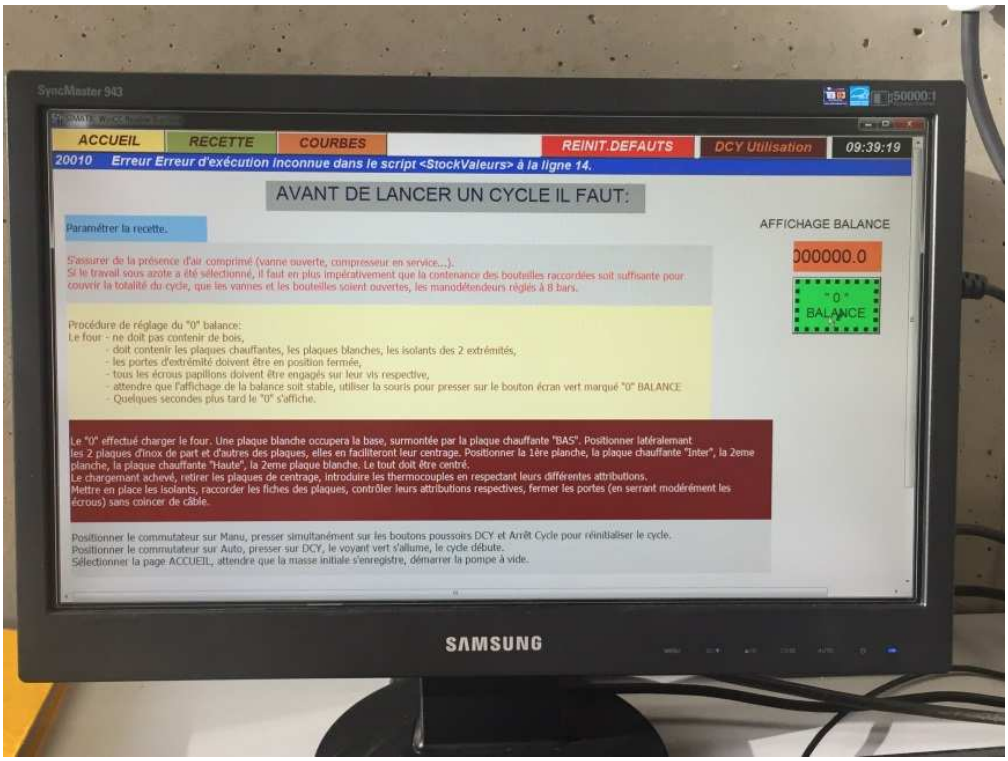

(c). RECETTE: to setting the process of vacuum reactor, normally we just chang the value on the horizontal row "*Intermd 1*", " *Intermd 2*", and " *Intermd 3*".

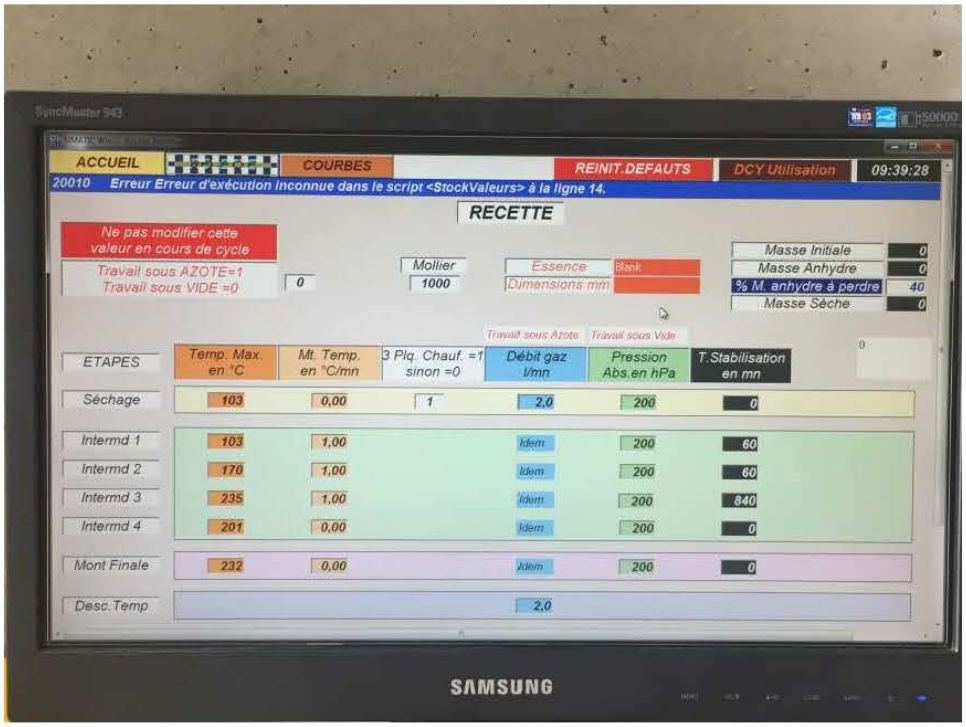

3. Clean condition

(1) Clean the hole inside the reactor.
(After wood heat treatment, it is necessary to do this to prevent the block of the hole)


(2) Put metal layout (**4 layouts**), heating plate (**3 heating plates**), and the ceramics layer (**2 ceramics layers**) inside the reactor.

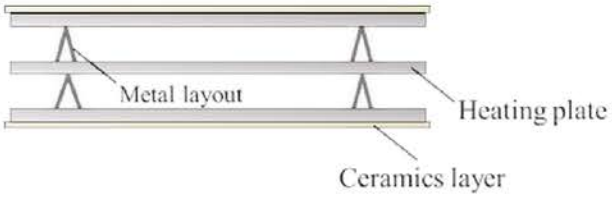


(3) Connect the heating plates and put the thermal couples inside the heating plate. Put the isothermal layer, then close the oven at the step.

(Be sure that connect the right number of thermal couple with the right heating plate, 1 to top, 2 to middle, 3 to bottom, otherwise, the system will alarm)

(4) After closing the door of reactor, wait for a few minute, and make ZERO

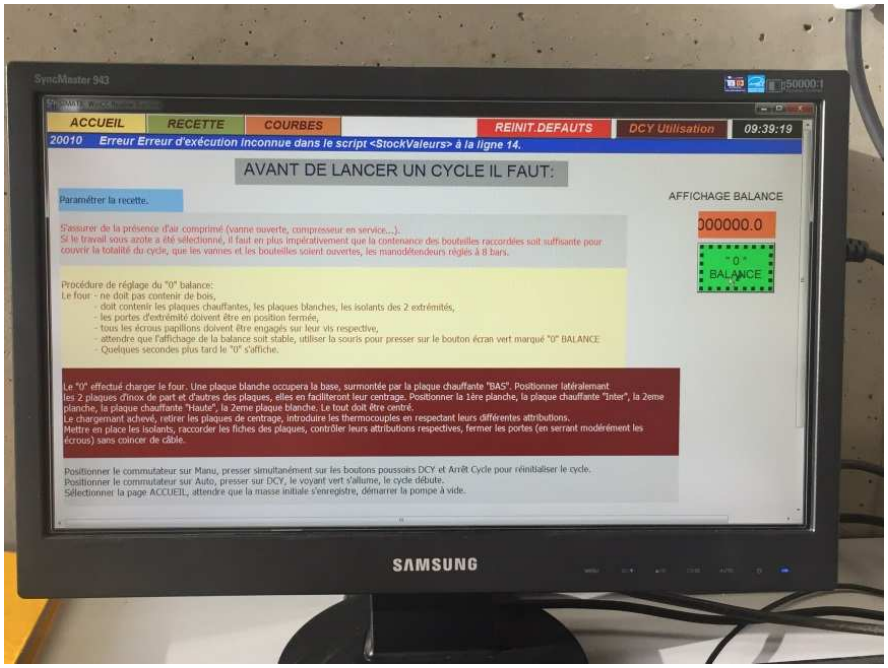

(5) After making zero, put the mass **(2 kg)** on the top of the reactor.

(6) Setting the temperature program for clean condition.

Step 1: 103 °C **for 60 min with heating rate of 1** °C **min^{-1}.**

Step 2: 170 °C **for 60 min with heating rate of 1** °C **min^{-1}.**

Step 3: 235 °C **for with 720 min heating rate of 1** °C **min^{-1}.**

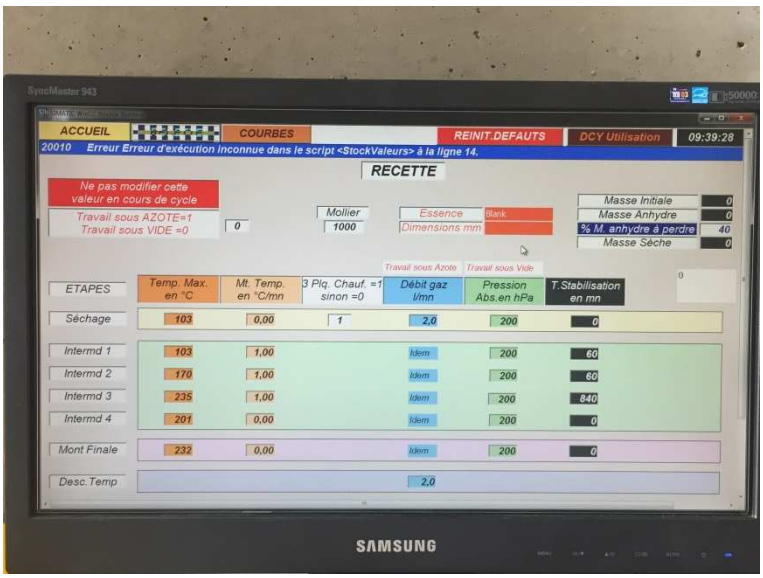

4. Blank condition

(1) After the clean condition, we just remove the mass (2 kg), and wait for a few minute, then make ZERO again.

(2) After making ZERO, put the mass (2 kg) again, and set the temperature program.

(3) Temperature program:

Step 1. 103 ˚C for 120 min with heating rate of 0.2 ˚C min^{-1}.

Step 2. 170 ˚C for 120 min with heating rate of 0.2 ˚C min^{-1}.

Step 3. 200~230 ˚C for 1000 min with heating rate of 0.2 ˚C min^{-1}.

5. **Wood heat treatment**

(1) After blank condition, remove the mass (2kg), and then open the door of reactor.

(2) Remove the metal layout (**4 layouts**), then close the door of reactor.

(3) Make **"ZERO"**.

(4) Take two boards from drier, and measure the density of wood. **(The density of two boards should be close)**

(5) Measure the mass from the balance, and record it. (**To check with the value of mass sensor and validate the value before the heat treatment**)

(6) Put the boards inside the reactor, and put the thermal couples inside the boards.

(7) Close the door of reactor, and set the program of heat treatment **(as the same condition of blank)**

(8) Wait a few minutes until mass stabilization, and then turn the mode to **auto**, and put the green bottom. After turn on the power of compressor to have vacuum condition.

(9) Waiting for the checking for the connection between heating plate and vacuum system, then wait for the results.

(10) Data storage: **Ordinateur > Sauvegarde TRAVAIL > LERMAB >FichiersFour**

A3. Validation of mass loss dynamics

The experimental data of solid yields displayed in this study were the average values between the two experiments, and its relative difference was controlled below 5%. The relative difference was the solid yield relative error, which is defined as:

$$\text{Relatvie error (\%)} = \left|\frac{SY_1 - SY_2}{SY_{average}}\right| \times 100$$

where SY_1 and SY_2 stand for the solid yield in the first and second runs, respectively, and $SY_{average}$ represents the average value of solid yield. For example: the solid yields of heat treated poplar at 230 °C after two experiments were 83.53 wt% and 82.63 wt% in dry basis, and the average solid yield was 83.08 %. The relative error was 1.08 %.

The experimental results with the statistical analysis are summarized and revised in the revised manuscript, as shown in **Table a1**. The results of repeatability from poplar and fir treated at 230 °C are also demonstrated in **Fig. a6**.

Table a1. Experimental results of solid yields and relative errors at the end of treatment.

Wood sample	**Treatment temperature (°C)**			
	200	**210**	**220**	**230**
Poplar				
Solid yield (%) [a]	91.73±0.15	88.25±0.32	85.61±0.24	83.08±0.45
Relative error (%)	0.32	0.72	0.56	1.08
Fir				
Solid yield (%) [a]	96.18±0.30	93.92±0.05	90.36±0.65	87.71±0.17
Relative error (%)	0.63	0.11	1.43	0.39

[a]: dry basis

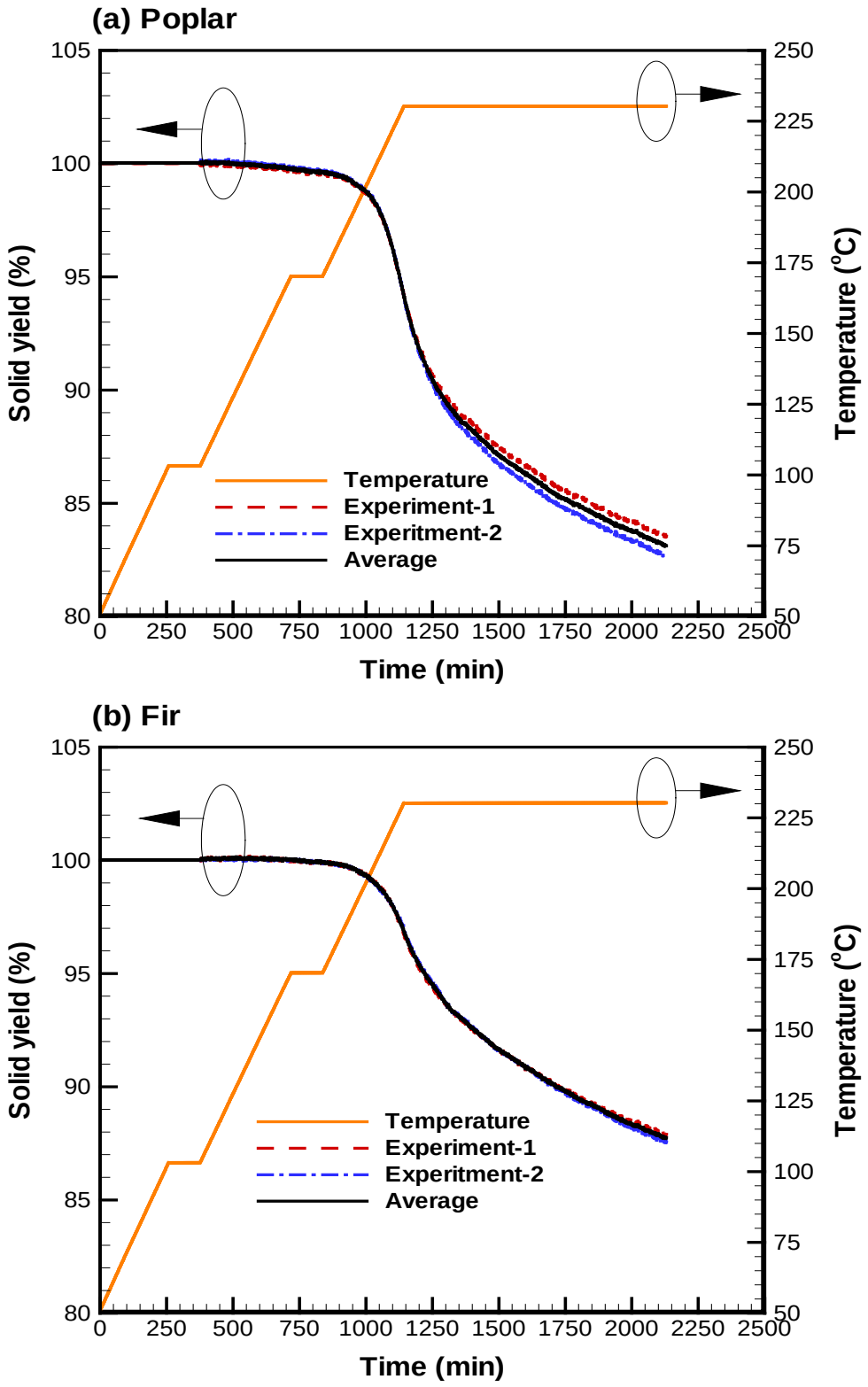

Fig. a6. Profiles of dynamic solid yields in poplar and fir at 230°C of treatment.

A4. Publications related to the thesis

Journal of Analytical and Applied Pyrolysis 130 (2018) 8–18

Contents lists available at ScienceDirect

Journal of Analytical and Applied Pyrolysis

journal homepage: www.elsevier.com/locate/jaap

Thermal degradation and compositional changes of wood treated in a semi-industrial scale reactor in vacuum

Bo-Jhih Lin[a], Baptiste Colin[a], Wei-Hsin Chen[b,c,*], Anélie Pétrissans[a,**], Patrick Rousset[d,e], Mathieu Pétrissans[a]

[a] Université de Lorraine, Inra, LERMaB, F88000, Epinal, France
[b] Department of Aeronautics and Astronautics, National Cheng Kung University, Tainan 701, Taiwan
[c] Research Center for Energy Technology and Strategy, National Cheng Kung University, Tainan, 701, Taiwan
[d] CIRAD, UPR BioWooEB, F34398, Montpellier, France
[e] Joint Graduate School of Energy and Environment- Center of Excellence on Energy Technology and Environment-KMUTT, Bangkok, 10140, Thailand

ARTICLE INFO

Keywords:
Wood heat treatment
Vacuum
Sustainable material
Devolatilization index

ABSTRACT

Heat treatment is an eco-friendly and efficient way to improve the defective properties of woods, such as hygroscopic nature, lack of dimensional stability, and low resistance against biological degradation, and to produce a green and sustainable wood material for construction and buildings. The aim of this study is to investigate the thermal degradation of a hardwood (poplar, *Populus nigra*) and a softwood (fir, *Abies pectinata*) in a semi-industrial scale reactor in which a vacuum environment is adopted to intensify the thermal degradation process. Four different stages of thermal degradation during wood heat treatment are defined, based on the intensity of differential mass loss (*DML*). Meanwhile, a number of analyses on untreated and treated woods are performed to evaluate their thermal degradation characteristics and compositional change during treatment. The FTIR analysis clearly demonstrates the thermal degradation through dehydration, deacetylation, depolymerization, and condensation reactions during the heat treatment. In addition, the XRD analysis indicates an increase in relative crystallinity of cellulose. The correlation of devolatilization index (*DI*) with respect to mass loss of the two wood species is strongly characterized by linear distribution, which is able to provide a simple and useful tool in predicting mass loss of wood treated in wood industry.

1. Introduction

Nowadays, energy shortage and environmental issues have been the biggest challenges facing the world. Accordingly, sustainability, industrial ecology, eco-efficiency, and green chemistry are guiding the development of materials, products, and processes [1]. Forests are the main greenhouse gas sinks in the world, and play an important role in mitigating the climate change. Trees absorb carbon dioxide and utilize water and sunlight to grow and produce oxygen as a byproduct. The resulted materials can be used in construction and paper production, and can provide chemical feedstocks. Furthermore, at the end of a product life cycle, the material constituents can be combusted or composted to return the chemical constituents to the grand cycles [2–4].

Woods are regarded as renewable and sustainable materials. However, the utilization of woods is limited by its poor resistance to fungal attack (low durability) and the lack of dimensional stability [5,6]. Among various techniques for overcoming these problems, Wood heat treatment is an eco-friendly technology because no chemicals are utilized and added into this process to improve the wood's durability and dimensional stability, whereas toxic chemicals may be used in other chemical modification methods [5,6]. The heat treated woods have longer durability and better dimensional stability, stemming from the reduction in water absorption and biological degradation which are caused from the thermal decomposition of hemicellulose, cellulose, and lignin [5,7]. Wood heat treatment (WHT), similar to mild pyrolysis or torrefaction [8], is conducted in an inert atmosphere at temperatures between 180 °C and 240 °C with a low heating rate (0.1–1 °C min^{-1}). Heat treatment of wood has been widely investigated and carried out since the early 20th century, and the technique has been improved quickly in developing countries and especially in Europe [4].

The vacuum process is a novel and promising technology which is suitable for biomass pyrolysis, carbonization, and wood heat treatment [9–11]. The applications of the aforementioned thermochemical

* Corresponding author at: Department of Aeronautics and Astronautics, National Cheng Kung University, Tainan 701, Taiwan.
** Corresponding author at: Université de Lorraine, Inra, LERMaB, F88000, Epinal, France.
E-mail addresses: chenwh@mail.ncku.edu.tw, weihsinchen@gmail.com (W.-H. Chen), anelie.petrissans@univ-lorraine.fr (A. Pétrissans).

https://doi.org/10.1016/j.jaap.2018.02.005
Received 4 December 2017; Received in revised form 12 January 2018; Accepted 5 February 2018
Available online 07 February 2018
0165-2370/

Applied Energy 231 (2018) 768–776

Contents lists available at ScienceDirect

Applied Energy

journal homepage: www.elsevier.com/locate/apenergy

Hygroscopic transformation of woody biomass torrefaction for carbon storage

Wei-Hsin Chen[a,b,*], Bo-Jhih Lin[a,c], Baptiste Colin[c], Jo-Shu Chang[b,d,*], Anélie Pétrissans[c], Xiaotao Bi[e], Mathieu Pétrissans[c]

[a] Department of Aeronautics and Astronautics, National Cheng Kung University, Tainan 701, Taiwan
[b] Research Center for Energy Technology and Strategy, National Cheng Kung University, Tainan 701, Taiwan
[c] Université de Lorraine, Inra, LERMaB, F88000 Epinal, France
[d] Department of Chemical Engineering, National Cheng Kung University, Tainan 701, Taiwan
[e] Department of Chemical and Biological Engineering, University of British Columbia, Vancouver V6T 1Z3, Canada

HIGHLIGHTS

- Color change and hygroscopic transformation of poplar and fir from torrefaction are analyzed.
- Total color difference linearly increases with increasing mass loss or torrefaction severity.
- Hygroscopic transformation of biomass is evaluated by equilibrium moisture content (EMC) and contact angle.
- Hygroscopicity reduction extent (HRE) can reach up to 57.39% at 230 °C.
- Carbon, hydrogen, and oxygen removals from torrefaction can be predicted by color change and HRE.

GRAPHICAL ABSTRACT

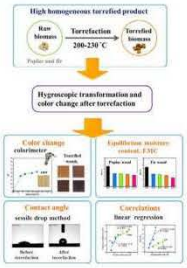

ARTICLE INFO

Keywords:
Torrefaction
Hygroscopicity
Equilibrium moisture content (EMC)
Contact angle
Color change
Devolatilization

ABSTRACT

Biochar is a potential medium for carbon storage, so its production and storage have been considered as is a crucial route to effectively achieve negative CO_2 emissions. Meanwhile, torrefaction is a thermochemical conversion process for producing biochar. Biochar is featured by its hydrophobicity, which makes it different from its parent biomass with hygroscopicity and is conducive to material storage. To evaluate the hygroscopic transformation of biomass from torrefaction, two woody biomass materials of poplar (hardwood) and fir (softwood) are torrefied at temperatures of 200–230 °C, and the variations of color, equilibrium moisture content, and contact angle of raw and torrefied samples are examined. The results indicate that the total color difference of torrefied woods increases linearly with increasing mass loss. The hygroscopicity reduction extent in torrefied fir is higher than in torrefied poplar, and can be increased by up to 57.39% at 230 °C. The tests of the contact angle suggest that the hygroscopicity of the raw woods is evidently exhibited, whereas the angles of the torrefied woods are in the range of 94–113°, showing their hydrophobic surfaces (> 90°). The decarbonization, dehydrogenation, and deoxygenation phenomena of the biomass during torrefaction are also analyzed. It is found that the three indexes can be correlated well by the total color difference and hygroscopicity reduction

* Corresponding authors at: Department of Aeronautics and Astronautics; Department of Chemical Engineering, National Cheng Kung University, Tainan 701, Taiwan.
E-mail addresses: chenwh@mail.ncku.edu.tw, weihsinchen@gmail.com (W.-H. Chen), changjs@mail.ncku.edu.tw (J.-S. Chang).

https://doi.org/10.1016/j.apenergy.2018.09.135
Received 29 May 2018; Received in revised form 3 September 2018; Accepted 12 September 2018
Available online 25 September 2018
0306-2619/

Industrial Crops & Products 131 (2019) 357–370

Contents lists available at ScienceDirect

Industrial Crops & Products

journal homepage: www.elsevier.com/locate/indcrop

Modeling and prediction of devolatilization and elemental composition of wood during mild pyrolysis in a pilot-scale reactor

Bo-Jhih Lin[a,b], Edgar A. Silveira[a,c], Baptiste Colin[a], Wei-Hsin Chen[b,d,*], Yu-Ying Lin[a,b], François Leconte[a], Anélie Pétrissans[a,*], Patrick Rousset[e,f], Mathieu Pétrissans[a]

[a] Université de Lorraine, Inra, LERMaB, F88000, Epinal, France
[b] Department of Aeronautics and Astronautics, National Cheng Kung University, Tainan, 701, Taiwan
[c] Mechanical Engineering Department, University of Brasília, Brasília, DF, 70910-900, Brazil
[d] Research Center for Energy Technology and Strategy, National Cheng Kung University, Tainan, 701, Taiwan
[e] CIRAD, UPR BioWooEB, F34398, Montpellier, France
[f] Joint Graduate School of Energy and Environment- Center of Excellence on Energy Technology and Environment-KMUTT, Bangkok, 10140, Thailand

ARTICLE INFO

Keywords:
Mild pyrolysis kinetics
Biochar
Elemental composition prediction
Wood heat treatment and torrefaction
Devolatilization
Higher heating value

ABSTRACT

Mild pyrolysis, operated at 200–300 °C in an inert atmosphere, is a promising technology to produce sustainable materials (i.e., heat treated woods for construction and building) and solid fuels (i.e., torrefied woods or biochars for combustion and gasification). To aid in process and reactor design, the aim of this work is to conduct thermal degradation kinetics of wood. A two-step kinetics model is developed to predict the elemental composition (C, H, and O) and devolatilization dynamics of wood materials during heat treatment in a pilot-scale reactor by kinetic analysis. A hardwood poplar (*Populus nigra*) and a softwood fir (*Abies pectinata*) sever as feedstock, and the experiments are carried out at 200–230 °C with a heating rate of 0.2 °C min^{-1} in a low-pressure environment (200 hPa). The predictions in the weight losses of the woods are in a good agreement with the experimental data. The evolutions of solids, volatiles, elements (C, H, and O), and the heating values of treated woods are further analyzed. The predictions suggest that the intermediate solid is the main product, and almost all the woods are converted when the treatment temperature is as high as 230 °C. The devolatilization process, which is responsible for the mass loss of wood, can be clearly identified, and the volatile liberation amounts from poplar and fir at 230 °C are 17.05 and 12.44 wt%, respectively. The predicted HHVs of treated woods from the empirical formula are between 19.62 and 20.55 MJ kg^{-1}, and the enhancement factors at the end of treatment are between 1.01 and 1.07 which is close to torrefied wood after light torrefaction. During the treatment, the extents of decarbonization, dehydrogenation, and deoxygenation in fir are all smaller than those in poplar, resulting from the lower intensity of devolatilization in the former.

1. Introduction

In recent years, the promotion of renewable resource-based bioeconomy has garnered much political support because it can contribute to diverse policy aims such as climate change mitigation, environmental protection, energy security, technological progress, growth, employment, and rural value creation (Pätäri et al., 2017; Purkus et al., 2018). Scholars and policymakers broadly understand bioeconomy as the transition from a fossil-based economy to another economy where the basic sources for products, chemicals, and energy would be derived from renewable biological resources (Giurca and Späth, 2017). For the greenhouse gas (GHG) mitigation, the Intergovernmental Panel on Climate Change (IPCC) has concluded that producing sustainable wood materials or energy from sustainably managed forests would generate the largest sustained mitigation benefits of GHG production (Geng et al., 2017).

Mild pyrolysis, which is performed in an inert atmosphere, is a promising process for upgrading wood materials through thermal modification to produce sustainable materials (e.g., heat treated woods) or solid fuels (e.g., torrefied woods) (Chen et al., 2015; Todaro et al., 2017). After this treatment, the properties of wood materials can be improved, such as rendering higher homogeneity, longer durability, and higher energy density (Chen et al., 2018; Kesik et al., 2014; Volpe et al., 2015a). Generally, mild pyrolysis is carried out in the temperature range of 200–300 °C. Prior to reaching the treatment temperature, different heating rates can be adopted, depending on the purpose of

* Corresponding author.
E-mail addresses: chenwh@mail.ncku.edu.tw, weihsinchen@gmail.com (W.-H. Chen), anelie.petrissans@univ-lorraine.fr (A. Pétrissans).

https://doi.org/10.1016/j.indcrop.2019.01.065
Received 22 November 2018; Received in revised form 28 January 2019; Accepted 31 January 2019
Available online 10 February 2019
0926-6690/

Available online at www.sciencedirect.com

ScienceDirect

Energy Procedia 158 (2019) 32–36

Energy Procedia

www.elsevier.com/locate/procedia

10th International Conference on Applied Energy (ICAE2018), 22-25 August 2018, Hong Kong, China

A study of hygroscopic property of biomass pretreated by torrefaction

Wei-Hsin Chen [a, b, *], Bo-Jhih Lin [a, c], Baptiste Colin [c], Anélie Pétrissans [c], Mathieu Pétrissans [c]

[a]*Department of Aeronautics and Astronautics, National Cheng Kung University, Tainan 701, Taiwan*
[b]*Research Center for Energy Technology and Strategy, National Cheng Kung University, Tainan 701, Taiwan*
[c]*Université de Lorraine, Inra, LERMaB, F88000 Epinal, France*

Abstract

Torrefaction is a thermochemical conversion process, and it is adopted to improve the drawbacks of raw biomass (such as high hygroscopicity, low calorific values and energy density). During this process, biomass is thermally degraded in an inert or nitrogen environment at temperature range of 200-300 °C for several minutes to several hours. In this study, high homogeneous torrefied wood samples were produced by torrefaction at 200, 210, 220, and 230 °C. The equilibrium moisture content (EMC) of raw and torrefied wood and the contact angle of sample surface are examined to evaluate the hygroscopicity changes of torrefied wood. The results indicate that the EMC of the torrefied wood decreased by 35% or more compared to the EMC of raw material. An increasing of contact angle of torrefied wood surface is observed with increasing torrefaction temperature, and it is in the range of 103-113 ° which is correspond to hydrophobic surface (>90°). Meanwhile, the detailed mechanisms about the changes of biomass hygroscopicity after torrefacion are also illustrated in the present work.

Peer-review under responsibility of the scientific committee of ICAE2018 – The 10th International Conference on Applied Energy.

Keywords: torrefaction, hygroscopicity, equilibrium moisture content (EMC), contance angle

* Corresponding author. Tel.: +886-6-2004456; fax: +886-6-2389940.
E-mail address: weihsinchen@gmail.com; chenwh@mail.ncku.edu.tw

Peer-review under responsibility of the scientific committee of ICAE2018 – The 10th International Conference on Applied Energy.
10.1016/j.egypro.2019.01.030

1. Introduction

Nowadays, energy shortage and environmental issues have been the biggest challenges facing the world. Accordingly, sustainability, industrial ecology, eco-efficiency, and green chemistry are guiding the development of materials, products, and processes [1]. Biomass is regarded as an attractive low-carbon resource, and has the following specific features: (1) it is abundant and easily generated; (2) biomass production is labor intensive and thus conducive to poverty reduction and increase of rural employment; and (3) it is easily converted to thermal energy and electricity [2]. Torrefaction is an eco-friendly process because no chemicals are utilized and added into this process to improve the natural defect of biomass and produce solid fuel. Torrefaction is operated between 200-300°C under an inert condition. Based on the pretreatment temperature, the conventional biomass torrefaction can be classified into light, mild, and severe torrefaction, where the temperatures are in the ranges of approximately 200-235, 235-275, and 275-300 °C, respectively [3]. Compared to raw biomass, torrefied biomass has a higher calorific values or energy density, lower atomic O/C and H/C ratios and moisture content, lower hygroscopicity, higher grindability, and more uniform properties.

Concerning to the improvement of hygroscopicity, biomass is hygroscopic in nature, because moisture can be absorbed into the cell walls by the hydroxyl groups attract which hold water molecules through hydrogen bonding [4,5]. When biomass undergoes torrefaction, the hydroxyl groups will be partly destroyed through dehydration, and this prevents the formation of hydrogen bonds [4]. Accordingly, hygroscopic biomass tends to be hydrophobic after torrefaction, and the equilibrium moisture content (EMC) in the biomass is reduced significantly [6]. The hygroscopic characteristic of biomass is usually examined by determining the EMC under a humidity range of 50-80%. Some studies pointed out that the hygroscopic property can also be observed via thermogravimetric analysis (TGA), where its weight loss is lower for heating temperatures between room temperature and 105 °C when compared to its parent materials [3].

The aim of this study is to investigate the hygroscopicity of lignocellulosic biomass after light torrefaction, which could produce higher homogeneous torrefied wood compared to mild or severe torrefaction [7]. To achieve this target, the examinations of EMC and contact angle are performed to evaluate the behaviour of water absorption in biomass after torrefaction.

2. Experiment

In this study, a softwood species (fir, *Abies pectinata*) which is abundant in Europe and widely used in the European wood industry have been chosen. The wood sample was dried in an oven at 103 °C until mass stabilization before experiments. The light torrefaction were carried out in a pilot scale system in the temperature range of 200-230 °C with a low heating rate (0.2°C min^{-1}) and under low pressure (200 hPa) for 1000 min of experiment to produce a high homogenous torrefied wood. It has been reported that the biochars obtained from low pressure of pyrolysis have more “open” pores and higher reactivity than atmospheric pyrolysis biochars [8], and also could provide torrefied products with greater homogeneity [9]. The proximate analysis was performed according to the ASTM standard procedures (i.e., moisture: E871; volatile matter: E872; fixed carbon: E1534; and ash: D1102) [10]. Before the proximate analysis, the wood samples were crushed with a grinder and sieved to the particle sizes ranging from 0.36 to 1.7 mm (i.e. 12-45 mesh). For the EMC and contact angle determination, the wood samples were cut to the dimensions 20 mm × 20 mm × 20 mm. The sieved and cut wood samples were dried in an oven at 105 °C for 24 h to provide a basis for analysis. Subsequently, the samples were placed in sealed plastic bags and stored in electronic cabinet at room temperature until experiments were performed.

The EMC analysis was carried out in a temperature and humidity chamber at 25 °C with 55 % relative humidity. EMC is defined as the weight ratio of sample with moisture content and the oven dried weight of sample. The measurement of contact angle was performed by using an optical contact angle apparatus, which was consisted of a video measuring system connected and a high-resolution CCD camera. A commercial software (FTA32) was connected with the system to measure and record the results.

3. Results and discussion

The values of solid yield, which is the weight ratio of torrefied wood and raw, under various torrefaction temperatures are given in **Table 1**. The solid yield is in the range of 87-97 wt%. When the biomass is torrefied at 200 °C, the solid yield is 96.18%, which means a very light thermal decomposition occurs. While the torrefaction temperature is at 230 °C, the solid yield is decreased to 87.71%. Overall, the decreasing of solid yield is mainly due to the thermal decomposition of hemicelluloses in this temperature range [11]. The HHVs of the samples are between 16.55 MJ kg^{-1} (raw) and 18.26 MJ kg^{-1} (230 °C of torrefaction), also shown in **Table 1**. The enhancement factor of HHV, which is the HHV ratio of torrefied biomass and raw biomass can be regarded as energy density, it has been widely used to examine the performance of torrefaction [12]. The enhancement factor of treated wood at the end of treatment is in the range of 1.02-1.10. This result is with a good agreement to the light torrefied wood [13]. The results of proximate analysis indicate that the volatile matter (VM) in the samples decreases after torrefaction, whereas the fixed carbon (FC) increases, resulting from the devolatilization reaction during treatment [4,14]. The increasing of FC could also be owing to the carbonaceous materials are formed during treatment due to thermal reticulation reactions [11].

Table 1. Solid yield, HHV, and proximate analysis of raw and torrefied wood.

Material	Solid yield (wt%)	HHV (MJ kg^{-1})	Enhancement factor	Volatile matter (wt%)	Fixed carbon (wt%)
Raw	100.00	16.55	1.000	85.53	14.28
200 °C	96.18	16.90	1.021	83.31	16.49
210 °C	93.92	17.08	1.032	82.59	17.18
220 °C	90.36	17.61	1.064	80.88	18.87
230 °C	87.71	18.26	1.103	79.72	20.03

The EMC is used in relation to a hygroscopic material, like biomass, and the lower EMC values examined means the lower behavior of water absorption [6]. The EMC of the torrefied wood is decreased while increasing torrefaction temperature, and it is in the range of 2.34-3.60 %. Moreover, the EMC decreased by 34-58 % of reduction compared to EMC of the raw material (**Fig. 1**).

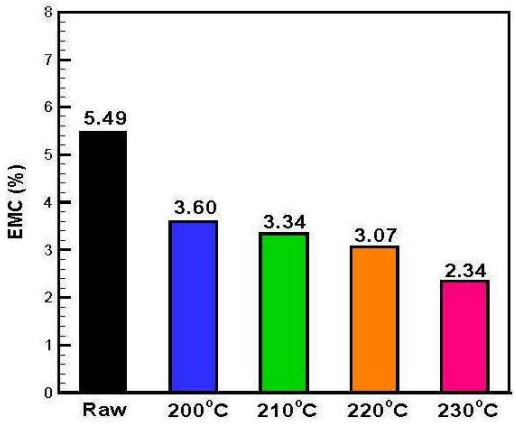

Fig. 1. EMC distribution of raw and torrefied biomass

The reduction of EMC is reflected to the improvement of biomass hygroscopicity. The hygroscopic property of biomass is contributed to the hydroxyl groups in biomass attract and hold water molecules through hydrogen bonding. The hemicelluloses and the amorphous reign of the cellulose chains are more prone to attract water due to

the availability of hydroxyl groups. While biomass after torrefaction, the hemicelluloses and the amorphous reign of cellulose are thermally decomposed. These results prevent the formation of hydrogen bonding to catch water molecules, so that the torrefied biomass tends to be hydrophobic. It is worthy to note that the solid yield of 200 °C torrefied wood is 96.18%, and it is implied a very light degradation of biomass. However, the reduction of EMC is as high as 34.9%, and it could be attributed the released of extractives which are mainly consisted of organic volatile products condensed inside the wood pores. The related study has reported that the lower saturated moisture content in torrefied biomass could also result from tar condensation inside the pores of torrefied biomass, obstructing the passage of moist air through the solid, and then avoiding the condensation of water vapor. In addition, the apolar character of condensed tar on the solid also prevents the condensation of water vapor inside the pores [4].

The measurement of contact angle is conducted by the sessile drop technique. This method is based on the observation of the profile of a drop deposited on a solid surface [15]. After the measurement, the small contact angles (<90°) correspond to hydrophilic surface (with hygroscopic property), while large contact angles (>90°) correspond to hydrophobic surface (with low wettability) [16,17]. **Fig. 2** and **Fig. 3**. display the results of contact angle on the surface of raw and torrefied wood. **In Fig. 2**, The water absorption behavior with time can be observed. The contact angle of raw biomass surface is around 86 ° in the beginning, and after 20 s, the contact angle of the surface tends to 0°. In contrast, the contact angles of torrefied biomass are always maintained at a certain value and higher than 90°, the range is from 103 to 113 °. Overall, the contact angels of all the torrefied samples in the present study are higher than 90°, indicating the reduction of wettability (or increase of hydrophobicity). In the related study, Li et al. [18] performed the contact angle determination of biomass (corncob) surfaces after torrefaction under N_2 and CO_2. They revealed that the contact angel increased as the torrefaction temperature elevated, and the high hydrophobicity of corncobs could be obtained while torrefaction occurred at a high temperature.

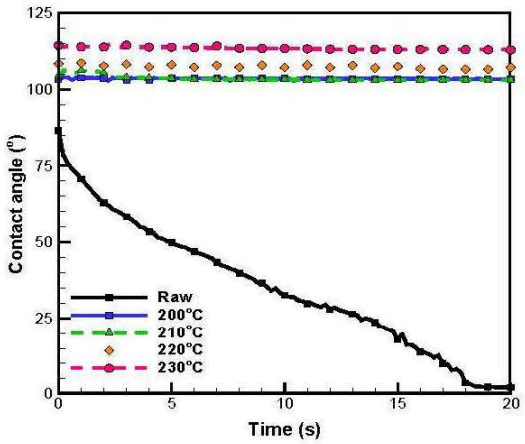

Fig. 2. Profiles of contact angle on the surface of raw and torrefied biomass

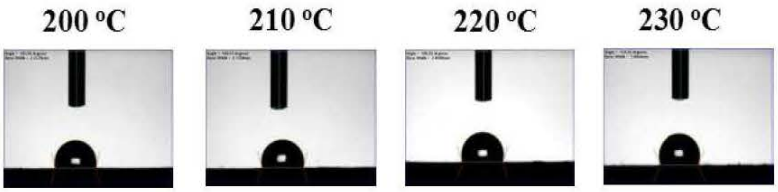

Fig. 3. Diagram of contact angle on the surface of torrefied biomass at different conditions

4. Conclusions

The torrefaction of fir (*Abies pectinata*) has been carried out at 200-230 °C under low pressure (200 hPa) to produce high homogenous torrefied wood in this study. The results point out that the EMCs of torrefied wood are decreased significantly while torrefaction temperature is increased, and it is in the range of 2.34-3.60 %. On the other hand, the solid yield of 200 °C torrefied wood is 96.18% (around 3.8 wt% of mass loss), which is implied a very light degradation of biomass. However, the reduction of EMC is reached up to 34 %, and it could be owing to release of extractives condensed inside the wood pores to prevent the water contact the wood surface directly. For the determination of contact angle on wood surface, the contact angels of all the torrefied samples in the present study are higher than 90° (in the range of 103-113 °), and it is increased with torrefaction temperature, indicating the reduction of wettability (or increase of hydrophobicity).

Acknowledgements

The authors gratefully acknowledge the financial support (MOST 106-2923-E-006-002-MY3) of the Ministry of Science and Technology in Taiwan, and the financial support under the program ANR-11-LABX-0002-01 (Lab of Excellence ARBRE) in France.

References

[1] Mohanty AK, Misra M, Drzal1 LT. Sustainable bio-composites from renewable resources: opportunities and challenges in the green materials world. Journal of Polymers and the Environment 2002;10:19-26.
[2] Dogan E, Inglesi-Lotz R. Analyzing the effects of real income and biomass energy consumption on carbon dioxide (CO2) emissions: Empirical evidence from the panel of biomass-consuming countries. Energy 2017;138:721-727.
[3] Chen WH, Kuo PC. A study on torrefaction of various biomass materials and its impact on lignocellulosic structure simulated by a thermogravimetry. Energy 2010;35:2580-2586.
[4] Chen WH, Peng J, Bi XT. A state-of-the-art review of biomass torrefaction, densification and applications. Renewable and Sustainable Energy Reviews 2015;44: 847-866.
[5] Pelaez-Samaniego MP, YadamamV, Lowell E, Espinoza-Herrera R. A review of wood thermal pretreatments to improve wood composite properties. Wood Science and Technology 2013;47:1285-1239.
[6] Esteves BM, Pereira HM. Wood modification by heat treatment: a review. BioResources2009;4(1):370-404.
[7] Chen WH, Lu KM, Tsai CM. An experimental analysis on property and structure variations of agricultural wastes undergoing torrefaction. Applied Energy 2012;100:318-325.
[8] Uras-Postma Ü, Carrier M, Knoetze J. Vacuum pyrolysis of agricultural wastes and adsorptive criteriadescription of biochars governed by the presence of oxides. Journal of Analytical and Applied Pyrolysis 2014;107:123-122.
[9] Ferrari S, Cuccui I, Allegretti O. Thermo-vacuum modification of some European softwood and hardwood species treated at different conditions. BioResources 2013;8(1):1100-1109.
[10] Chen YC, Chen WH, Lin BJ, Chang JS, Ong HC. Impact of torrefaction on the composition, structure and reactivity of a microalga residue. Applied Energy 2016;181:110-119.
[11] Chaouch M, Pétrissans M, Pétrissans A, P. Gérardin P. Use of wood elemental composition to predict heat treatment intensity and decay resistance of different softwood and hardwood species. Polymer Degradation and Stability 2010;95:2225-2259.
[12] Chen WH, Hsu JJ, Kumar G, Budzianowski WM, Ong HC. Predictions of biochar production and torrefaction performance from sugarcane bagasse using interpolation and regression analysis. Bioresource Technology 2017;246:12-19.
[13] Colin C, Dirion JL, Arlabosse P, Salvador S. Quantification of the torrefaction effects on the grindability and the hygroscopicity of wood chips. Fuel 2017;197:232-239.
[14] Park SW, Jang CH, Baek KR, Yang JK. Torrefaction and low-temperature carbonization of woody biomass: Evaluation of fuel characteristics of the products. Energy 2016;45:676-685.
[15] Pétrissans M, Gerardin P, El bakali I, Serraj M. Wettability of Heat-Treated Wood 2003;57:301-307.
[16] Law KY. Definitions for hydrophilicity, hydrophobicity, and superhydrophobicity: getting the basics right. Journal of Physical Chemistry Letters 2014;5:686-688.
[17] Hakkou M, Pétrissans M, Gérardin P, A. Zoulalian A. Investigations of the reasons for fungal durability of heat-treated beech wood. Polymer degradation and stability 2006;91: 393-397.
[18] Li SX, Chen CZ, Li MF, Xiao X.Torrefaction of corncob to produce charcoal under nitrogen and carbon dioxide atmospheres. Bioresource Technology 2018;249:348-353.

Available online at www.sciencedirect.com

ScienceDirect

Energy Procedia 158 (2019) 111–116

Energy Procedia

www.elsevier.com/locate/procedia

10th International Conference on Applied Energy (ICAE2018), 22-25 August 2018, Hong Kong, China

Prediction of higher heating values (HHVs) and energy yield during torrefaction via kinetics

Bo-Jhih Lin [a, b], Edgar A. Silveira [a, c], Baptiste Colin [a], Wei-Hsin Chen [b, d, *], Anélie Pétrissans [a, †], Patrick Rousset [e, f], Mathieu Pétrissans [a]

[a]Université de Lorraine, Inra, LERMaB, F88000 Epinal, France
[b]Department of Aeronautics and Astronautics, National Cheng Kung University, Tainan 701, Taiwan
[c]Mechanical Engineering Department, University of Brasília, Brasília, DF 70910-900, Brazil
[d]Research Center for Energy Technology and Strategy, National Cheng Kung University, Tainan 701, Taiwan
[e]CIRAD, UPR BioWooEB, F34398 Montpellier, France
[f]Joint Graduate School of Energy and Environment- Center of Excellence on Energy Technology and Environment-KMUTT, Bangkok 10140, Thailand

Abstract

Torrefaction is a promising process to upgrade biomass and produce solid biofuel. The purpose of this study is to predict the higher heating values (HHVs) of biomass and energy yield during torrefaction. A two-step model and a direct method are adopted to obtain the torrefaction kinetics and the prediction of elemental composition in the present study. The experiments were performed at the temperature range of 200-230 °C in a pilot-scale reactor, which can record the mass loss dynamics during the treatment. The results point out that the prediction of solid yield and elemental composition profiles are in good agreement with the experiments. The predicted HHVs are calculated from C, H, and O based on an empirical equation. As a while, the HHVs of torrefied wood are in the range of 19.85-20.71 MJ kg^{-1} and the energy yields are in the range of 92.3-97.4 %.

Peer-review under responsibility of the scientific committee of ICAE2018 – The 10th International Conference on Applied Energy.

Keywords: torrefaction; two-step kinetics; sustainable material; mild pyrolysis

* Corresponding author. Tel.: +886-6-2004456; fax: +886-6-2389940.
E-mail address: weihsinchen@gmail.com; chenwh@mail.ncku.edu.tw
† Corresponding author.
E-mail address: anelie.petrissans@univ-lorraine.fr

Peer-review under responsibility of the scientific committee of ICAE2018 – The 10th International Conference on Applied Energy.
10.1016/j.egypro.2019.01.054

1. Introduction

Bioenergy is an important renewable energy and it has been extensively employed worldwide. Solid biomass can be burned directly to get heat and power. The moisture, oxygen and hydrogen contents as well as the volume of raw biomass are high, whereas its calorific value is low. Therefore, the utilization efficiency of untreated biomass is low. Torrefaction is a mild pyrolysis process in the temperature range of 200-300 °C conducted to improve the poor properties of biomass. In recent years, numerous studies concerning biomass torrefaction have been performed and the advantages of the pretreatment method have been reported [1]. In order to identify the behavior of degradation during biomass torrefaction, kinetic analysis have to be conducted. In the literature, some studies have proposed kinetic models to represent the thermal degradation of biomass during torrefaction. These models, usually applied to TGA (thermogravimetric analysis) data to simulate the intrinsic decomposition of biomass, can be sorted in two major sections: the detailed models and the pseudo-components models. The most used of the detailed models was initially proposed by Ranzi et al. [2] and further developed by Blondeau and Jeanmart [3], Gauthier et al. [4] and Anca-Couce et al. [5]. This model considers separately the decomposition of the three biopolymer components (hemicelluloses, cellulose, and lignin) in biomass and predicts the volatile matters that are produced. It is the only model based on the description of the chemical reactions occurring during the treatment. However, this model is complex and hard to extend to various species or torrefaction conditions. The pseudo-components models are the most used in the literature because of their simplicity. They aim to represent the global mass loss and can be based on a one-step reaction scheme [6], on several reactions in parallel schemes [7,8] or on several steps in series schemes [9,10]. These models, even if they are simpler, present the advantage to be easily adaptable.

In the present work, a two-step in series model is adopted to obtain the associated kinetic constants and the torrefaction kinetics from the experimental results. Poplar (*Populus nigra*), a common European wood species, was chosen for the torrefaction. The contents of hemicelluloses, cellulose, and lignin in poplar are 22.45, 49.91 and 24.61wt% respectively. The torrefaction experiments were carried out at 200, 210, 220, and 230 °C in a pilot-scale reactor, which could record the mass loss dynamics during the treatment. The detailed informations about experiments have been reported in a previous study [11]. The aim of the present study is to predict higher heating values (HHVs) and energy yields from the torrefaction kinetics. A direct method is also introduced to simulate the elemental composition during torrefaction. The obtained results will be relevant to evaluate the torrefaction performances and provide a useful insight about the mechanisms of biomass thermal degradation.

2. Methodology

The two-step kinetic scheme was originally applied for isothermal pyrolysis by Di Blasi and Lanzetta [12] to describe pure hemicellulose (xylan) decomposition. The kinetic scheme consists of two series-reactions, as shown in **Fig.1**. In this model, it is assumed that raw wood material A is converted to an intermediate solid B and volatiles V_1. The intermediate solid B reacts afterwards to form solid residue C and additional volatiles V_2.

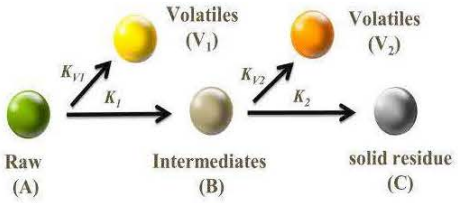

Fig. 1. Two-step kinetic scheme

Assuming that all reactions are of first order, the solid yield equations for the solids (A, B, C) and volatiles (V_1, V_2) can be written as:

$$\begin{cases} \frac{dm_A(t)}{dt} = -(k_1 + k_{V1}) \times m_A(t) \\ \frac{dm_B(t)}{dt} = k_1 \times m_A(t) - (k_2 + k_{V2}) \times m_B(t) \\ \frac{dm_C(t)}{dt} = k_2 \times m_B(t) \\ \frac{dm_{V1}(t)}{dt} = k_{V1} \times m_A(t) \\ \frac{dm_{V2}(t)}{dt} = k_{V2} \times m_B(t) \end{cases} \quad (1)$$

where m_i is the mass of each pseudo-component (i = A, B, C, V_1, V_2). The rate constants obey the Arrhenius law: $k_i=A_i \exp(-E_i/RT)$, in which A_i and E_i are respectively the pre-exponential factor and the activation energy of the component i, R is the universal gas constant and T is the absolute temperature. A numerical approach (MATLAB®) was used to obtain the kinetic parameters for poplar wood. Eight parameters for the four pre-exponential factors (A_i) and four activation energies (E_i) were assumed to start the calculation. A minimizing function and ODE resolutions were used to obtain the optimized values for the rate constants (k_i) and calculate the components yields (A, B and C) during heat treatment.

The calculation for the elemental composition (Ci, Hi, Ni, Oi) of the pseudo-components i is expressed in the matrix form below:

$$\begin{bmatrix} Y_A^{(200)} & Y_B^{(200)} & Y_C^{(200)} \\ Y_A^{(210)} & Y_B^{(210)} & Y_C^{(210)} \\ Y_A^{(220)} & Y_B^{(220)} & Y_C^{(220)} \\ Y_A^{(230)} & Y_B^{(230)} & Y_C^{(230)} \end{bmatrix}_j \times \begin{bmatrix} C_A & H_A & O_A & N_A \\ C_B & H_B & O_B & N_B \\ C_C & H_C & O_C & N_C \end{bmatrix}_j = \begin{bmatrix} C_S^{(200)} & H_S^{(200)} & O_S^{(200)} & N_S^{(200)} \\ C_S^{(210)} & H_S^{(210)} & O_S^{(210)} & N_S^{(210)} \\ C_S^{(220)} & H_S^{(220)} & O_S^{(220)} & N_S^{(220)} \\ C_S^{(230)} & H_S^{(230)} & O_S^{(230)} & N_S^{(230)} \end{bmatrix}_j \quad (2)$$

where i = A, B, C and S represent the pseudo-components A, B, C and the solid after torrefaction (S), respectively; j denotes the data point; $Y_i^{(T)}$ and $X_i^{(T)}$ are the mass fraction and the relative elemental content of the component i at a temperature T, and X = C, H, N, O. The elemental composition of each pseudo-component and thus the treated wood at any temperature and time will be obtained after substituting the ultimate analyses of the initial untreated wood and treated wood at the end of treatment, as well as the instantaneous fraction into the matrix [13].

3. Results and discussion

A two-step kinetic model is established and used to predict dynamic mass loss during wood treatment. The mass loss is predicted by a curve-fitting to fit to the experimental data (as shown in **Fig. 2**).

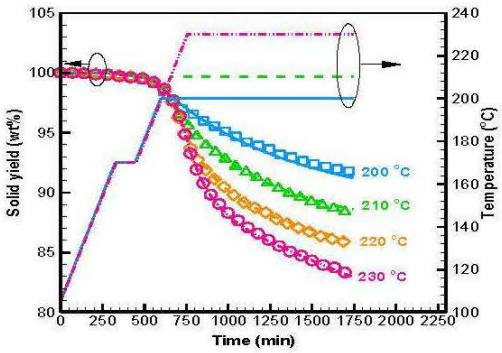

Fig. 2. Profiles of predicted (lines) and experimental (symbols) solid yield during torrefaction

It is found that accurate fits between the simulated and experimental data are achieved in **Fig. 2**. As a result, kinetic parameters are in a reasonable range compared with the kinetic parameters for the degradation of xylan reported in the literature [12]. The pre-exponential factors and activation energies are: A_1=4.80 x 10^8 s^{-1}, E_1=104.42 kJ mol^{-1}; A_{V1}=9.65 x 10^9 s^{-1}, E_{V1}= 125.10 kJ mol^{-1}; A_2=3.2 x 10^6 s^{-1}, E_2=97.60 kJ mol^{-1}; A_{V2}=2.75 x 10^7 s^{-1}, E_{V2}=111.57 kJ mol^{-1}. It is found that reaction rates are higher during the degradation of the initial wood material (A) to form the intermediate (B), than those in the second step during the further decomposition of the intermediate to produce the final solid [13].

Table 1. Elemental analysis of raw and torrefied biomass.

Material	C (wt%[a])	H (wt%)	N (wt%)	O (wt%)[b]
Raw (Poplar)	46.61	6.32	0.28	46.79
Wood torrefied at 200 °C	49.44	6.27	0.28	44.01
Wood torrefied at 210 °C	50.54	6.12	0.36	42.98
Wood torrefied at 220 °C	51.02	5.95	0.38	42.65
Wood torrefied at 230 °C	52.25	5.88	0.45	41.42

[a]: dry-ash-free; [b]:by difference.

According to the elemental analysis of torrefied wood (**Table 1**) and the torrefaction kinetics, the predicted elemental compositions of wood during torrefaction are obtained, as plotted in **Fig. 3**. The results point out that the C, H, and O profiles are in good agreement with expected composition changes in the wood materials after torrefaction (i.e. higher carbon, lower hydrogen and lower oxygen contents at stronger thermal intensity of treatment). When increasing the treatment temperature, the elemental compositions in treated wood tend to be changed more aggressively. At the temperature of 230 °C, the carbon content in treated poplar quickly increases and the oxygen content dramatically decreases. This result is attributed to the thermal cross-linking reactions that obviously occur at higher temperature [11,14]. Overall, the prediction of elemental composition of torrefied wood works well at any treatment temperature and time.

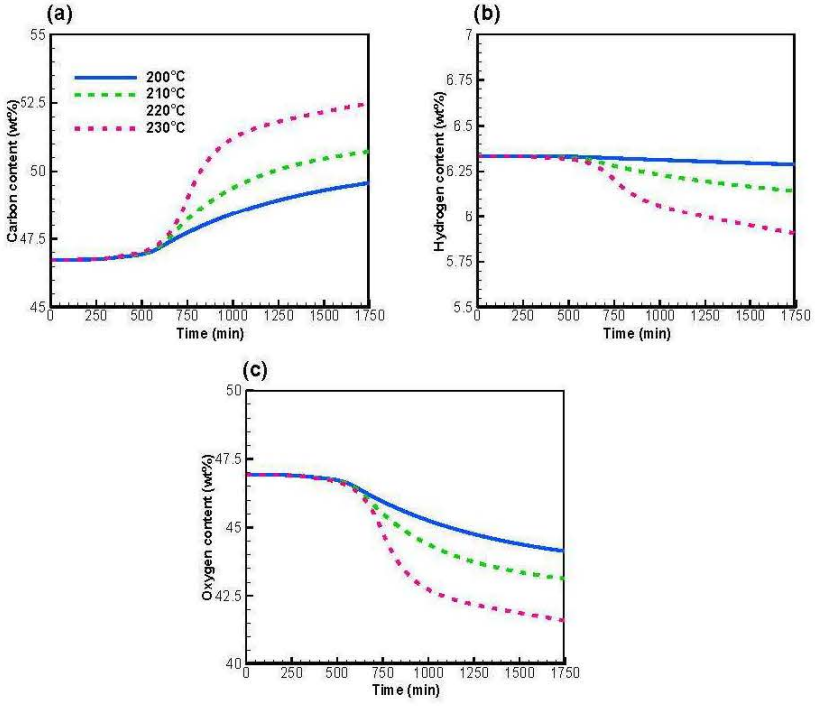

Fig. 3. Profiles of predicted (a) carbon, (b) hydrogen and (c) oxygen contents during torrefaction

The higher heating value (HHV) of torrefied wood is obtained from the predicted elemental composition by the empirical equation. The obtained HHV can be applied to evaluate the potential opportunity for solid fuel in the end of use. The HHVs of untreated and torrefied wood are calculated based on the correlation by Boie [10] presented in Eq. (3):

$$HHV = 0.3517C + 1.16249H + 0.10467S - 0.1195O + 0.0628N \quad (3)$$

where the C, H, O, and N are the mass percentages of carbon, hydrogen, oxygen, and nitrogen on a dry-ash free basis. The results are displayed in **Fig. 4a**. The HHV started to increase at the thermal homogenization stage, and it is owing to the removal of extractives and light volatile matters [11]. As a while, the HHVs of poplar tend to increase with increasing temperature, and they are in the range of 19.85-20.71 MJ kg^{-1}. The increasing of HHV is mainly due to the changes of elemental composition in treated wood. Chen *et al.* [1] pointed out that carbon and hydrogen in a fuel are the major sources of heat released during the combustion. However, more hydrogen contained in a fuel is usually accompanied by a lower content of carbon. Oxygen contained in biomass is conducive to fuel burning, but it reduces the heating value of biomass. Based on the results of solid yields and HHVs, the energy yields can be determined [1], as expressed as:

$$\text{Energy yield}(\%) = \text{Solid yield}\ (\%) \times \frac{HHV\ of\ torrefied\ biomass}{HHV\ of\ raw\ biomass} \quad (4)$$

The results indicated that the energy yield is in the range of 92-98%, as shown in **Fig. 4b**. With these obtained results, it can be conducted with other informations, such as energy consumption and manufacturing cost, to optimize the biomass torrefaction process.

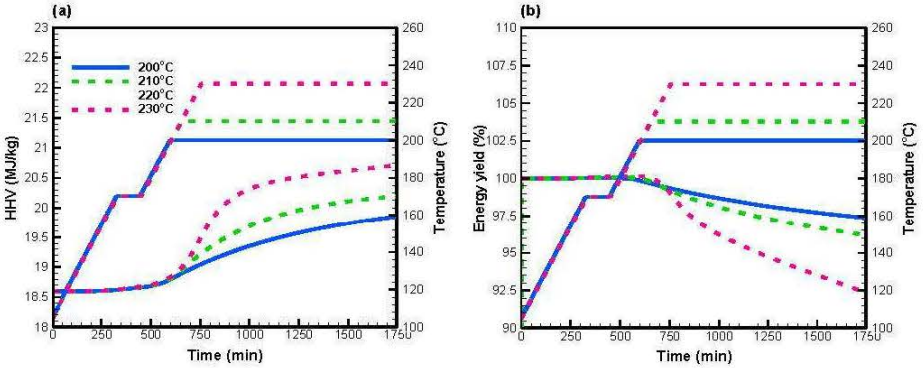

Fig. 4. Profiles of predicted (a) HHVs and (b) energy yields during torrefaction

4. Conclusions

The prediction of higher heating values (HHVs) and energy yields of torrefied wood in a pilot-scale reactor have been investigated in this study. One common European wood species (poplar) and four different treatment temperatures (200, 210, 220 and 230 °C) have been employed. A two-step model was adopted to evaluate the torrefaction kinetics and a direct method was applied to predict the elemental composition. The results point out that the C, H, and O profiles are in good agreement with expected composition changes in the wood materials after torrefaction. The HHVs of treated wood are computed from the predicted elemental composition by an empirical equation. As a while, the HHVs of torrefied poplar tend to increase with increasing temperature, and they are in the

range of 19.85-20.71 MJ kg^{-1}. Concerning the energy yield of treated wood, it is in the range of 92-98% which is close to the results of light torrefied biomass [1].

Acknowledgements

The authors gratefully acknowledge the financial support under the program ANR-11-LABEX-0002-01 (Lab of Excellence ARBRE) in France, the financial support (MOST 106-2923-E-006-002-MY3) of the Ministry of Science and Technology in Taiwan.

References

[1] Chen WH, Peng J and Bi XT. A state-of-the-art review of biomass torrefaction, densification and applications. Renewable and Sustainable Energy Reviews 2015; 44:847-866.
[2] Ranzi E, Cuoci A, Faravelli T. Chemical kinetics of biomass pyrolysis. Energy & Fuels 2008; 22(6):4292-4300.
[3] Blondeau J and Jeanmart H. Biomass pyrolysis at high temperature: prediction of the gaseous species yields from an anisotropic particle. Biomass and Bioenergy 2012; 41:107-121.
[4] Gauthier G, Melkior T, Salvador S, Corbetta M, Frassoldati A, Pierucci S, Ranzi E, Bennadji H and Fisher EM. Pyrolysis of thick biomass particles: experimental and kinetic modelling. Chemical Engineering Transactions 2013; 32:601-606.
[5] Anca-Couce A, Mehrabian R, Scharler R, and Obernberger I. Kinetic scheme to predict product composition of biomass torrefaction. Chemical Engineering Transactions 2014; 37:43-48.
[6] Repellin V, Govin A, Rolland M and Guyonnet R. Modelling of weight loss of wood chips during torrefaction in a pilot kiln. Biomass and Bioenergy 2010; 34(5):602-609.
[7] Ratte J, Fardet E, Mateos D and Héry JS. Mathematical modelling of a continuous biomass torrefaction reactor: TORSPYD™ column. Biomass and Bioenergy 2011; 35(8):3481-3495.
[8] Cavagnol S, Sanz E, Nastoll W, Roesler JF, Zymla V and Perré P. Inverse analysis of wood pyrolysis with long residence times in the temperature range 210-290°C: Selection of multi-step kinetic models based on mass loss residues. Thermochimica Acta 2013; 574:1-9.
[9] Joshi Y, de Vries H, Woudstra T and de Jong W. Torrefaction: unit operation modelling and process simulation. Applied Thermal Engineering 2014; 74:83-88.
[10] Peduzzi E, Boissonnet G, Haarlemmer G, Dupont C and Maréchal F. Torrefaction modelling for lignocellulosic biomass conversion process. Energy 2014; 70:58-67.
[11] Lin BJ, Colin B, Chen WH, Pétrissans A, Rousset P and Pétrissans M. Thermal degradation and compositional changes of wood treated in a semi-industrial scale reactor in vacuum. Journal of Analytical and Applied Pyrolysis 2018; 130:8-18.
[12] Di Blasi C and Lanzetta M. Intrinsic kinetics of isothermal xylan degradation in inert atmosphere. Journal of Analytical and Applied Pyrolysis 1997; 40-41:287-303.
[13] Bach QV, Chen WH, Chu YS and Skreiberg Ø. Predictions of biochar yield and elemental composition during torrefaction of forest residues. Bioresource Technology 2016; 215:239-246.
[14] Chaouch M, Pétrissans M, Pétrissans A and Gérardin P. Use of wood elemental composition to predict heat treatment intensity and decay resistance of different softwood and hardwood species. Polymer Degradation and Stability 2010; 95(12):2255-2259.

Etudes de bois traités par pyrolyse douce dans un réacteur semi-industriel pour une production de matériaux durable: comportement thermique, changements de propriétés et modélisation cinétique

Résumé

La pyrolyse douce est un procédé prometteur et largement utilisé, mené à une température de 200 à 300 °C dans une atmosphère inerte afin de produire des matériaux durables (bois traité thermiquement) ou des combustibles solides (bois torréfié). Le but de cette étude est d'étudier les bois traités thermiquement dans un réacteur à l'échelle semi-industrielle. Une essence de feuillus (Populus nigra) et une essence de résineux (Abies pectinata), sont utilisées pour réaliser les expériences. Dans la première partie de cette étude le comportement thermique des planches de bois est étudié dans un réacteur à l'échelle semi-industrielle. Les expériences sont effectuées à 200-230 °C sous vide (200 hPa) avec une vitesse de chauffe de 0.2 °C min^{-1}. Quatre étapes différentes de dégradation thermique lors du traitement du bois sont définies en fonction de la perte de masse. Les caractéristiques de dévolatilisation du bois traité sont évaluées à l'aide de l'indice de dévolatilisation (ID) basé sur les résultats de l'analyse immédiate. La corrélation de l'ID par rapport à la perte de masse des deux essences de bois est fortement caractérisée par une distribution linéaire, ce qui permet de fournir un outil simple et utile pour prédire la perte de masse du bois. Dans la seconde partie de l'étude, plusieurs analyses (spectroscopie infrarouge, diffraction des rayons X, mesure du changement de couleur, teneur en humidité à l'équilibre et angle de contact) ont été réalisées. Les résultats obtenus montrent clairement les réactions de déshydratation, de désacétylation, de dépolymérisation et de condensation au cours du traitement thermique. Les phénomènes de changement de couleur et de transformation hygroscopique observés sont illustrés et discutés en détail. La décarbonisation, la déshydrogénation et la désoxygénation des bois traités sont également évaluées. Il s'avère que les trois indices peuvent être bien corrélés à la variation de couleur totale et à l'étendue de la réduction de l'hygroscopicité (HRE). Dans la dernière partie, une modélisation cinétique du traitement thermique du bois est développée. Le modèle obtenu permet de prédire avec succès le rendement en solide de planches de bois lors du traitement dans un réacteur à l'échelle semi-industrielle. Dans le même temps, une prévision de la composition élémentaire est proposée. Celle-ci est basée sur les analyses élémentaires du bois non traité et du bois traité, ainsi que sur les rendements instantanés en solides. Les résultats indiquent que la prédiction des profils C, H et O est en accord avec les changements de composition attendus dans le matériau au cours du traitement. En résumé, les résultats obtenus et la cinétique établie sont propices à l'identification des mécanismes de dégradation thermique du bois et peuvent être utilisés pour le traitement thermique et la conception de réacteurs dans l'industrie afin de produire des matériaux bois adaptés à diverses applications.

Mots clés: Cinétique de pyrolyse, Comportement thermique, Dévolatilisation, Pyrolyse légère, Traitement thermique du bois, Torréfaction.

Investigations of wood treated by mild pyrolysis in a semi-industrial reactor for sustainable material production: thermal behavior, property changes and kinetic modeling

Abstract

Mild pyrolysis is a promising and widely applied process conducted at 200-300 °C in an inert condition to produce sustainable materials (i.e. heat treated wood) or solid fuel (i.e. torrefied wood). The aim of this study is to investigate the woods heat treated in a semi-industrial scale reactor for sustainable material production. Two different European wood species, a hardwood species (poplar, *Populus nigra*) and a softwood species (fir, *Abies pectinata*), are used to perform the experiments. The present research is divided into three parts. In the first part, the thermal behavior of wood boards is studied in a semi-industrial scale reactor. The experiments are carried out at 200-230 °C with a heating rate of 0.2 °C min^{-1} in a vacuum condition (200 hPa) to intensify the thermal degradation. Four different stages of thermal degradation during wood heat treatment are defined based on the intensity of differential mass loss (DML). The devolatilization characteristics of treated woods are evaluated by the devolatilization index (DI) based on the results of proximate analysis. The correlation of DI with respect to mass loss of the two wood species is strongly characterized by linear distribution, which is able to provide a simple tool to predict the mass loss of wood. In the second part of the study, a number of analyses, such as Fourier-transform infrared spectroscopy, X-ray diffraction, measurement of color change, equilibrium moisture content, and contact angle) are performed to evaluate the property changes of treated woods. The obtained results clearly demonstrate the thermal degradation through dehydration, deacetylation, depolymerization, and condensation reactions during the heat treatment. The observed phenomena of color change and hygroscopic transformation are illustrated and discussed in detail. The decarbonization, dehydrogenation, and deoxygenation of the treated woods are also evaluated. It is found that the three indexes can be well correlated to the total color difference and hygroscopicity reduction extent (HRE). In the last part of the study, the kinetic modeling of wood heat treatment is developed based on a two-step kinetic scheme. The obtained kinetics successfully predict dynamic solid yield of wood boards during the treatment in the semi-industrial reactor. Meanwhile, the prediction of elemental composition is also performed by a direct method based on the elemental analyses of untreated and treated woods at the end of the treatment, as well as the instantaneous solid yield. The results point out that the prediction of C, H, and O profiles are in good agreement with expected composition changes in the wood materials during treatment. In summary, the obtained results and established kinetics are conducive to recognizing the mechanisms of wood thermal degradation and can be used for heat treatment process and reactor design in industry to produce wood materials for various applications.

Keywords: Pyrolysis kinetics, Thermal behavior, Devolatilization, Mild pyrolysis, Wood heat treatment, Torrefaction.